25/1222

NUREG/CR-1222

Techniques of Analysis of Load-Displacement Records by J-Integral Methods

NEWARK PUBLIC LIBRARY

FEB 19 1980

U. S. GOVT. PUBS.
DEPOSITORY 376

Prepared by H.A. Ernst, P.C. Paris

The Center for Fracture Mechanics
Washington University

Prepared for
U. S. Nuclear Regulatory
Commission

READEX FICHE

Y 3.N 88:

NOTICE

This report was prepared as an account of work sponsored by an agency of the United States Government. Neither the United States Government nor any agency thereof, or any of their employees, makes any warranty, expressed or implied, or assumes any legal liability or responsibility for any third party's use, or the results of such use, of any information, apparatus product or process disclosed in this report, or represents that its use by such third party would not infringe privately owned rights.

Available from

GPO Sales Program
Division of Technical Information and Document Control
U. S. Nuclear Regulatory Commission
Washington, D. C. 20555

and

National Technical Information Service
Springfield, Virginia 22161

NUREG/CR-1222

Techniques of Analysis of Load-Displacement Records by J-Integral Methods

Manuscript Completed: November 1979
Date Published: January 1980

Prepared by
H.A. Ernst, P.C. Paris

The Center for Fracture Mechanics
Washington University
St. Louis, Missouri 63130

Prepared for
Division of Reactor Safety Research
Office of Nuclear Regulatory Research
U.S. Nuclear Regulatory Commission
Washington, D.C. 20555
NRC FIN No. B6288

Techniques of Analysis of Load-Displacement Records by J-Integral Methods

By

Hugo A. Ernst* and Paul C. Paris**

Abstract

Exact methods are used to obtain J from a single load displacement record for different configurations based on dimensional analysis and deformation theory of plasticity to imply the dependence of the load on crack length and displacement. The methods also permit the evaluation of the crack length increment a and hence complete J-R curves can be constructed. Formulae for T_{mat} and T_{app} are presented as well. Conditions for the existence of the so-called η-factor are stated, and subsequent simplifications of the general method by its use are shown. Results of analysis of experimental work for different configuration material combinations are presented showing the adequacy of the general methodology.

The substance of this work was the D.Sc. dissertation of Hugo A. Ernst, submitted in partial fulfillment of the requirements for the D.Sc. degree at Washington University.

---

* Research Assistant, Center for Fracture Mechanics, Washington University, St. Louis, Missouri 63130.

** Professor of Mechanics and Director, Center for Fracture Mechanics, Washington University, St. Louis, Missouri 63130.

TABLE OF CONTENTS

No.		Page
1.	Preliminaries	
1.1	Introduction	1
1.2	The J integral	7
1.3	J as the Strength of the Crack Tip Singularity	12
1.4	J as a Fracture Criterion	17
1.5	Estimates on J	18
1.6	The J-R Curve	29
1.7	J and the Growing Crack	32
1.8	J Controlled Crack Growth	33
1.9	A Treatment on the Subject of Tearing Instability	36
1.10	Summary	42
2.	The Analysis of Load-Displacement Relationships to Determine J-R Curves and Tearing Instability Material Properties	
2.1	Introduction	44
2.2	Development of a Convenient Form for the J-integral	49
2.3	Dimensional Analysis of Relationship Between Load, Crack Length and Plastic Displacement	52
2.4	Analysis to Determine J using the First Special Functional Form F_1	54
2.5	Determination of Crack Length Change and T using the First Special Functional Form	57
2.6	Pure Bending of a Small Remaining Ligament	60
2.7	The Compact Specimen	63

TABLE OF CONTENTS
(continued)

No.		Page
2.8	Determination of F_1 and its Derivatives for Compact Specimens	67
2.9	Bending Test Specimens of the 3-Point and 4-Point Bending Type	72
2.10	Applications to Predominately Tension Loading	73
2.11	The Round Bar in Tension	76
2.12	Applied Tearing Modulus	79
3.	Theorems on Conditions for Separability	
3.1	Introduction	85
3.2	J integral Separability	85
3.3	P Separability	91
3.4	Existence of the η-factor	94
3.5	Summary	98
4.	An Approach to Development of Plastic Work Factors	
4.1	Introduction	99
4.2	The Elastic η-factor	100
4.3	Plastic η-factors	102
4.4	A General Condition for the Existence of η_{pl}	107
4.5	Examples of Specific Conditions for which η_{pl} exists	109
4.6	Plastic Factors for the Tension Specimen	113
4.7	Plastic Factors in the Small Scale Yielding Regime	120
4.8	Examples of Conditions where η_{pl} does not Rigorously Exist	128

TABLE OF CONTENTS
(continued)

No.		Page
	4.9 Summary and Discussion	130
5.	Experimental Results	131
	5.1 Introduction	131
	5.2 An Initial Experimental Investigation of Tearing Instability Theory	131
	5.3 Analysis of Data for Compact Tension Specimen Nongrowing Crack	151
	5.4 Analyis of Three Point Bend Specimens s/W = 4 Ni- Cr- Mo- V Rotor Steel	160
	5.5 Analysis of Three Point Bend Specimens s/W = 8 Recalculation of Previous Results	164
	5.6 Analysis of H.Y. 130 Steel Compact Specimens	170
	5.7 Analysis of H.Y. 130 Steel Compact Specimens by an Experimentally Obtained Calibration Function	175
6.	Concluding Remarks	194
7.	Acknowledgements	199
8.	Bibliography	200
9.	Appendix	207

TECHNIQUES OF ANALYSIS OF LOAD DISPLACEMENT RECORDS BY J-INTEGRAL METHODS

1. PRELIMINARIES

1.1 INTRODUCTION

It has been an important task through the years to be able to predict the load level at which a body would fail. This problem goes back as far as man himself.

At the turn of the XV century Leonardo da Vinci [57]*, was probably the first to conduct systematic tests to determine critical loads on wires of different lengths and diameters. He came to the conclusion that the load required to cause failure was on the average bigger for shorter wires of the same material and diameter. Significant differences in the failure load values were observed, for equivalent numbers of specimens tested of the different lengths. These results are now explained on the basis of cracks present in the body. The longer the wire, the bigger the probable number and size of the largest cracks (or microcracks) present in the body.

*Numbers in brackets in the text indicate references in the Bibliography.

During the 19th and 20th centuries but mostly in the last thirty years, significant effort has been devoted to the stress analysis of cracked bodies. Some interesting examples are:

In 1890, Love [37] included, in his extensive treatise of elasticity, the comment that fracture is not well understood. Later on, in 1920, Griffith [1] introduced the principles of an energy balance theory. This theory, based on a linear elastic behavior of the material, predicted the failure of the cracked body when a critical value of the energy rate supplied to the moving crack tip was attained. This energy G, or the elastic energy made available per unit extension of the cracked area, is

$$G = - \frac{dU}{dA} \tag{1.1}$$

where U is the potential energy, and A is the cracked area.

More recently, in the mid-1950's, George Irwin [2,58,60] developed the analytical basis of a crack tip stress field theory, which in turn was the starting point of modern Fracture Mechanics. In his theory he defined a parameter, the crack tip stress field intensity factor, K, which is a combination of applied load P, specimen configuration and crack length, a,

$$K = P.\ F(a, \text{geometry}) \tag{1.2}$$

K is said to be the controlling parameter of such a field, because stresses and displacements are proportional to it. In general

$$\sigma_{ij} = \frac{K}{\sqrt{r}} f_{ij}(\theta)$$
$$u_i = K\sqrt{r}\, g_i(\theta) \qquad (1.3)$$

at points near the crack tip where σ_{ij} and u_i are the components of the stress tensor and displacement vector respectively, and r and θ are the usual polar coordinates with the origin taken from the crack tip [3] [38].

Initially with this approach it was assumed that failure occurs when K reaches a critical value K_c. Later more sophisticated failure criteria were introduced, as shall be noted subsequently herein. Irwin [2,58,60] also proved that there is a unique relationship between K and Griffith's G

$$G = \frac{K^2}{E} \qquad (1.4)$$

and so the consistency of the two theories was apparent.

From there on, a large variety of test programs were conducted to measure K_c (plane stress) and K_I* (plane strain) values for different configurations (specimen geometry and crack length). The result was that for brittle materials K_{IC} is reasonably independent of configuration and it only depends on temperature, strain rate,

*The subscript "I" stands for what is called mode I loading, meaning that the load is applied perpendicular to the crack plane [3], and in addition that the local stress state within the plastic zone at the crack tip is plane strain.

and the material, provided the state of stresses is that of plane strain. This critical value of K is often referred to, in Fracture Mechanics, as toughness of the material: the ability to carry load or deform plastically in the presence of a notch or crack [4].

It was also found, that for plane stress a substantial amount of crack growth occured prior to fracture, and then the so-called Resistence R-Curve methodology was introduced [18] in order to better characterize the material behavior. The idea of fracture resistence curve concept can be described as follows.

If a loading system is applied to a cracked body, a zone where the material yields develops ahead of the crack tip, providing the material resistence to crack growth. This material resistence R increases with the plastic zone size which increases with the applied load. At the same time the applied parameter G also increases with the increasing load and with the slightly increased crack length a. The process goes on in such a way that at any stage an equilibrium state is reached i.e.

$$G = R \tag{1.5}$$

However, as loading progresses, at a certain point G may increase faster, with an increment of crack length, than R, thus causing sudden and substantial growth to ensue in an unstable manner. Figure 1.

The mathematical conditions for the instability are (for dead load, P, applied)

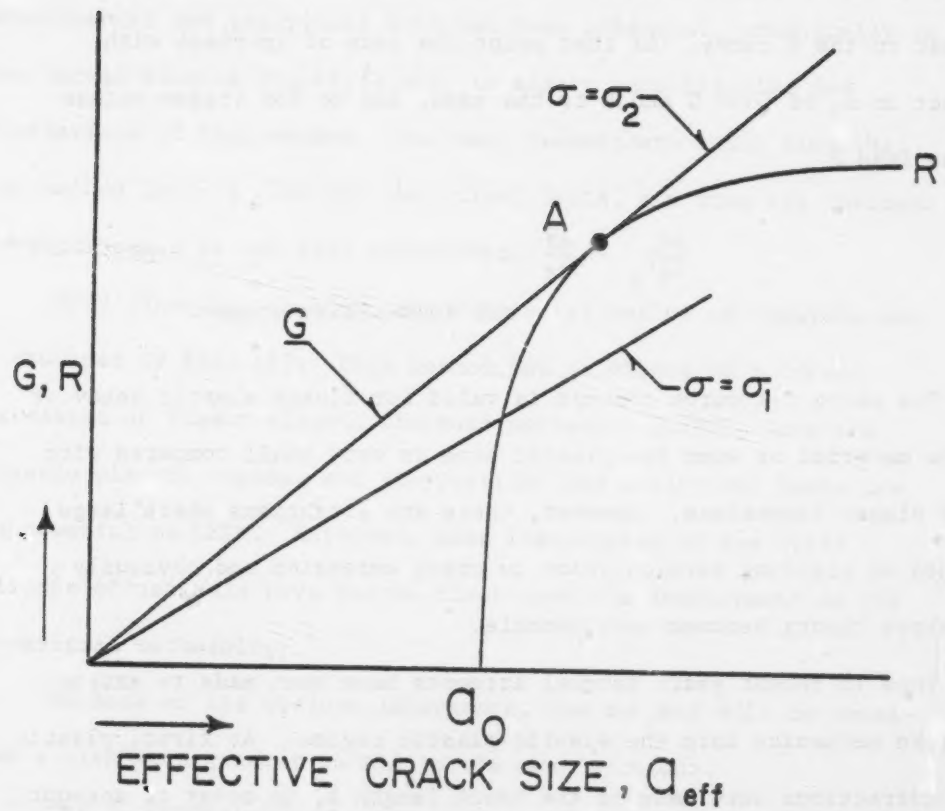

Fig. 1 G-R Curve

$$G = R \quad \text{and}$$

$$\left(\frac{\partial G}{\partial a}\right)_P \geq \frac{dR}{da} \tag{1.6}$$

Figure 1 shows a plot of G and R as functions of effective crack size a_{eff}. At any level of applied load below A, G = R and a small amount of crack growth occurs. When A is reached the G curve is tangent to the R curve. At that point the rate of increase with respect to a, of both G and R is the same, and so for bigger values of the load P

$$\left(\frac{\partial G}{\partial a}\right)_P > \frac{dR}{da} \tag{1.7}$$

and instability occurs.

The above G-R curve concept is valid for linear elastic behavior of the material or when the plastic zone is very small compared with other planar dimensions. However, there are situations where large amounts of yielding develop prior to crack extension and obviously the above theory becomes questionable.

Thus in recent years several attempts have been made to extend fracture mechanics into the elastic-plastic regime. At first, plastic zone corrections were made to the crack length a, in order to account for the extra deformation due to plasticity [5] [60]. These corrections proved to be insufficient to handle problems ranging from large scale yielding to fully plastic regimes.

Later on, in 1961 Wells [6] proposed that the fracture behavior could be characterized by parameters related to the opening of the

crack surfaces at the original crack tip, namely the crack opening displacement (COD). He showed that COD could be related to G, in the presence of small amounts of plasticity, and thus critical values of COD could be related to K_{IC}.

This method uses the Dugdale-Bilby-Cottrell model [7] [39] [43], to relate COD to applied load and crack length. Extensive experimental and analytical work has been conducted, principally in the United Kingdom [61,62,63,64], to assert possibilities and limitations of this method. But many researchers still find that the method lacks a flexible analytical basis, and that its rational physical basis is not well understood.

More recently, in 1968, the J-integral method of analysis was introduced by Rice [8]. This method can be viewed as a direct extension of linear elastic fracture mechanics (LEFM), into the elastic plastic regime, and its physical and analytical basis are as powerful as LEFM. Moreover, some limitations of the other methods of analysis have become clear upon the development of the J-integral methodology.

Because of its obvious importance, the subject will be considered with much greater detail in the next sections.

1.2 THE J-INTEGRAL

Consider a homogeneous body which presents an elastic (linear or non linear) behavior; free of body forces, with a crack or notch parallel to the x-axis and subjected to a 2-D deformation field (all $\sigma_{ij} = \sigma_{ij}(x,y)$), as shown in Figure 2. Then Rice proved that

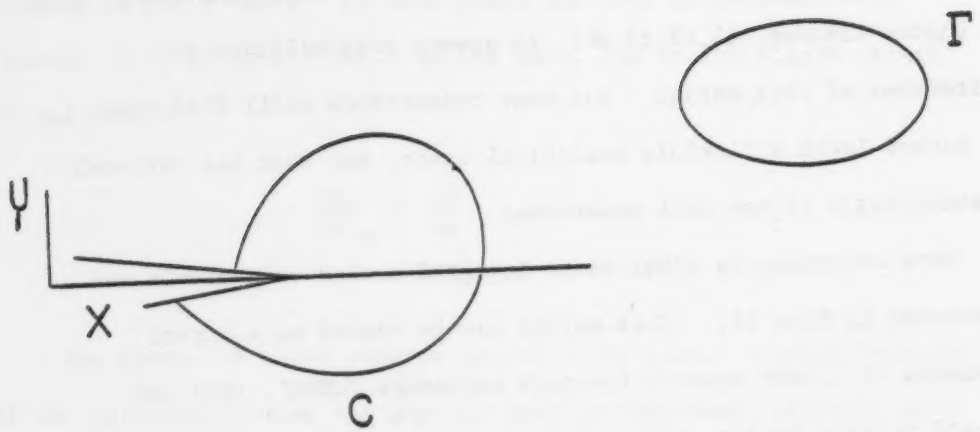

$$J=\int_C W dy - T_i \frac{\partial u_i}{\partial x}\, ds$$

Fig. 2. Different types of contours

$$\int_{\Gamma} W_s \, dy - T_i \frac{\partial u_i}{\partial x} \, ds = 0 \qquad (1.8)$$

where W_s is the strain energy density, T_i are the components of the traction vector, u_i are the displacement vector components, and Γ is any closed curve lying completely inside the body (not encompassing any singularities).

As a consequence, if now C represents an open curve surrounding the crack tip going from the lower surface to the upper one, and lying completely inside the body, the integral taken along any C type curve gives a unique value, which Rice called J. Then J is said to be path independent since it is the same if computed on any C type curve.

And so

$$J = \int_{C} W_s dy - T_i \frac{\partial u_i}{\partial x} \, ds \qquad (1.9)$$

The uniqueness of the result or path independence of the integral implies that J is a crack tip characterization parameter. That is, the crack tip is the only point enclosed by all C type curves, and thus J is related to the state at or near the crack tip, such as the intensity or the stress-strain singularity there. At the same time, its value can be evaluated on a large contour from conditions far from the crack tip.

A more physical meaning can be obtained [9] for J by considering Figure 3. Here, let C be some contour around the crack tip where crack extension takes place carrying the contour with it. Then

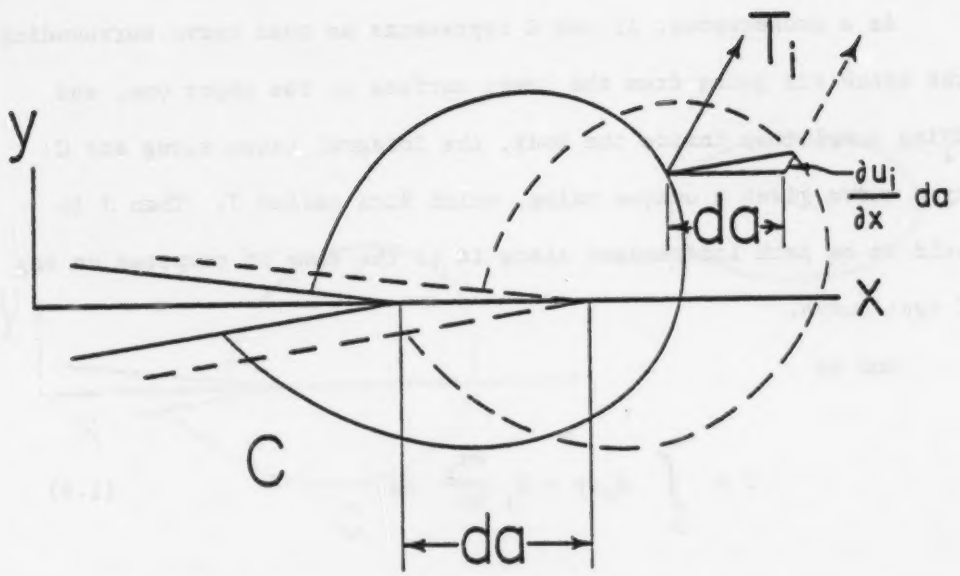

Fig. 3 J around contour C at a crack tip

$$J\,da = \int_C W_s\,dy\,da - T_i \frac{\partial u_i}{\partial x}\,ds\,da \qquad (1.10)$$

The first term on the right-hand side is the strain energy gained by moving the contour with the crack tip, and the second one is the work done by tractions in moving. So J da is the total energy coming across the contour (any C surrounding the crack tip) for a cracked area da (per unit thickness) for an elastic (linear or non linear) material.

$$J = -\frac{dU}{da} \qquad (1.11)$$

As a result for linear elasticity J coincides with both G and K by

$$J = G = \frac{K^2}{E} \qquad (1.12)$$

An alternative interpretation was also provided by Rice [10]: J can be interpreted as the rate of change of potential energy per unit crack length. That is

$$J = -\frac{dU}{da} \qquad (1.13)$$

where U is the potential energy. The potential energy of a body of area A, and with a boundary S is given by

$$U = \int_A W_s\,dx\,dy - \int_{S_T} \bar{T}.\bar{u}\,ds \qquad (1.14)$$

The first term is the strain energy contained in the body, or simply the work done by the external forces; in the second term S_T refers to that portion of the boundary S, where stresses are prescribed as boundary conditions.

On a load load-point displacement P-δ record, for slightly different crack lengths in otherwise identical specimens, the area between curves is J da. Figure 4 shows J da in the constant load and constant displacement. The additional triangular area is a second order term and may therefore be neglected. Hence J is the same independently of the parameter held constant (P or δ).

Therefore an alternative, equally valid definition of J, for an elastic material is

$$J = -\frac{dU}{da} = -\int_0^{\delta} \left(\frac{\partial P}{\partial a}\right)_{\delta} d\delta = \int_0^{P} \left(\frac{\partial \delta}{\partial a}\right)_{P} dP \qquad (1.15)$$

From this alternative form, various procedures for evaluating J are found. These procedures will be discussed later.

1.3 J AS THE STRENGTH OF THE CRACK TIP SINGULARITY

In the aim of extending LEFM into the elastic plastic regime, analytical work was devoted to find a single parameter capable of characterizing the stress-strain field surrounding the crack tip. It was anticipated that such a parameter might be related to J, in order to have consistency with linear elasticity where the controlling parameter is K, and is

$$K = \sqrt{G\,E} = \sqrt{J_{el}\,E} \qquad (1.16)$$

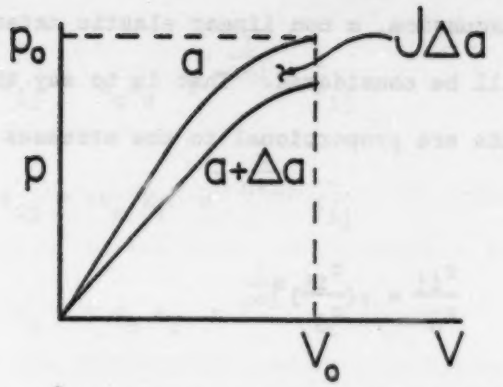

a) CONSTANT DISPLACEMENT

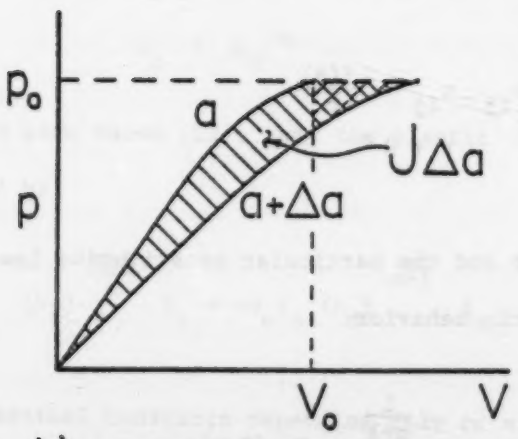

b) CONSTANT LOAD

Fig. 4 Graphical measurement of J

This work was done by Hutchinson [11] [12], and Rice and Rosengren [13], and can be summarized as follows.

In the present discussion, a non linear elastic material, of the pure power type will be considered. That is to say that the strain tensor components are proportional to the stresses raised to the power n.

$$\frac{\varepsilon_{ij}}{\varepsilon_o} = \gamma\left(\frac{\sigma_{ij}}{\sigma_o}\right)^n$$

For such materials the stress-strain singularities have been discussed [11], [12], [13].

They showed that the product of stress and strain approaches a 1/r singularity as r (distance to the crack tip), tends to 0.

$$\sigma_{ij}\ \varepsilon_{ij} \underset{r \to 0}{=} \frac{f(\theta)}{r} \tag{1.17}$$

This type of behavior and the particular constitutive law used here, requires the asymptotic behavior

$$\sigma_{ij} \to r^{-\frac{1}{n+1}}\ \Sigma_{ij}(\theta,n) \tag{1.18}$$

$$\varepsilon_{ij} \to r^{-\frac{n}{n+1}}\ E_{ij}(\theta,n)$$

The functions Σ_{ij} and E_{ij} can be obtained from the set of equilibrium, and compatibility equations, the constitutive law, and

the stress free surface boundary conditions of the problem.

Equation (1.18) can be written more precisely [11], as

$$\sigma_{ij} = \sigma_o k_\sigma \, r^{-\frac{1}{n+1}} \, \tilde{\sigma}_{ij}$$

$$\varepsilon_{ij} = \gamma \varepsilon_o \, k_\varepsilon \, r^{-\frac{n}{n+1}} \, \tilde{\varepsilon}_{ij} \qquad (1.19)$$

$$u_i = \gamma \, \varepsilon_o \, k_\varepsilon \, r^{\frac{1}{n+1}} \, \tilde{\mu}_i$$

where σ_{ij} ε_{ij} and μ_i are dimensionless functions dependent of the angle, θ, and the hardening exponent, n. And k_ε and k_σ are the plastic strain and stress intensity factors respectively, related by

$$k_\varepsilon = (k_\sigma)^n \qquad (1.20)$$

It has also been shown [12], that the plastic intensity factors are related to J by

$$J = \gamma \sigma_o \varepsilon_o \, (k_\varepsilon)^{\frac{n+1}{n}} \, I_n = \gamma \sigma_o \varepsilon_o \, (k_\sigma)^{n+1} \, I_n \qquad (1.21)$$

where I_n are numerical constants depending only on n. Values of I_n for different n are given in [11].

Using (1.19) and (1.21), the stress and strain fields can be written in terms of J as

$$\sigma_{ij} = \sigma_o \left(\frac{J}{r\sigma_o\varepsilon_o}\right)^{\frac{1}{n+1}} \bar{\Sigma}_{ij}(\theta,n)$$

$$\varepsilon_{ij} = \varepsilon_o \left(\frac{J}{r\sigma_o\varepsilon_o}\right)^{\frac{1}{n+1}} \bar{E}_{ij}(\theta,n) \qquad (1.22)$$

The advantage of choosing J as the parameter to characterize the crack tip field instead of the plastic intensity factors is that J can be evaluated experimentally independent of stress-strain properties and calculated with less difficulty.

The role of J is then the governing intensity parameter of the stress-strain field.

The parameter J has proven to be a very useful parameter which is capable of characterizing the crack tip stress-strain fields, as well as to represent the elastic energy release rate per unit crack extension. At the same time, an alternative definition of J, in terms of the "macro parameters" load P, and displacement δ has been given. But so far all these approaches assume an elastic (linear or non linear) behavior of the material. In real situations, an elastic-non reversible plastic behavior is more likely to occur.

Now, when plasticity is treated by deformation theory [40,41], there is no difference between an elastic plastic behavior and a pure non-linear elastic one, provided no unloading occurs. In other words, assume that both the non linear elastic and the elastic plastic stress-strain curves are identical for monotonically increasing load, and that the only difference between the two is their response to unloading. If the bodies are loaded identically then the same

stress-strain response is expected, at any point in both bodies, provided no unloading occurs.

Moreover, recent numerical studies by Shih [26], McMeeking [27], Hayes [42], Carlsson [44] and others, show that J values calculated from deformation theory are essentially the same as those obtained from flow theory; J being for the latter also essentially path independent. This behavior of J can be explained by the fact that, in many practical situations, a state of stresses that closely approaches proportional loading is present nearby the crack tip, giving therefore identical results for deformation and incremental theories.

J then can be viewed as the intensity of the singular crack tip fields for non linear elastic materials, playing essentially the same role as K or (K^2) does for LEFM. But the numerical studies mentioned above suggested the possibility that J is a reasonable enough parameter to characterize the stress-strain fields even for elastic-plastic (non-reversible) material behavior.

These observations lead to the conclusion that Begley and Landes' [14,20] suggestion that fracture itself might be governed by J is very reasonable.

1.4 J AS A FRACTURE CRITERION

As was mentioned before J can be related to the area between the load displacement diagrams, for two otherwise identical specimens having neighboring crack sizes. That is

$$J = -\int_0^{\delta} \frac{\partial P}{\partial a})_{\delta} \, d\delta = \int_0^{P} \frac{\partial \delta}{\partial a})_{P} \, dP. \qquad (1.15)$$

This result was used by Begley and Landes [14,20] to do the first experimental evaluation of J for different materials and geometries.

They simply obtained P-δ records for a wide range of crack sizes, in otherwise identical specimens. They calculated the area under each curve for different values of the displacement δ, Figure 5a.

Then they plotted these areas vs crack length a, with δ as a parameter Figure 5b, and finally calculating the slopes of these curves they obtained J, (using $J = - dU/dA$) Figure 5c, as a function of a and δ.

With this method they were able to calculate J, as a function of crack length and displacement, at the point of initiation of crack growth (J_{IC}), for different materials and geometries. They found that the value of J_{IC} obtained from small specimens, where large amounts of yielding had occured, was the same (for the same material) as that for big specimens where the plastic zone was very small compared with other planar dimensions. In both cases abrupt unstable crack extension ensues upon reaching J_{IC}. That is

$$J_{IC} \text{ (plastic tests)} = J_{IC} \text{ (elastic tests)} = \frac{K_{IC}^2}{E} \qquad (1.23)$$

This finding, that was not obvious beforehand, provided the possibility of using J as a more general fracture parameter than G or K. Indeed, J coincides with G for LEFM but it has proven to be adequate for large yielding too.

1.5 ESTIMATES ON J

After the critical experiments of Begley and Landes, significant effort was devoted to evaluate J as a function of the applied load, or

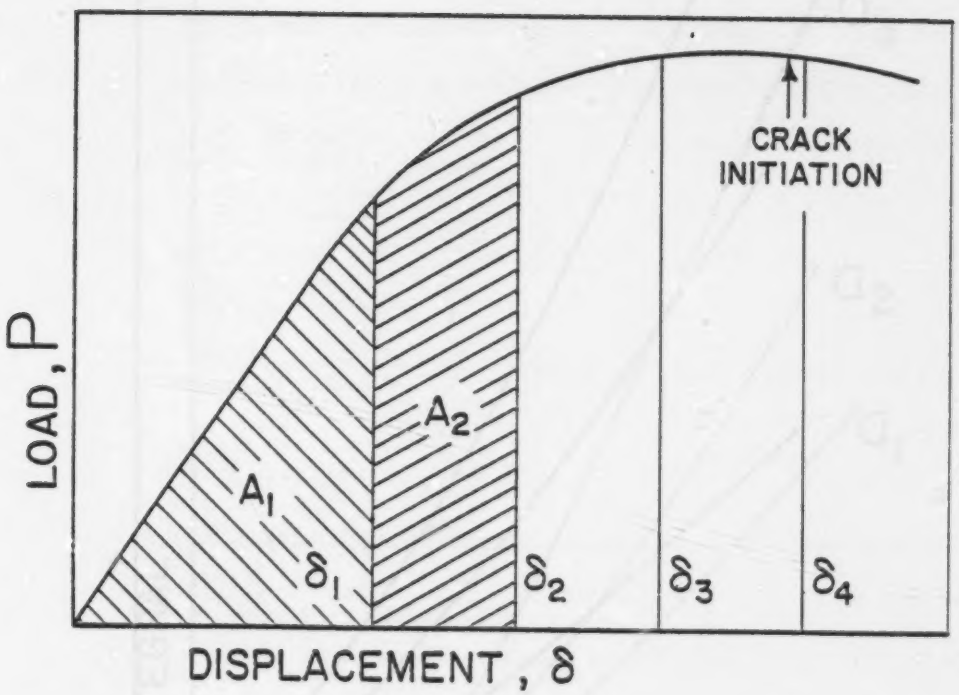

Figure 5a. Illustration of work to a given displacement

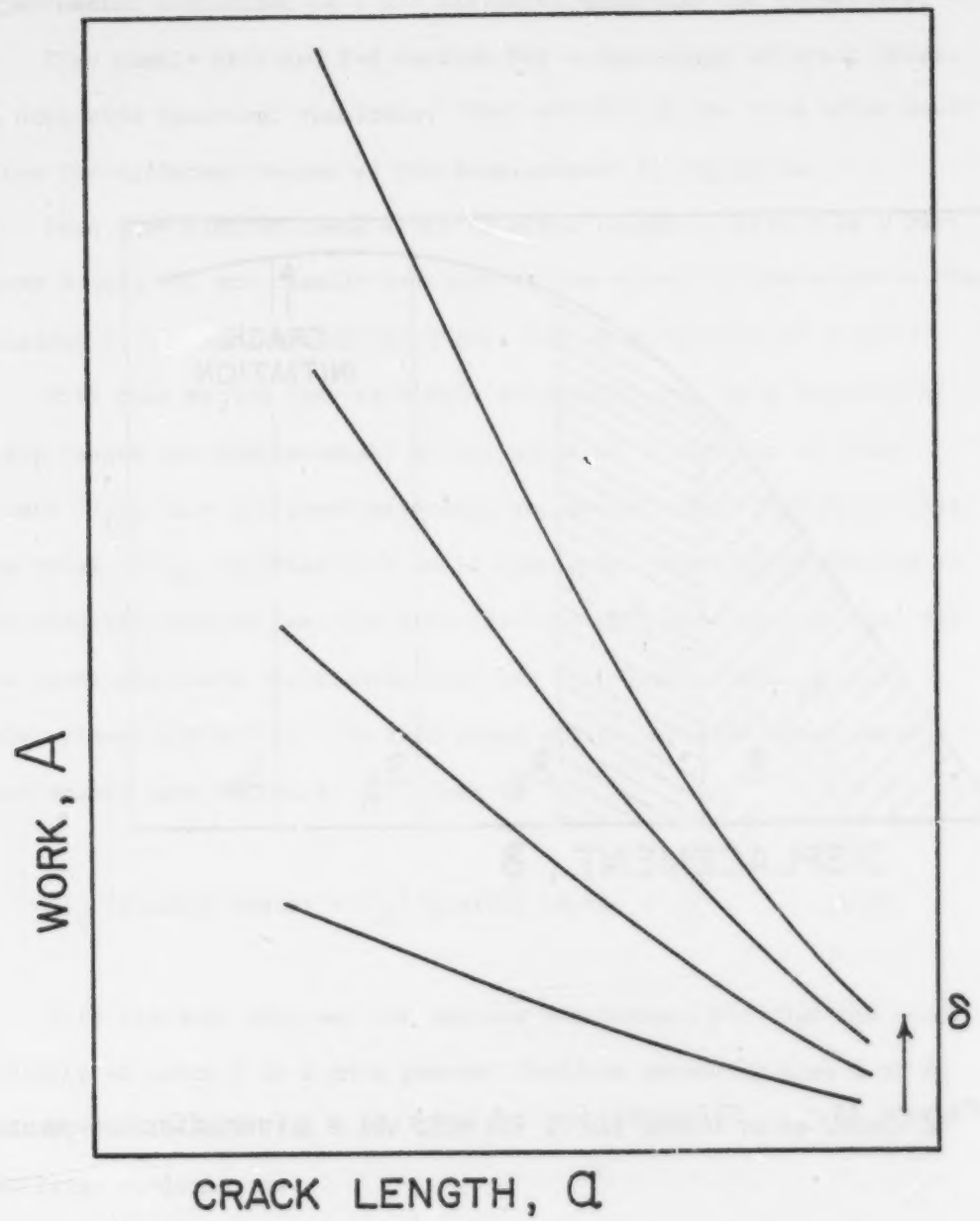

Fig. 5b. Work done as function of crack length

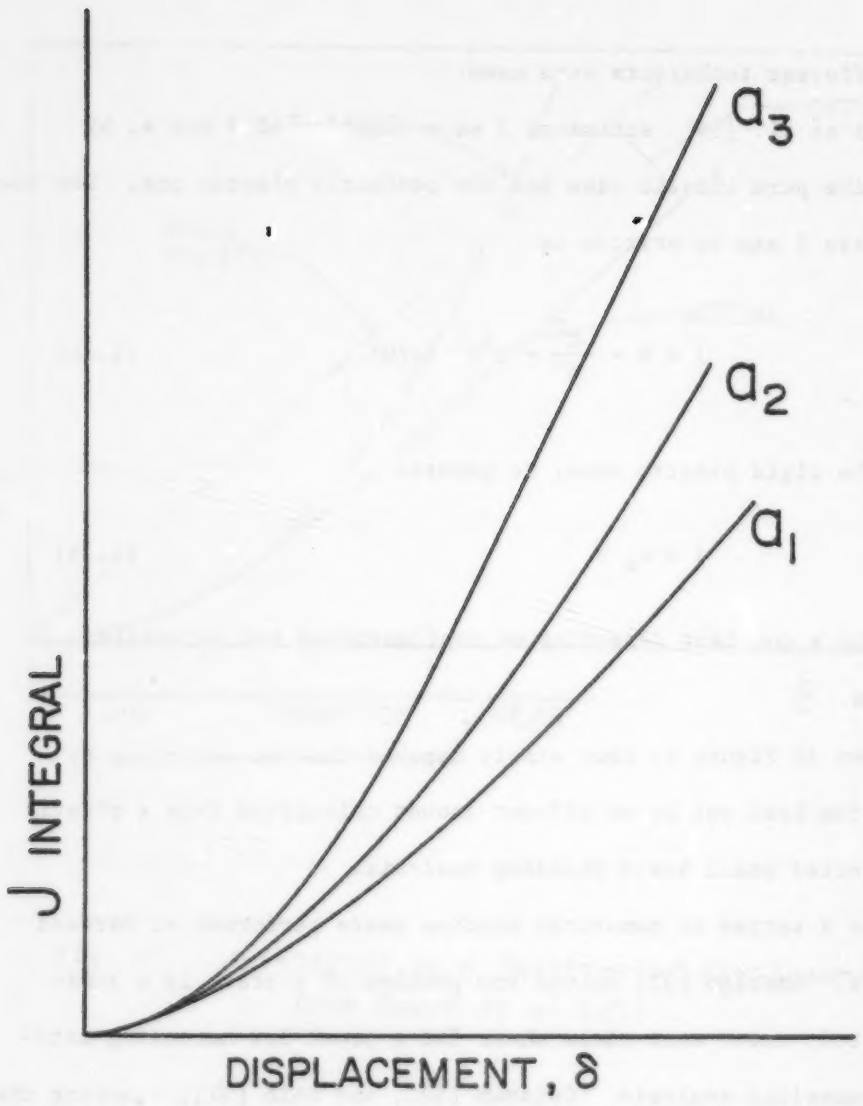

Fig. 5c. J-integral vs displacement

displacement, and the crack length a.

$$J = J(P, a) = J(\delta, a) \tag{1.24}$$

and so different techniques were used.

Bucci et al. [35], estimated J as a function of δ and a, by matching the pure elastic case and the perfectly plastic one. For the elastic case J can be written as

$$J = G = \frac{K^2}{E'} = \delta^2 f \quad (a/W). \tag{1.25}$$

And for the rigid plastic case, in general

$$J = s_o \delta \tag{1.26}$$

where s_o is a constant depending on configuration and materials properties.

As is shown in Figure 6, they simply matched the two solutions by shifting the last one by an off-set amount calculated from a plastic zone corrected small scale yielding analysis.

Later a series of numerical studies where performed at Harvard University. Amazigo [33] solved the problem of a crack in a semi-infinite body under anti plane shear for a power law hardening material by numerical analysis. Goldman [32], and Shih [31], studying the same material behavior performed numerical calculations for different configurations and loading conditions. In general they considered

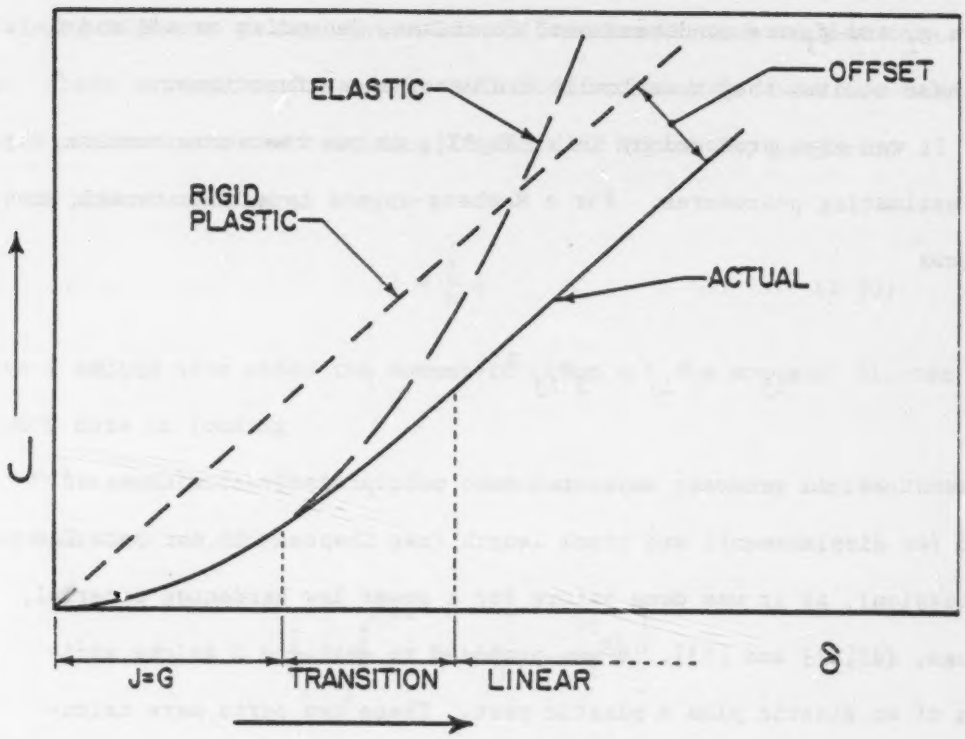

Fig. 6 J-integral as a function of displacement from Bucci et al [35]

$$J = \alpha\gamma_o\varepsilon_o \; a\,(1-a/W)\; g_1\,(a/W,n) \;\; (P/P_o)^{n+1}$$

$$\delta = \alpha\,\varepsilon_o\; a\; g_3\,(a/W,n)\;(P/P_o)^n \qquad (1.27)$$

where g_1 and g_3 are nondimensional functions, depending on a/W and n. In these studies they numerically evaluated these functions.

It was also proposed by Shih [31,53], to use the above results, for estimating procedures. For a Ramberg-Osgood type of material, as follows

$$\varepsilon_{ij} = c_1\sigma_{ij} + c_2\sigma_{ij}^{\;n} \qquad (1.28)$$

J cannot be, in general, separated into multiplicative functions of load (or displacement) and crack length (see Chapter III for detailed discussion), as it was done before for a power law hardening material, though, in [31] and [53], it was proposed to evaluate J as the addition of an elastic plus a plastic part. These two parts were calculated as follows.

The elastic part was obtained by setting n=1 and $a=a_{eff}$ in the g_i functions. The effective crack length, a_{eff}, being the original one plus the usual r_y correction from small scale yielding. The plastic part was calculated by using the g_i functions for the desired n and original crack length a.

$$J = J(a_{eff},\, n = 1) + J\,(a,n) \qquad (1.29)$$

Another approach to the problem was presented by Rice et al [36]. They developed a method based on dimensional analyses, for calculating $J = J(\delta,a)$, from a single test record, for different configurations. This method assumes a very deep crack, meaning that the ratio of the remaining ligament to any other planar dimension is much smaller than one. Their expression for a semi-infinite cracked body where the only length parameter is the remaining ligament b, Figure 7a, subjected to pure moment applied at $-\infty$ is

$$J = \frac{2}{b} A \tag{1.30}$$

where A is the area under the moment-rotation (of the moments) diagram or work done in loading.

For a similar analysis of the center cracked panel in tension Figure 7b they obtained

$$J = G + \frac{2}{b}\left[\int_0^{\delta_{pl}} P \; d\delta_{pl} - \frac{P\delta_{pl}}{2}\right] \tag{1.31}$$

This work, since its publication in 1973, was the only available tool for calculating J from a single test record, and has been of common and general use since then. It has often been used in situations beyond its assumptions for which it was not intended to serve. As a result, several works were presented [54,55], comparing J values obtained from this method with others and with the J_{DEF}. The comparison went as far as values of .6 of b/W for the compact tension specimen. The original hypothesis of $b/W \ll 1$ was largely forgotten. Moreover, some investigators reached the rather ironical conclusion

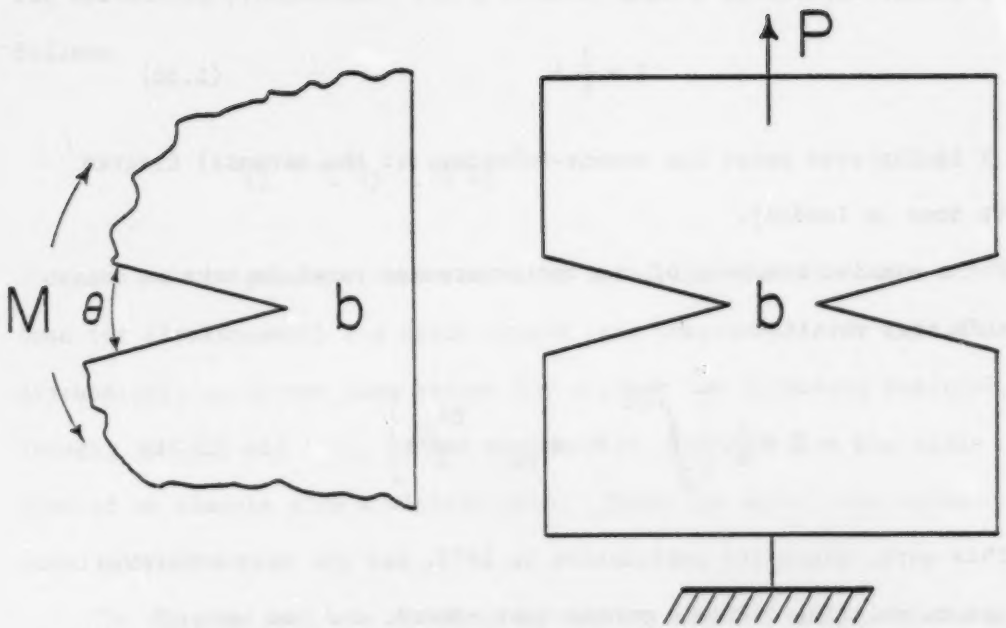

7 a) 7 b)

Fig. 7 Small remaining ligament subject to a) pure bending and b) tension

that the method itself was in error. A much greater detailed discussion on this method, will be provided later.

Subsequently Sumpter and Turner [51] performed also some numerical calculations of J. They separate J as

$$J = \frac{\eta_{el}}{b} A_1 + \frac{\eta_{pl}}{b} A_2 \qquad (1.32)$$

where A_1 and A_2 are the elastic and plastic part of the area under the P-δ record respectively. The η_{el} and η_{pl} are functions of a/W only η_{el} can be calculated from available functions [30]; and η_{pl} was obtained from the numerical results. This method makes use of the interesting idea of separating J into an elastic and plastic part, but leaves unclear the validity and method for evaluation of η_{pl} for a given test specimen in an actual situation.*

Most recently McCabe [52] presented some evidence of the possibilities of the so called off-set secant method for analyzing P-δ records. Joining the origin with the point of interest, Figure 8, and calculating the slope of the straight line, he could calculate the crack length a_{eff} associated with that compliance, from the linear elastic solution. With the value obtained for a_{eff} he then calculated the corresponding K, and thus G. He found that those values of $G = J_{el}$ were in excellent agreement with the so called J definition (J_{DEF}) values which were calculated using the Begley and Landes multispecimen technique.

*Recent cooperative effort between Turner [82] and the Washington University Group is attempting this clarification.

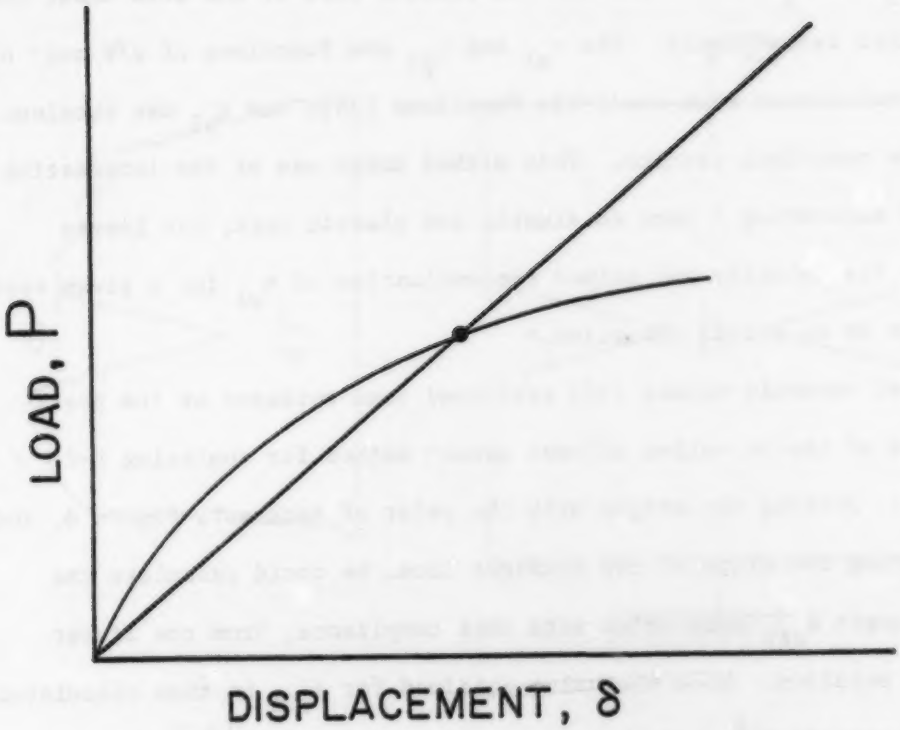

Fig. 8 Secant offset method

The results are in rather surprising agreement, considering that the method applied small scale yielding analysis to conditions well into the fully plastic state and calculated the K using the effective crack length, $a_{eff} = a_0 + r_y$, where, as was mentioned, the r_y is no longer a small correction term. Further explanation is obviously required.

Many other studies on estimates for J have been done since 1972, which are not mentioned here. However, a number of them that can be found in the literature, clearly show the interest in the possibility of evaluating J from a single specimen test record.

1.6 THE J-R CURVE

Up to this point J has been shown to be a suitable parameter to extend LEFM into the elastic plastic regime. It is a parameter capable of characterizing the stress-strain field, associated with the pseudo-elastic energy release rate per unit crack extension and it furnishes a criterion for initiation of crack growth, J_{IC}. Subsequently additional discussion was devoted to completing the picture of EPFM, having in J its basis, as an extension of K or G in LEFM. A further natural extension was the developing of J-R curves instead of G-R curves, but for plane strain as well as plane stress.

Landes and Begley [15], Clarke et al [16], Logdson [17] and others [18], have plotted applied field intensity, J vs Δa to characterize the material's resistence response or R-curve. A schematic J-R curve is shown in Figure 9. As the load is applied to the cracked body, the crack tip blunts, giving a linear dependence between the apparent Δa and $J(\Delta a \approx J/2\sigma_o)$ [19]. As the level of applied J

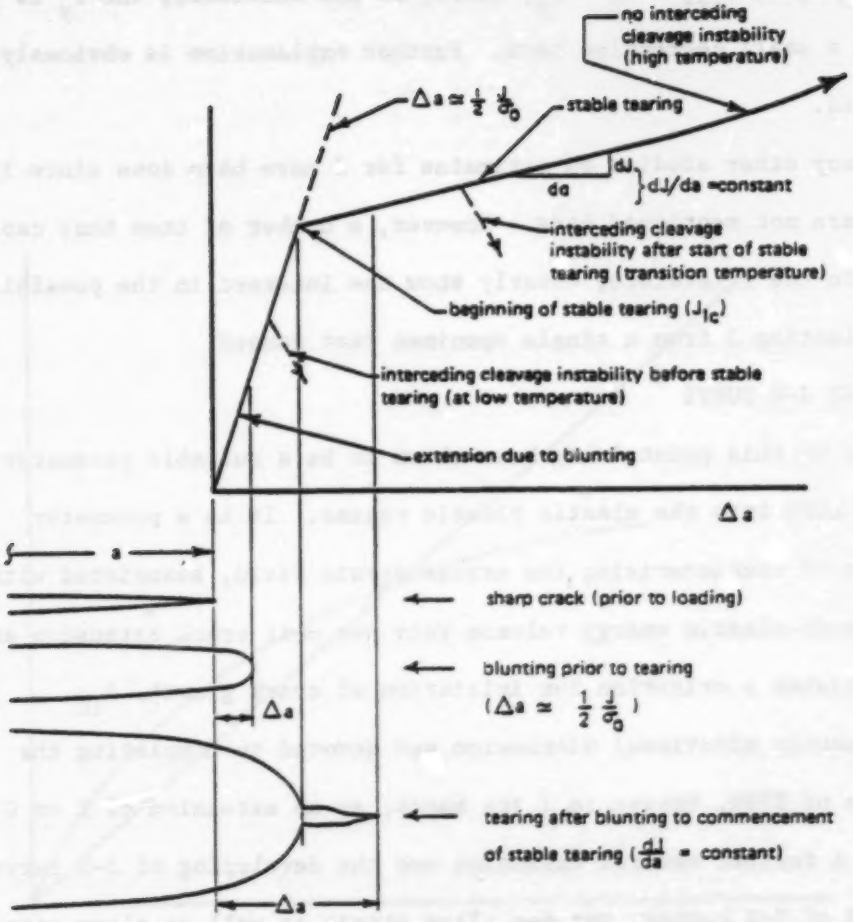
no interceding cleavage instability (high temperature)
$\Delta a \simeq \frac{1}{2} \frac{J}{\sigma_0}$
stable tearing
dJ
da
dJ/da =constant
interceding cleavage instability after start of stable tearing (transition temperature)
beginning of stable tearing (J_{Ic})
interceding cleavage instability before stable tearing (at low temperature)
extension due to blunting
Δa
a
sharp crack (prior to loading)
blunting prior to tearing
($\Delta a \simeq \frac{1}{2} \frac{J}{\sigma_0}$)
Δa
tearing after blunting to commencement of stable tearing ($\frac{dJ}{da}$ = constant)
Δa

Fig. 9 The J-R curve.

increases the blunting goes on until a certain state is achieved ahead of the blunted crack tip. At that point, a process of stable tearing may occur depending on the temperature, and other properties of the material.

The specimen may fail in an unstable manner by cleavage before any stable tearing is observed, if the temperature is lower than a certain value. On the other hand, if the temperature is high enough, stable tearing may be observed for values of J beyond J_{IC}, up to a certain level where instability occurs. In the intermediate range of temperature mixture of small amounts of tearing follow by cleavage is likely to occur.

Plane strain conditions (in the fracture process zone) are assumed to be present [15] [9] [19] [85] as long as the test specimen thickness and remaining ligament are large enough by the criterion [28]

$$\text{size} \geq 25\ J/\sigma_o \qquad (1.33)$$

If this condition is met, the J-R curve is size independent [16] and is also reasonably independent of configuration, with some reservation [20].

Significant work on R curves was done by McCabe and Heyer [21,22, 23] and others [24], that showed that they appear to be a material property if the requirements above mentioned were met. Those two investigators also introduced a method [23] [25] to evaluate the whole G-R curve from a single specimen. They simply tested the specimen in a displacement controlled apparatus i.e. applying displacement instead

of load to the specimen. In this way they obtained several test points at increased crack length Δa as a function of applied G, before failure of the specimen. Their crack length was calculated from the unloading compliance [16] and G was calculated from available formulas.

1.7 J AND THE GROWING CRACK

In their experimental work, Begley and Landes [14,20] carefully avoided the question of unloading due to crack growth, and so their work was directed essentially to crack initiation, rather than propagation. With no unloading the difference between non linear elasticity and elasto-plasticity was not of significance to their approach.

For the more general case of a growing crack, however, the crack tip field is far more complex than for the stationary crack, and so far no complete solution of such a field is available for an extending crack. This is because of mathematical complexities in the continuum formulation.

McClintock and Irwin [45] and Rice [46], approached the problem on incremental basis, considering an elastic perfectly plastic material, and quasi-static crack growth. The important conclusion of these studies is that the singular behavior of the strain field near the crack tip, is much weaker than for the stationary crack. In fact, the field for an advancing crack presents a log r singularity, compared to a 1/r singularity for the non-growing crack. This weaker singularity is probably due to the extending of the crack into the zone where the material is less plastically deformed. This reduced crack tip strain field intensity may be one of the main reasons for stable crack growth.

In general, as discussed by Rice [19], at a given material point, there is an incompatible elastic strain increment due to crack growth, which is not derivable from a displacement increment. This incompatible elastic strain induces, in turn plastic strain. Nevertheless, recent numerical studies by Shih [26], Anderson [47], and others, show that for a growing crack J is nearly path independent, under certain conditions.

Most recently, Shih [48], presented some results where J seemed to be even closer to path independence if it is calculated on a contour traveling with the crack in its growth. In the same work, some effort was devoted to establishing a theory to explain stable vs unstable crack growth. Anderson [47], suggested that the crack would grow when a certain critical crack tip opening angle (CTOA) was reached, and the growth would proceed in such a way as to maintain the CTOA constant. Even though, there is some ambiguity in the definition of CTOA, because, as was pointed out by Rice [46], the crack tip profile experiences a vertical tangent and so an arbitrary extra length parameter has to be introduced. Finally, the picture emerging from all the above is that, in contrast with the static crack, the mechanics of crack growth has not been yet completely understood. Thus even though J-R curves were constructed, the role of J as a parameter characterizing the stress-strain fields in the presence of crack growth was found objectionable without further insight.

1.8 J CONTROLLED CRACK GROWTH

As was pointed out above, the role of J as the controlling parameter for a growing was doubted.

On this question the work of Hutchinson and Paris [49] sheds some light. They showed that even for a growing crack there is an annular region where J still dominates, provided some sufficient conditions are met. To show this, consider a material obeying a pure power hardening law,

$$\varepsilon_{ij} = \alpha\sigma_{ij}^{n} \tag{1.34}$$

The strain field of the dominant singularity at the crack tip according to deformation theory is

$$\varepsilon_{ij} = k_n J^{\frac{n}{n+1}} r^{-\frac{n}{n+1}} \tilde{\varepsilon}_{ij}(\theta,n) \tag{1.35}$$

where r and θ are planar-polar coordinates centered at the tip; the function $\tilde{\varepsilon}_{ij}$ depends on the angle θ as well as on n and on whether plane stress or plane strain pertains; k_n is a dimensional constant.

Now, let R denote the characteristic outer radius of the zone controlled by J which, in general, it is at least fraction of the plastic zone. Since there will be an internal region of distinctly non-proportional plastic loading, which will be of the order of the crack growth increment Δa, the first condition for J-controlled growth is

$$\Delta a \ll R \tag{1.36}$$

Examine now, the strain increments due to a simultaneous increase in J and crack length a. For deformation theory the strain field,

Equation (1.35) continues to hold with the origin relocated at the current crack tip.

$$d\varepsilon_{ij} = k_n J^{\frac{n}{n+1}} r^{-\frac{n}{n+1}} \frac{n}{n+1} \left\{ \frac{dJ}{J} \tilde{\varepsilon}_{ij} + \frac{da}{r} \tilde{\beta}_{ij} \right\} \qquad (1.37)$$

where $\tilde{\beta}_{ij}(\sigma) = \cos\theta\, \tilde{\sigma}_{ij} + \frac{n+1}{n} \sin\frac{\partial}{\partial\theta} \tilde{\sigma}_{ij}$

The first term in the brackets corresponds to proportional loading increments, the second is the non proportional one. Taking $\tilde{\varepsilon}_{ij}$ and $\tilde{\beta}_{ij}$ to be of the same order of magnitude, the condition to have just proportional loading is

$$\frac{da}{r} << \frac{dJ}{J} \qquad (1.38)$$

Combining (1.36) and (1.38) the annular region in which J is the controlling parameter is defined by

$$\Delta a << r < R < b \qquad (1.39)$$

In particular for a specimen in which the whole remaining ligament has yielded, R will be a fraction of b. Introducing a new parameter

$$\omega = \frac{b}{J} \frac{dJ}{da} \qquad (1.40)$$

the condition for J-controlled crack growth can be restated as

$$\omega >> 1 \qquad (1.41)$$

together with (1.39). As was pointed out by the authors, the condition $\omega >> 1$, is a sufficient condition for J-controlled crack growth. In other words having $\omega >> 1$ assures J-control, but the question still remains to be answered on which is the smallest value of ω which will assure J-control. The answer will probably depend on specimen geometry as well as on strain hardening but has not yet been given.

1.9 A TREATMENT ON THE SUBJECT OF TEARING INSTABILITY

Even though the potential of J as the governing parameter of the crack tip stress strain field was established earlier, the question of stable vs unstable crack growth remained unresolved until very recently. For examining stability under fully plastic condition it is evident that such a theory requires including the influence of material properties, specimen geometry, crack length and overall behavior of the structure. The specimen, or structural member, is normally constrained by the rest of the structure in such a way, that neither an exclusively load-controlled, nor a displacement-controlled situation is realistic, but more likely a mixed one, where the compliance C_M of the rest of structure ($C_M \neq 0$, $C_M \neq \infty$), has to be taken into account.

In 1977, Paris et al [71,72] proposed a theory to explain stable vs unstable crack growth. They introduced a non dimensional quantity called the tearing modulus T

$$T_{mat} = \frac{E}{\sigma_o^2} \frac{dJ}{da} \tag{1.42}$$

where E is the Young's modulus and σ_o is the flow stress.

If dJ/da is taken from the J-R curve, the obtained tearing modulus is a material property,

$$T = \frac{E}{\sigma_o^2} \left(\frac{dJ}{da}\right)_{mat} \tag{1.43}$$

On the other hand, if dJ/da is taken to be the increment of the externally applied J field per unit crack extension, the tearing modulus is the characterizing parameter of the potential of the applied source of deformation to cause instability.

$$T_{app} = \frac{E}{\sigma_o^2} \left(\frac{dJ}{da}\right)_{app} \tag{1.44}$$

The basic idea given in [71,72], is then that the condition of instability is

$$J_{app} = J_{mat} \qquad \text{Equilibrium for } J_{app} > J_{IC}$$

and (1.45)

$$T_{app} > T_{mat}$$

Let the applied tearing modulus T_{app}, be considered here with more detail.

Suppose a total displacement δ_{tot} is applied to a structure, composed by a specimen (sp) and the rest of the apparatus, or machine (M),

$$\delta_{tot} = \delta_M + \delta_{sp} \tag{1.46}$$

or separating the elastic and plastic parts of δ_{sp}

$$\delta_{tot} = \delta_M + \delta_{el} + \delta_{pl} \tag{1.47}$$

At any level of the applied δ_{tot}, there is a well defined value of the applied J

$$J_{app} = J(\delta_{sp}, a) \tag{1.48}$$

Consider now a virtual crack extension that takes place at that particular stage of the applied displacement δ_{tot}, which is thought to be constant during the crack extension process so,

$$d\delta_{tot} = d\delta_M + d\delta_{sp} = 0$$

or

$$d\delta_M + d\delta_{el} + d\delta_{pl} = 0 \tag{1.49}$$

Elastic displacements are (normally) linearly proportional to load and have the form:

$$\delta_{el} = \frac{P}{BE} \cdot f\left(\frac{a}{W}, \frac{B}{W}, \frac{L}{W}, \text{ etc.}\right) \tag{1.50}$$

where f( ) is a nondimensional function of the specimen dimensions. The plastic displacement, δ_{pl}, presuming we are at limit load for the cracked section, will have a linear relationship to the crack opening stretch, δ_t, or

$$\delta_{pl} = \delta_t \cdot g\left(\frac{a}{W}, \frac{B}{W}, \frac{L}{W}, \text{ etc.}\right) \tag{1.51}$$

and finally the testing machine will be regarded as a linear spring or

$$\delta_M = \frac{P}{K_M} \tag{1.52}$$

where K_M is the spring constant. The load, P, is assumed to be at limit load, P_L, which will depend linearly on the flow stress, σ_o, and thickness, B, therefore

$$P = P_L = \sigma_o B\, W\, h\left(\frac{a}{W}, \frac{B}{W}, \frac{L}{W}, \text{etc.}\right) \tag{1.53}$$

and the usual relationship between J and δ_t is assumed with a constant, β, adjustable approximately to suit the configuration, or

$$\delta_t = \beta \frac{J}{\sigma_o} \tag{1.54}$$

Now during an increment of crack extension, da, the variables in the above expressions, which change are, a, P, δ_t and J to cause changes in the dispiacements writing the differentials of Eqs. (1.44) through (1.48) gives

$$d\delta_{el} = \frac{dP}{BE} \cdot f(\,) + \frac{P}{BE} \frac{\partial f(\,)}{\partial a}\, da \tag{1.50a}$$

$$d\delta_{pl} = d\delta_t g(\,) + \delta_t \frac{\partial g(\,)}{\partial a}\, da \tag{1.51a}$$

$$d\delta_M = \frac{dP}{K_M} \tag{1.52a}$$

$$dP = dP_L = \sigma_o B\, W \frac{\partial h(\,)}{\partial a}\, da \tag{1.53a}$$

and

$$d\delta_t = \beta \frac{dJ}{\sigma_o} \tag{1.54a}$$

Now substituting (1.53) (1.54) (1.53a) and (1.54a) in the right hand sides of (1.50a), (1.51a), and (1.52a) so that the remaining differentials there are da and dJ, gives:

$$d\delta_{el} = \frac{\sigma_o W}{E} \frac{\partial}{\partial a} [h(\,) \cdot f(\,)]\, da \tag{1.50b}$$

$$d\delta_{pl} = \beta \frac{dJ}{\sigma_o} g(\,) + \frac{\beta J}{\sigma_f} \frac{\partial g(\,)}{\partial a}\, da \tag{1.51b}$$

$$d\delta_M = \frac{\sigma_o BW}{K_M} \frac{\partial h(\,)}{\partial a}\, da \tag{1.52b}$$

Finally substituting (1.50b) through (1.52b) into (1.49) and rearranging gives

$$\frac{dJ}{da} \frac{E}{\sigma_o^2} = \frac{W}{\beta g(\,)} \frac{\partial}{\partial a} [h(\,) \cdot f(\,)] + \frac{EB}{K_M} \frac{\partial h(\,)}{\partial a} + \frac{\beta J E}{W \sigma_o^2} \frac{\partial g(\,)}{\partial a} \tag{1.55}$$

But (1.55) can be further simplified by noting that (with signs chosen for usual behavior):

$$-\frac{W}{g(\,)} \frac{\partial}{\partial a} [h(\,) \cdot f(\,)] = p\left(\frac{a}{W}, \frac{B}{W}, \frac{L}{W}, \text{ etc.}\right)$$

$$-\frac{W}{g(\,)} \frac{\partial h(\,)}{\partial a} = q\left(\frac{a}{W}, \frac{B}{W}, \frac{L}{W}, \text{ etc.}\right) \tag{1.56}$$

and

$$\frac{W}{g(\,)} \frac{\partial g(\,)}{\partial a} = r\left(\frac{a}{W}, \frac{B}{W}, \frac{L}{W}, \text{ etc.}\right)$$

Therefore substituting (1.56) into (1.55), the simplification leads to

$$T = \frac{dJ}{da}\frac{E}{\sigma_o^2} \leq \frac{1}{\beta}\left[p(\,) + \frac{EB}{K_M}q(\,) - \frac{JE}{W\sigma_o^2}r(\,)\right] \qquad (1.57)$$

as the general form for the tearing instability criterion for any specimen under fully plastic conditions.

All of the tearing instability criteria given in the first sections of [71] fit this general form, Equation (1.57). In those criteria a rigid testing machine was assumed, i.e. $K_M = \infty$, so the term with q( ) did not enter. Moreover, considering Equations (1.51) and (1.56) for most configurations, g( ) did not contain crack size, thus r( ) was zero; (except for the deeply cracked compact specimen where h( ) · f( ) did not contain crack size, thus p( ) was zero; and r( ) turns out positive thus assuring an always stable situation).

Moreover, even though the microcrack within the flow field ahead of the crack does not fit the physical model here as depicted by Figure 7, the criterion which resulted still fits the form of (1.57). Thus it is regarded as a very general result!

Finally, all of these tearing instability criteria have $T = \frac{dJ}{da}\frac{E}{\sigma_o^2}$ as a key material parameter in resisting tearing instability. Also note that the term with r( ) sometimes also enters as a partly geometrical term assisting resistance to tearing instability.

1.10 SUMMARY

In this discussion the J-integral method of analysis was presented as a direct extension of LEFM. Its role was examined showing its significance and applications. They can be summarized as follows.

1) The value of J is the numerical result of a line integral from the lower to the upper surface of a crack, independent of the particular path of integration.

2) J is the strength of the crack tip elastic plastic stress strain field singularity, thus it may be regarded as the characteristic parameter of said field.

3) J may be seen as the potential energy release rate per unit crack extension for the non-linear elastic counterpart of an elastic plastic material.

4) J may be interpreted as the difference in the work performed in deforming the body with two different crack lengths a and a+da (area between the two load displacement records).

5) J may be used as a fracture initiation criterion by reasoning that for a given material, equal J values mean equal intensities of geometrically identical surrounding crack tip stress strain fields. Thus, crack growth begins when a critical value of the strength of that field is attained.

6) J can be evaluated without great difficulty by numerical procedures using its line integral definition, or by methods using load-displacement diagrams.

7) J appears to be a good parameter to correlate crack growth data even for situations beyond the limits of strict applicability of deformation theory of plasticity.

8) J can be used for constructing material property J-R curves, as an extension of the G-R curves of LEFM, even for significant amounts of crack growth under certain restrictions. The J-R curves can also be used to analyze the conditions for instability of ductile tear.

2. THE ANALYSIS OF LOAD-DISPLACEMENT RELATIONSHIPS TO DETERMINE J-R CURVE AND TEARING INSTABILITY MATERIAL PROPERTIES

2.1 INTRODUCTION

This analysis is based on recent work of Hutchinson and Paris [49] and Paris et al. [71,72], which suggested that load-displacement records for pure bending could be analyzed to determine J-R curve and instability related material properties. However, here the analysis will be generalized and shown to be applicable to all configurations (2-D) and that it is especially useful for typical test configurations such as compact, 3 point bend, center cracked, etc. configurations. Some of these additional results have been presented in [73,74].

Indeed, the analysis to be presented is "exact", from an analytical viewpoint, and is based on dimensional considerations in the spirit of Rice-Paris-Merkle analysis [36] based on Rice's J-integral concepts [8]. The strict deformation theory of plasticity interpretation of J will be used here which has been shown to be "exact" under the size restrictions described by Hutchinson and Paris [28,49] for application to determining J-R curves and related material properties, and for structural applicatiions.

Finally, the analysis will lead to the following useful results:

(1) Correct (exact) methods for computing J from load-displacement records with crack growth present.

(2) Methods for determining crack length change, Δa, from load-displacement records (without further instrumentation).

(3) Using the results of (1) and (2), construction of J-R curves from load-displacement records alone.

(4) Moreover, material tearing instability properties, i.e. the tearing modulus, T_{mat}, may be determined from load-displacement records (without further instrumentation).

(5) Similarly, a system's tendency for tearing instability, T_{appl}, may be found from further analysis and load-displacement information from the system.

Therefore, the methods to be developed here are anticipated to have extensive applicability to J-R curve methods of determining material properties controlling crack extension and stability. Moreover, since only load-displacement records are required the methods ideally suited to solve certain special testing problems, such as hot cell testing of irradiated materials and/or dynamic testing (both of which present especially difficult problems if additional instrumentation is required).

A Note on Tearing Instability

The basis of the theory for stable or unstable crack growth were clearly set down by Paris et al. [71,72], and by Hutchinson and Paris [49], although here some of these concepts will be repeated as an introduction to the analysis of the next sections.

Consider a specimen (in plane strain or plane stress) with a crack length a, characterized by deformation theory.

As shown in Figure 10, let P be the generalized load per unit thickness acting on the specimen and let δ be the load-point displacement. The specimen is deformed in series with a linear spring of compliance C_M, that can be identified with the testing machine, and so let δ_{tot} be the total displacement or

$$\delta_{tot} = PC_M + \delta. \tag{2.1}$$

It is important at this point to make a distinction between the values of J lying on the material resistance J-R curve, and the applied values of J. The former will be called J_{mat} and will be regarded as a function of the crack length increment, Δa, only.

$$J_{mat} = J_{mat}(\Delta a)$$

The latter can be regarded as a function of load (or displacement) and the current crack length a ($a = a_o + \Delta a$), thus

$$J_{app} = J(a,P) = J(a,\delta)$$

At any stage of the deformation process, equilibrium requires that

$$J_{app} = J_{mat} \tag{2.2}$$

This analysis will be considered with the total load-point displacement, δ_{tot}, held fixed (or other similar condition specified), and so, following [49,71,72], stability will be ensured if

$$T_{app} = \frac{E}{\sigma_o^2}\left(\frac{\partial J}{\partial a}\right)_{\delta_{tot}} < \frac{E}{\sigma_o^2}\frac{dJ_{mat}}{da} = T_{mat} \tag{2.3}$$

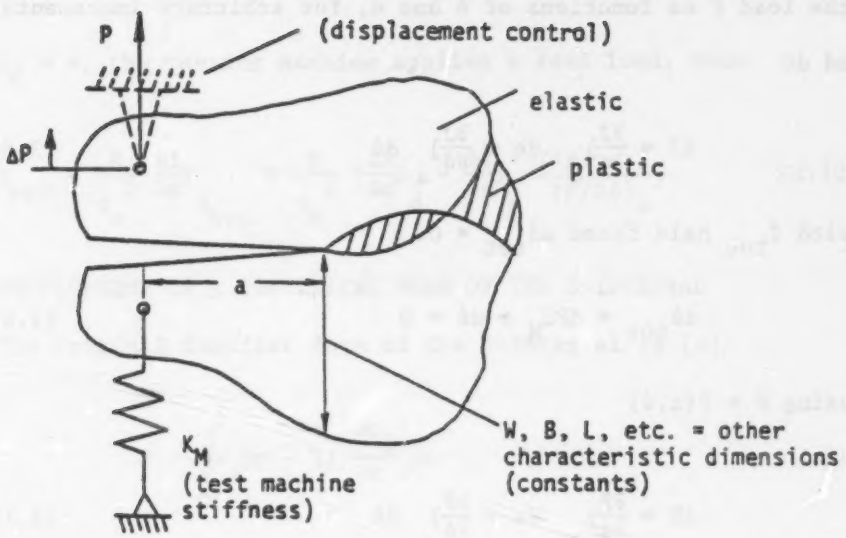

Fig. 10 An Arbitrary Configuration.

On the other hand, instability will occur if

$$T_{mat} < T_{app} \tag{2.4}$$

In the next sections, the applied tearing modulus T_{app} is calculated. A general expression for dJ is derived, by regarding J and the load P as functions of δ and a, for arbitrary increments in da and $d\delta$

$$dJ = \left(\frac{\partial J}{\partial a}\right)_{\delta} da + \left(\frac{\partial J}{\partial \delta}\right)_{a} d\delta \tag{2.5}$$

But with δ_{tot} held fixed $d\delta_{tot} = 0$.

$$d\delta_{tot} = dPC_M + d\delta = 0 \tag{2.6}$$

and using $P = P(a,\delta)$

$$dP = \left(\frac{\partial P}{\partial a}\right)_{\delta} da + \left(\frac{\partial P}{\partial \delta}\right)_{a} d\delta \tag{2.7}$$

Considering Equations (2.6) and (2.7)

$$\frac{d\delta}{da} = -\frac{C_M(\partial P/\partial a)\delta}{1 + C_M(\partial P/\partial \delta)_a} \tag{2.8}$$

And so dividing Equation (2.5) by da and using Equation (2.8)

$$T_{app} = \frac{E}{\sigma_o^2}\left(\frac{\partial J}{\partial a}\right)_{\delta_{tot}} = \frac{E}{\sigma_o^2}\left\{\left(\frac{\partial J}{\partial a}\right)_{\delta} - \left(\frac{\partial J}{\partial \delta}\right)_{a} \frac{(\partial P/\partial a)\delta}{\left[\frac{1}{C_M} + \left(\frac{\partial P}{\partial \delta}\right)_{a}\right]}\right. \tag{2.9}$$

If C_M is identified with the compliance of the testing machine, specialization to the two limiting cases ($C_M = 0$; $C_M \to \infty$) can be made. With $C_M = 0$, rigid testing machine, Equation (2.9) becomes

$$T_{app} = \frac{E}{\sigma_o^2} \left(\frac{\partial J}{\partial a}\right)_{\delta_{tot}} = \frac{E}{\sigma_o^2} \left\{\left(\frac{\partial J}{\partial a}\right)_{\delta}\right\} \tag{2.10a}$$

with $C_M \to \infty$, the testing machine applies a dead load, thus

$$T_{app} = \frac{E}{\sigma_o^2} \left(\frac{\partial J}{\partial a}\right)_{\delta_{tot}} = \frac{E}{\sigma_o^2} \left\{\left(\frac{\partial J}{\partial a}\right)_{\delta} - \left(\frac{\partial J}{\partial \delta}\right)_a \frac{(\partial P/\partial a)_\delta}{(\partial P/\partial \delta)_a}\right\} \tag{2.10b}$$

2.2 DEVELOPMENT OF A CONVENIENT FORM OF THE J-INTEGRAL

The original familiar form of the J-integral is [4]:

$$J = \int_C W_s dy - Ti \frac{\partial u_i}{\partial x} ds \tag{2.11}$$

which, based on deformation theory, is path independent when integrating around a crack tip, and can be equally well represented by the alternate forms [4]:

$$J = \int_0^P \left(\frac{\partial \delta}{\partial a}\right)_P dP = - \int_0^\delta \left(\frac{\partial P}{\partial a}\right)_\delta d\delta \tag{2.12}$$

where, δ is the work producing component of load point displacement for the load, P. It is noted that Equation (2.12) appropriately implies either $\delta = \delta(a, P)$ or $P = P(a, \delta)$ as functional relationships between the variables including the crack length, a, as the third variable.

In the analysis to follow here, it is convenient to divide J into elastic and plastic parts, J_{el} and J_{pl}. This is done by noting that for actual elastic-plastic situations the displacement, δ, may always be divided into its linear-elastic and nonlinear elastic (plastic) parts. That is

$$\delta = \delta_{el} + \delta_{pl} \tag{2.13}$$

Then the first form in Equation (2.2) may be written:

$$J = \int_0^P \left(\frac{\partial \delta_{el}}{\partial a}\right)_P dP + \int_0^P \left(\frac{\partial \delta_{pl}}{\partial a}\right)_P dP \tag{2.14}$$

Now the first term in Equation (2.14) is the linear-elastic component, J_{el}, of J, which is also the Griffith, G. That is

$$J_{el} = \int_0^P \left(\frac{\partial \delta_{el}}{\partial a}\right)_P dP = G(P, a) \tag{2.15}$$

Moreover, the second term in Equation (2.14), J_{pl}, may be reinterpreted by referring to Figure 11. This figure shows schematically load, P, vs. plastic displacement, δ_{pl}, curves for crack sizes a and a + da. The area between curves is noted to be $J_{pl}da$ by integrating over elements of the area by

$$J_{pl}(da) = \int_0^P \left(\frac{\partial \delta_{pl}}{\partial a}\right)_P dP(da) \tag{2.16}$$

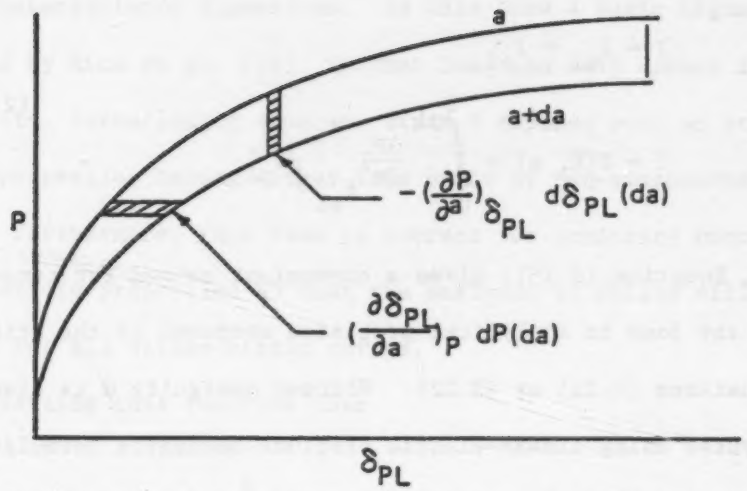

Fig. 11 Plastic part of J from P vs δ_{pl} record.

But using the alternate element, it is observed that two forms are equally appropriate, i.e.

$$J_{pl} = \int_0^P \left(\frac{\partial \delta_{pl}}{\partial a}\right)_P dP = -\int_0^{\delta_{pl}} \left(\frac{\partial P}{\partial a}\right)_{\delta_{pl}} d\delta_{pl} \qquad (2.17)$$

Now substituting Equations (2.15) and (2.17) into Equation (2.14), the result is:

$$J = J_{el} + J_{pl}$$

or

$$J = G(P, a) - \int_0^{\delta_{pl}} \frac{\partial P}{\partial a}\Big)_{\delta_{pl}} d\delta_{pl} \qquad (2.18)$$

This form, Equation (2.18), gives a convenient method for computing J without any loss in analytical precision compared to the original forms, Equations (2.11) or (2.12). Without ambiguity G is always to be computed using linear-elastic fracture mechanics formulas using the actual load, P, and crack length, a (without plastic zone correction). It remains to be shown here that the second term of Equation (2.18) may be appropriately evaluated.

2.3 DIMENSIONAL ANALYSIS OF RELATIONSHIPS BETWEEN LOAD, CRACK LENGTH AND PLASTIC DISPLACEMENT

Normally the plasticity in a cracked member of a specimen is confined to the remaining ligament at the cracked section. Thus in order to avoid certain ambiguities requiring some modifications in the analysis, plasticity confined to the ligament region is assumed here. Under this condition, dimensional analysis leads to the

following form for the relationship between load, P, crack length, a, and plastic displacement:

$$\frac{\delta_{pl}}{W} = f\left(\frac{P}{W}, \frac{a}{W}, \frac{L}{W}, \frac{B}{W}, \text{etc.}\right) \tag{2.19}$$

where P is taken as load per unit thickness, W is a typical characteristic (non-varying) dimension such as width, and L, B, etc. are other characteristic dimensions. In this form a basic argument, as proposed by Rice et al. [36], is that load can only appear as P/W with units, force/length squared, since f depends only on stress-strain properties having either like units or non-dimensional units. Furthermore, this form is correct for arbitrary monotonic stress-strain properties so that the analysis to follow will be "exact" for all stress-strain curves.

Inverting this function then

$$\frac{P}{W} = F\left(\frac{\delta_{pl}}{W}, \frac{a}{W}, \frac{L}{W}, \frac{B}{W}, \text{etc.}\right) \tag{2.20}$$

Now more appropriate forms for analysis can be found by defining the width of the remaining uncracked ligament, b, from other dimensions, such as W-a. Then either b/W or $(b/W)^2$ may be factored out of F( ) to give the special forms of Equation (2.20):

$$P = \frac{b^2}{W} F_1\left(\frac{\delta_{pl}}{W}, \frac{a}{W}, \frac{L}{W}, \frac{B}{W}, \text{etc.}\right) \tag{2.21a}$$

or

$$P = b\, F_2\left(\frac{\delta_{pl}}{W}, \frac{a}{W}, \frac{L}{W}, \frac{B}{W}, \text{etc.}\right) \tag{2.21b}$$

Indeed, an additional form which is equally appropriate dimensionally and similar to Equation (2.21b) is

$$P = b\, F_3\left(\frac{\delta_{pl}}{b}, \frac{a}{W}, \frac{L}{W}, \frac{B}{W}, \text{ etc.}\right) \qquad (2.21c)$$

Now it will be shown that these forms, in combination with Equation (2.18) will lead to significant results. Indeed, all of the results in [3], as well as important new results will follow.

2.4 ANALYSIS TO DETERMINE J USING THE FIRST SPECIAL FUNCTIONAL FORM, F_1

The first functional form, Equation (2.21a) may be substituted into Equation (2.18), noting that db = - da, to give:

$$J = G + \frac{2b}{W}\int_0^{\delta_{pl}} F_1(\ )\, d\delta_{pl} - \frac{b^2}{W^2}\int_0^{\delta_{pl}} \frac{\partial F_1}{\partial\left(\frac{a}{W}\right)}\, d\delta_{pl} \qquad (2.22)$$

Resubstituting for $F_1(\ )$ from Equation (2.21a) into the first integral of Equation (2.22) leads to

$$J = G + \frac{2}{b}\int_0^{\delta_{pl}} P\, d\delta_{pl} - \frac{b^2}{W^2}\int_0^{\delta_{pl}} \frac{\partial F_1}{\partial\left(\frac{a}{W}\right)}\, d\delta_{pl} \qquad (2.23a)$$

or using the total area under the load displacement record

$$A = \int_0^{\delta_{pl}} P d\delta_{pl} + \frac{P^2 C}{2}$$

The expression for J becomes

$$J = \underbrace{\frac{2A}{b}}_{\text{Rice's term}} + \underbrace{\left[\left(G - \frac{P^2C}{b}\right) - \frac{b^2}{w^2}\int_0^{\delta_{pl}} \frac{\partial F}{\partial a/w}\, d\delta_{pl}\right]}_{\text{Correction term}} \qquad (2.23b)$$

Where A is the area upon the load-displacement record. It is noted that Equation (2.23) is an exact form for computing J from any load displacement record but prior to the initiation of crack growth. Indeed, it is observed that the first term in Equation (2.23 the usual Rice et al. [36] area under the load-displacement curve (work) with the normal 2/b coefficient and the second is a correction term, which is however, in Equation (2.23b), "exact".

Now Equations (2.23) may be used to evaluate J for any configuration, however, as will be discussed later, it is best applied when the correction term, the final integral, is small compared to the others, which in this case will be the situation where the uncracked ligament is subject principally to bending.

In developing J-R curves it is appropriate to extend this analysis to the situation where crack growth has commenced. In order to do that it is most clearly accomplished by taking the differential of Equation (2.22), noting that the integral terms are functions of the independent variables, the crack size, a or b, and the plastic displacement, δ_{pl}. The differential of Equation (2.22) is thus:

$$dJ = dG + \left[\frac{2b}{W} F_1 - \frac{b^2}{W^2} \frac{F_1}{\partial(\frac{a}{W})}\right] d\delta_{pl}$$

$$+ \left[-\frac{2}{W}\int_0^{\delta_{pl}} F_1(\ )\, d\delta_{pl} + \frac{4b}{W^2}\int_0^{\delta_{pl}} \frac{\partial F_1}{\partial(\frac{a}{W})}\, d\delta_{pl}\right.$$

$$\left. - \frac{b^2}{W^3}\int_0^{\delta_{pl}} \frac{\partial^2 F_1}{\partial(\frac{a}{W})^2}\, d\delta_{pl}\right] da \qquad (2.24)$$

Now it is convenient for integration of Equation (2.24) to first define $\tilde{J}_{pl}$ as the last two terms in Equation (2.22), i.e. it is J_{pl} computed as if no crack growth occurred, or

$$\tilde{J}_{pl} = \frac{2b}{W}\int_0^{\delta_{pl}} F_1 d\delta_{pl} - \frac{b^2}{W^2}\int_0^{\delta_{pl}} \frac{\partial F_1}{\partial(\frac{a}{W})}\, d\delta_{PL} \qquad (2.15)$$

Reintegrating Equation (2.24) with crack growth from the initial crack size, a_o, to a size, a, and plastic displacement 0 to δ_{pl} is appropriate over any path, which gives

$$\tilde{J} = G + \tilde{J}_{pl}\Big|_{b=b_o} + \int_{a_o}^{a} \frac{1}{b}\left[-\tilde{J}_{pl} + \frac{3b^2}{W^2}\int_0^{\delta_{pl}} \frac{\partial F_1}{\partial(\frac{a}{W})}\, d\delta_{pl}\right.$$

$$\left. - \frac{b^3}{W^3}\int_0^{\delta_{pl}} \frac{\partial^2 F_1}{\partial(\frac{a}{W})^2}\, d\delta_{pl}\right] da \qquad (2.26)$$

It is to be noted that Equations (2.23) also applies for a growing crack if the terms are interpreted in a somewhat different manner. In fact if b is the actual (final) length of the remaining ligament

and the integrals are taken along the curve that would have had a cracked specimen initially with that b (or crack length a), Equation (2.22) still applies. But that curve is not known in general since it is not the actual load displacement record.

However, Equation (2.26) in combination with Equation (2.25), defines an exact method of computing J in any configuration. The actual load displacement record may be used to obtain F_1. Applied in a general way, it could be very complicated to compute in terms involving F_1 in Equations (2.25) and (2.26). However, in applications to be cited here, the cases will be restricted to situations where the second term in Equation (2.25) is small compared to the first and in such cases it will be possible to ignore the terms in Equation (2.26) explicitly containing F_1.

2.5 DETERMINATION OF CRACK LENGTH CHANGE AND T USING THE FIRST SPECIAL FUNCTIONAL FORM

Equation (2.21a), the first form, expresses the load, P, as a function of crack length a or b and plastic displacement, δ_{pl}, and other fixed quantities. Forming the differential of P, it is

$$dP = \frac{b^2}{W^2} \frac{\partial F_1}{\partial(\frac{\delta_{pl}}{W})} d\delta_{pl} + \left[\frac{b^2}{W^2} \frac{\partial F_1}{\partial(\frac{a}{W})} - \frac{2b}{W} F_1\right] da \qquad (2.27)$$

Solving this expression for the crack length change, da, it is

$$da = \frac{\frac{b^2}{W^2} \frac{\partial F_1}{\partial(\frac{\delta_{pl}}{W})} d\delta_{pl} - dP}{\frac{2b}{W} F_1 - \frac{b^2}{W^2} \frac{\partial F_1}{\partial(\frac{a}{W})}} \qquad (2.28)$$

or noting that

$$\delta_{el} = PC \qquad \text{where C is the compliance of the cracked specimen}$$

and

$$d\delta_{el} = dPC + \frac{PC'}{W}da$$

$$d\delta_{pl} = d\delta - d\delta_{el}$$

Equation (2.28a) can be rewritten as

$$da = \frac{\left(\frac{b^2}{W^2}\frac{\partial F}{\partial \delta_{pl}/W}\right)d\delta + \left(1 + \frac{b^2}{W^2}\frac{\partial F}{\partial a/W}C\right)dP}{\frac{2b}{W}F + \frac{b^2}{W^2}\frac{\partial F}{\partial a/W}PC' - \frac{b^2}{W^2}\frac{\partial F}{\partial a/W}} \qquad (2.28b)$$

Assuming that F_1 and the initial remaining ligament, b, are known, the crack length change can be found during an increment along a load-displacement record, dP and $d\delta_{pl}$ or $d\delta$. Note also Figure 12 that da can be calculated by comparing points as A and B for which the δ is the same, so $d\delta = 0$. Then Equation (2.28b) is further simplified to give

$$da = \frac{\left(1 + \frac{b^2}{W^2}\frac{\partial F}{\partial a/W}C\right)dP}{\frac{2b}{b}F + \frac{b^2}{W^2}\frac{\partial F}{\partial a/W}\left(\frac{PC'}{W} - 1\right)} \qquad (2.28c)$$

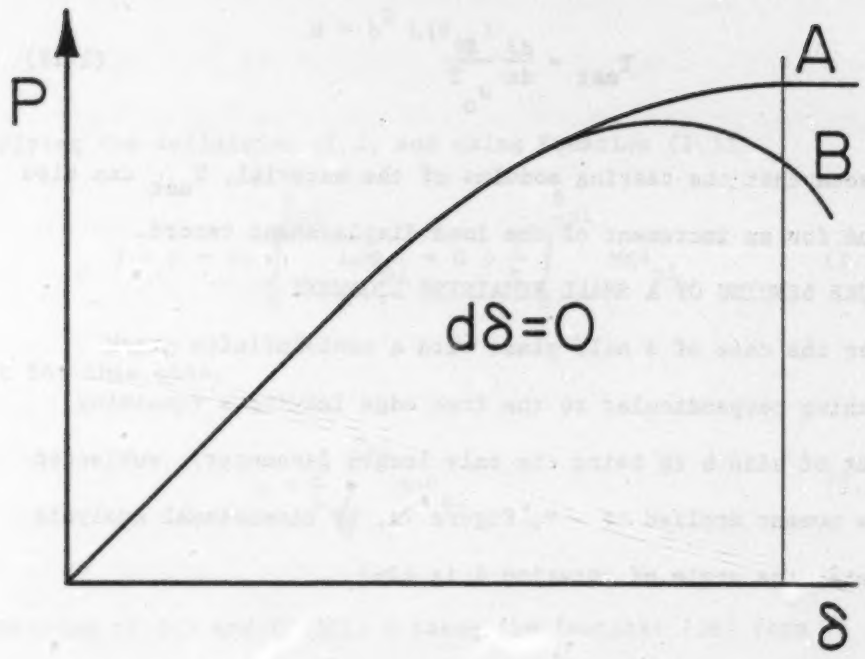

Fig. 12 Points at same displacement in a P vs δ record.

where all quantities are taken at point A and dP is the difference in load between points A and B.

During the increment, dJ can also be found using Equation (2.24). Substituting the results from Equation (2.24) and (2.28) into the definition of the tearing modulus i.e.

$$T_{mat} = \frac{dJ}{da} \frac{E}{\sigma_o^2} \tag{2.29}$$

It is seen that the tearing modulus of the material, T_{mat} can also be found for an increment of the load displacement record.

2.6 PURE BENDING OF A SMALL REMAINING LIGAMENT

For the case of a half plane with a semi-infinite crack approaching perpendicular to the free edge leaving a remaining ligament of size b (b being the only length parameter), subjected to pure moment applied at $-\infty$, Figure 7a, by dimensional analysis arguments, the angle of rotation θ is [36]

$$\theta = \theta\left(\frac{M}{b^2}, \text{ mat prop}\right) \text{ or } M = b^2 H(\theta) \tag{2.30}$$

Now it can be noted [30] that for the elastic part of the angle θ_{el}, a similar functional form holds

$$\theta_{el} = \theta_{el}\left(\frac{M}{b^2}\right) \tag{2.31}$$

So from Equations (2.30) and (2.31), the plastic part θ_{pl} must also be a function of the same variable M/b^2

$$\theta_{pl} = \theta - \theta_{el} = f\left(\frac{M}{b^2}\right) \tag{2.32}$$

or inverting

$$M = b^2\, s(\theta_{el}) \qquad M = b^2\, L(\theta_{pl}) \tag{2.33}$$

Applying the definition of J, and using Equation (2.33)

$$J = G + 2b \int_0^{\theta_{pl}} L d\theta_{pl} = G + \frac{2}{b} \int_0^{\theta_{pl}} M d\theta_{pl} \tag{2.34}$$

But for this case,

$$G = \frac{2}{b} \int_0^{\theta_{el}} M d\theta_{el} \tag{2.35}$$

Combining (2.34) and (2.35), J takes the familiar [36] form

$$J = \frac{2}{b} \int_0^{\theta} M d\theta = \frac{2}{b} \text{ Area} \tag{2.36}$$

Moreover, Equation (2.34) becomes upon differentiation

$$dJ = dG + [2b\, F_1] d\theta_{pl} + \left[-\frac{2}{b^2} \int_0^{\theta_{pl}} F_1 d\theta_{pl}\right] da$$

or

$$dJ = 2b\, L d\theta - \frac{J}{b}\, da \tag{2.37}$$

Reintegrating to give a result analogous to (2.26) leads to

$$J = 2b_o \int_0^{\theta} \frac{M}{b^2}\, d\theta - \int_{a_o}^{a} \frac{J}{b}\, da \tag{2.38}$$

The analogue of Equation (2.28) becomes

$$da = \frac{b \frac{\partial L}{\partial \theta}\, d\theta - \frac{dM}{b}}{dL} \tag{2.39}$$

and hence Equations (2.34) and (2.36) can be substituted into (2.29) to give

$$T_{mat} = \frac{E}{\sigma_o^2} \frac{dJ}{da} = \frac{E}{\sigma_o^2} \left[\frac{4b^2 L^2}{b^2 \frac{\partial L}{\partial \theta} - \frac{dM}{d\theta}} - \frac{J}{b} \right] \tag{2.40}$$

Therefore, given F_1, it is noted that Equation (2.39) can be used to compute crack length changes increment by increment along a load-displacement (M vs. θ) record. Then Equation (2.38) may be used to compute J and Equation (2.40) may be used to obtain T_{mat} at any point on the record. These results for pure bending were obtained in [49,71,72] and in both, a simple experimental method of determining them was discussed. Of course L could also be determined by analytical methods, such as finite element method, using the stress-strain curve for the material to which the present analysis is applied. It is emphasized that this analysis, Equations (2.37) through (2.40) is exact, independent of material property assumptions for this example case of pure bending.

This example, pure bending, has been given because it produces the simplest results and is most likely to be familiar to the reader. However, more important is the application of these procedures to configurations which will be used for testing or the analysis of structural cracking problems. In such applications for any configuration any one of the special forms, Equations (2.21a), (2.21b) or (2.21c) may be used. However, careful choice of the form, for most configurations, will lead to much more practical results. Moreover, the proper procedures for applying the results to load-displacement record analysis bears further comments here.

2.7 THE COMPACT SPECIMEN

For a compact specimen which is deeply cracked, say $a/W \geq 0.8$, the remaining ligament, $b(=W-a)$, is subjected to substantially pure bending with other planar dimensions, a, W, H, etc. very large compared to b. In this case the analysis of pure bending in the preceding section may be applied with reasonable accuracy. However, in such applications J must be computed using analysis, such as Equation (2.38), where the second integral is required to correct for the effects of crack growth on J. This correction has not been used throughout the previous literature except for [49,71, 86]. Indeed, the reader is cautioned that J-R curves in the literature are only approximately correct and that their slopes, dJ/da, for the crack growth portion may be in error by 20 to 30% due to neglect of this correction term in previous work. Thus, it is clear that more careful analysis is warranted in even the simplest cases and specially those used in testing, where materials

properties so evaluated will reside permanently in the published literature. It is relevant then to proceed with a general analysis of the compact specimen for all a/W values and neglect terms only where they are justifiably small compared to others.

In general the remaining ligament of a compact specimen is subjected mostly to bending but also to a moderate axial force which cannot be entirely neglected. For such cases where bending is a dominant factor, the use of the first special functional form, F_1, as defined by Equation (2.21a) is most appropriate. This is because in applying the analysis using that form, Equations (2.22) through (2.29), the terms involving derivatives with respect to a/W of F_1 will be weak, i.e. considerably smaller than the main terms. It will be noted here that some of these terms may then be neglected justifiably to simplify the analysis.

Reviewing the analysis, Equations (2.22) through (2.29), they will be repeated with appropriate modifications for the compact specimen. First for the determination of J <u>prior to crack growth</u> Equations (2.23) and (2.25) may be used, hence

$$J = G + \tilde{J}_{pl}$$

where

$$\tilde{J}_{pl} = \frac{2}{b_o} \int_0^{\delta_{pl}} P d\delta_{pl} - \frac{b_o^2}{W^2} \int_0^{\delta_{pl}} \frac{\partial F}{\partial (\frac{a}{W})} \, d\delta_{pl} \qquad (2.41)$$

Now the second term in Equation (2.41) involving $\partial F_1 / \partial (\frac{a}{W})$ is, as noted previously, a correction type term which is known to be smaller than other terms but which disappears only at very high a/W

values. Now this term cannot be neglected in Equation (2.41) but if the computation of J with growing cracks is considered using Equation (2.26). Then it is noted that the integral term in Equation (2.26) is small compared to other terms and within that integral the terms in the integrand involving explicitly the derivations of F_1 are small compared to J_{pl}. Thus their effect on the overall J can be neglected. That is to say that with small amounts of crack growth present compared to the ligament size, b, Equation (2.26) may simplified for compact specimens to give

$$J = G + \tilde{J}_{pl} - \int_{a_o}^{a} \frac{\tilde{J}_{pl}}{b} \, da$$

where (as before)

$$\tilde{J}_{pl} = \frac{2b_o}{W} \int_0^{\delta_{pl}} F_1 d\delta_{pl} - \frac{b_o^2}{W^2} \int_0^{\delta_{pl}} \frac{\partial F_1}{\partial (\frac{a}{W})} d\delta_{pl} \qquad (2.42)$$

(for all small Δa, $0 \leq \Delta a << b$)

Now the limitation of Equation (2.41) to small Δa is no loss in generality, since J-controlled crack growth is restricted to small crack length changes [49]. That is to say that for large amounts of crack growth, J-controlled crack tip fields disappear so that J analysis itself tends to become inappropriate.

Therefore, Equation (2.42) is a general form which may be used to compute J accurately in compact specimens. It is noted that two types of "correction terms" exist, i.e. the last terms of both parts of Equation (2.42). The term involving $\partial F_1/\partial(\frac{a}{W})$ is similar

to the Merkle-Corten correction now in use [67], but F_1 obviously depends on material properties and is thought to be strongly influenced by hardening, etc. The conclusion here is that until demonstrated otherwise, Equation (2.42) or its equivalent is the only sure way to obtain accurate J values from compact specimen results.

In order to evaluate increments of crack length change, da, in compact specimens, Equation (2.28) may be used without modification. It is, again

$$da = \frac{\frac{b^2}{W^2}\frac{F_1}{\partial(\frac{\delta_{pl}}{W})}d\delta_{pl} - dP}{\frac{2b}{W}F_1 - \frac{b^2}{W^2}\frac{\partial F_1}{\partial(\frac{a}{W})}} \qquad (2.43)$$

It is likely that the term in the denominator with $\partial F_1/\partial(\frac{a}{W})$ will be negligible, but it is carried here for further evaluation. At this point it is seen that Equations (2.42) and (2.43) are sufficient to evaluate crack length changes, da, and J, so that J-R curves may be constructed, given F_1 and a load-displacement record. Subsequently, the means of evaluating F_1 shall be discussed. However, first it is relevant to develop the procedure to directly evaluate T_{mat}.

Adopting the usual definition of T_{mat}, see Equation (2.29), the remaining component required is dJ. This is obtained most directly by differentiating Equation (2.42) and referring to earlier expressions such as Equation (2.24). The simplest format neglecting terms appropriately is:

$$dJ = dG + \left[\frac{2b}{W} F_1 - \frac{b^2}{W^2} \frac{\partial F_1}{\partial(\frac{a}{W})}\right] d\delta_{pl} - \left[\frac{2}{W} \int_0^{\delta_{pl}} F_1 \, d\delta_{pl}\right] da \quad (2.44)$$

Then using Equation (2.29), and substituting Equations (2.43) and (2.44), T_{mat} becomes

$$T_{mat} = \frac{E}{\sigma_o^2}\left[\frac{dG}{da} + \frac{\left[\frac{2b}{W} F_1 - \frac{b^2}{W^2} \frac{\partial F_1}{\partial(\frac{a}{W})}\right]^2}{\frac{b^2}{W^2} \frac{\partial F_1}{\partial(\frac{\delta_{pl}}{W})} - \frac{dP}{d\delta_{pl}}} - \frac{2}{W} \int_0^{\delta_{pl}} F_1 d\delta_{pl}\right] \quad (2.45)$$

Therefore, for a compact specimen Equations (2.42) through (2.45) are not only sufficient to construct a J-R curve, but also to evaluate T_{mat} directly at any point of a load displacement record, if F_1 and its derivatives, $\partial F_1/\partial(\frac{\delta_{pl}}{W})$ and $\partial F_1/\partial(\frac{a}{W})$, are known.

2.8 DETERMINATION OF F_1 AND ITS DERIVATIVES FOR COMPACT SPECIMENS

As defined by Equation (2.21a), F_1 is the relationship between load and plastic displacement, for a given set of specimen proportions, including a/W, and for a given material's stress-strain curve. Then it is evident that one way to obtain the function, F_1, is analytically through finite element method or other such methods. For example, it would be relevant to tabulate this function and its derivatives for common test configurations, such as the standard compact specimen, for Ramberg-Osgood stress-strain curves of various hardening coefficients, n.

However, it is also possible to experimentally determine F_1 and its derivatives for the actual material to be considered in a reasonably practical way. The procedure shall be described here.

More specifically it is assumed that a single load-displacement record is to be used to determine a material's crack growth properties. But in order to calibrate the method, i.e. to determine F_1 and its derivatives, then assume a few sub-size specimens of the same material are also available, where the sub-size specimens are made in exactly the same dimensional proportions as the full-size specimen, except their initial a/W values vary slightly from that of the full-size specimen to larger values. Now let all of the load-displacement records from these specimens be plotted on the basis of $\frac{PW}{b_o^2}$ vs. $\frac{\delta}{W}$ as shown on Figure 13a. The elastic parts of the displacement on Figure 13a may be noted, using initial slopes for each of the specimens, to develop Figure 13b a plot of $\frac{PW}{b_o^2}$ vs. $\frac{\delta_{pl}}{W}$ in which case $\frac{PW}{b_o^2}$ is F_1. Now the sub-sized specimens will go to larger deformations, $\frac{\delta_{PL}}{W}$, prior to having crack growth occur. Therefore, each plot of data from a sub-sized specimen is F_1 associated with its a/W value up to its own initiation of crack extension. Furthermore, the slopes of the sub-sized specimen curves give $\partial F_1/\partial(\frac{\delta_{pl}}{W})$ and the spacing of curves will give $\partial F_1/\partial(\frac{a}{W})$. Therefore, all of the information on F_1 required for analysis using Equations (2.42) through (2.45) is available. Then the full-size specimen's load displacement curve may be analyzed fully using Equations (2.42) through (2.45), integrating along this curve increment by increment as indicated by the equations to determine J, Δa and T_{mat} which can then be used to plot a J-R curve if desired.

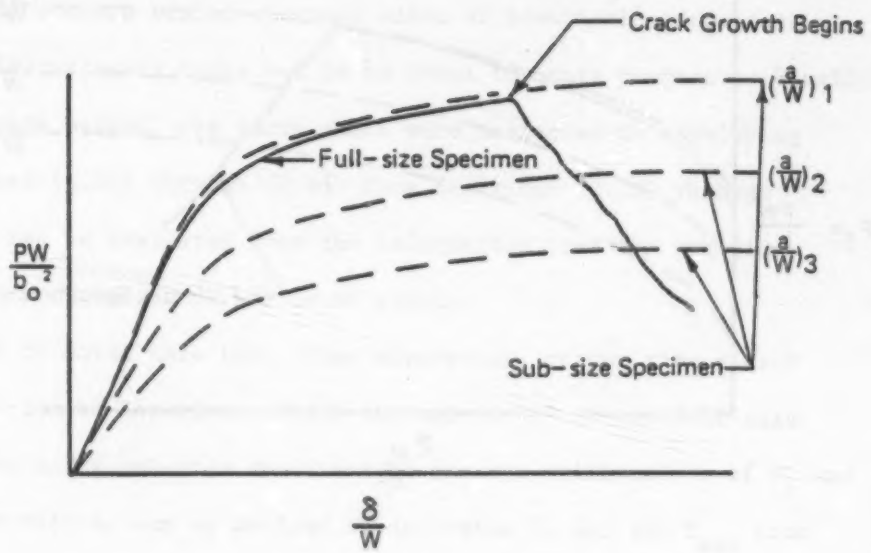

Fig. 13.a F - function vs normalized displacement.

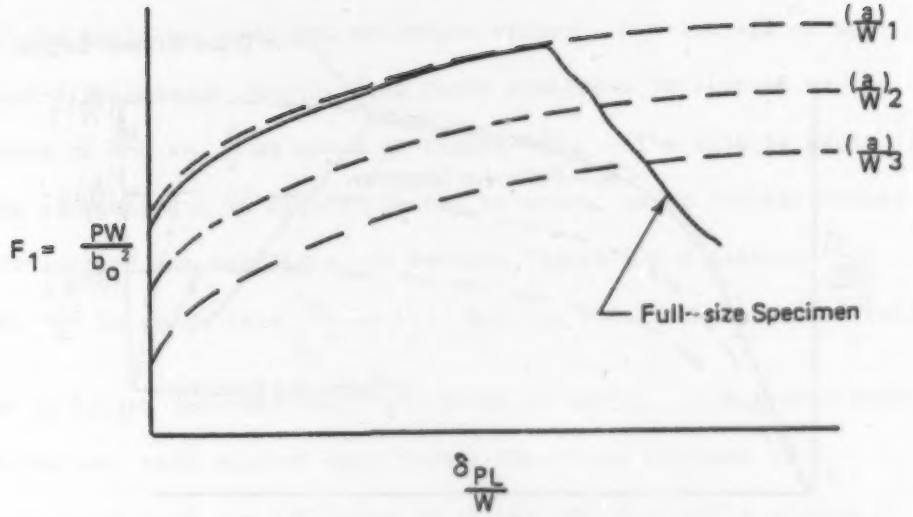

Fig. 13 b F - function vs normalised plastic displacement.

All of the theory behind this procedure is exact. It is calibrated for the actual material tested employing exactly the same degree of plane stress vs. plane strain in the sub-size specimens of the identical proportion and material. (Indeed, after testing a full-size compact specimen, the broken halves contain enough material to make four sub-size specimens just slightly smaller than half size.) (Moreover, many reactor surveillance programs contain scaled specimen sizes of identical proportions which fortuitously turns out to be ideal for this purpose.) Finally, using this method, the terms which were neglected in developing Equations (2.42) through (2.45) from Equations (2.22) through (2.29) can be evaluated from the information from the sub-size specimens technique if any doubt exists.

It is noted here that other approaches, rather than direct application of Equations (2.42) through (2.45) to the full-size specimen using sub-size specimens as passive calibrations of F_1 and its derivatives can be devised to determine J, Δa, and T_{mat} from this test information. However, each makes less than maximum use of information from the full-size specimen and therefore, is regarded as less precise. Finally, it is noted that a set of full-size specimens when tested can be used to calibrate each other, (i.e. determine F_1 and derivatives without sub-size specimens), but this would be less than precise if points of beginning of crack extension, etc. were not clearly distinguishable. The practical aspects of such short cuts are to be left to experimental programs.

In summary, for evaluation of a material's cracking properties from compact specimens, the calibration method described here along with Equations (2.42) through (2.45) forms a precise and practical basis for determining J, Δa, T_{mat}, etc. from nothing more than load-displacement records. Since other methods require costly additional instrumentation, etc., this method shows great promise.

2.9 BENDING TEST SPECIMENS OF THE 3-POINT AND 4-POINT BENDING TYPE

For typical bend test specimens with a/W large enough so that plasticity is confined to the remaining ligament region, the analysis in the preceding sections on compact specimens also applies. However, all terms involving $\partial F_1/\partial(\frac{a}{W})$ become very weak and can be neglected within normal accuracy requirements. Thus simply repeating Equations (2.42) through (2.45), deleting these terms, the results are:

$$J = G + \tilde{J}_{pl} - \int_{a_o}^{a} \frac{\hat{J}_{pl}}{b} \, da$$

where

$$\hat{J}_{pl} = \frac{2}{b_o} \int_0^{\delta_{pl}} P d\delta_{pl} \tag{2.46}$$

and

$$da = \frac{\frac{\omega^2}{W^2} \frac{\partial F_1}{\partial(\frac{\delta_{pl}}{W})} d\delta_{pl} - dP}{\frac{2b}{W} F_1} \tag{2.47}$$

and

$$T_{mat} = \frac{E}{\sigma_o^2}\left[\frac{dG}{da} + \frac{\left[\frac{2b}{W} F_1\right]^2}{\frac{b^2}{W^2}\frac{\partial F_1}{\partial(\frac{\delta_{pl}}{W})} - \frac{dP}{d\delta_{pl}}} - \frac{2}{W}\int_0^{\delta_{pl}} F_1 d\delta_{pl}\right] \qquad (2.48)$$

using Equations (2.46) through (2.48) and a single sub-size specimen to determine F_1, the evaluation procedures described in the previous section hold to determine J, Δa, T_{mat}, etc. from a load-displacement record of a full-size specimen. On the other hand, if doubt exists on the precision or deleting terms containing $\partial F_1/\partial(\frac{a}{W})$ here, then the previous analysis, Equations (2.42) through (2.45) can be employed in full (with further sub-size specimens required) to evaluate the effect of neglecting these terms.

It seems relevant to point out here that the final form of Equation (2.33), for 3-point bending, has been erroneously used in the past. In this connection it should be noted that the first form of Equation (2.46) contains G and that it must be modified for 3-point bending of a finite specimen whereas the plastic term remains reasonably accurate (based on θ_{crack}). The errors were the result of the inappropriate use of linear-elastic components of the analyses. Moreover, it is also noted here that in developing J-R curves from bending tests, the final term in Equation (2.46), correcting for the effect of crack growth has been neglected throughout the literature.

2.10 APPLICATIONS TO PREDOMINATELY TENSION LOADING

Any of the three special functional forms, Equations (2.21a), (2.11b) and (2.11c) may be applied to any 2-dimensional configuration.

Therefore for predominately tension, the form F_1 and its associated analysis, Equations (2.22) through (2.29), could be correctly employed. However, in that analysis the terms involving $\partial F_1/\partial(\frac{a}{W})$ and its second derivative as well, would become dominant and difficult to evaluate accurately. Thus for configurations subjected principally to tension, it is equally correct but significantly more practical to apply the alternate forms F_2 and/or F_3.

The latter form, F_3, is of substantial advantage because its dependence on a/W is anticipated to be very weak. In fact, when the remaining ligament, b, is very small compared to other dimensions, W, L, a, etc., F_3 is a function only of δ_{pl}/b and other variables disappear, as discussed originally in [36]. Consequently the further discussion here will be centered on the functional form, F_3, from Equation (2.21c).

Substituting Equation (2.21c) into Equation (2.8) gives

$$J = G + \int_0^{\delta_{pl}} \left\{ F_3 d\delta_{pl} - \frac{1}{b} \int_0^{\delta_{pl}} \frac{\partial F_3}{\partial \delta_{pl}/b} \delta_{pl} \right\} d\delta_{pl} - \frac{b}{W} \int_0^{\delta_{pl}} \frac{\partial F_3}{\partial a/W} d\delta_{pl} \tag{2.49}$$

$$J = G + \frac{2}{b} \left\{ \int_0^{\delta_{pl}} P d\delta_{pl} - \frac{P\delta_{pl}}{2} \right\} - \frac{b}{W} \int_0^{\delta_{pl}} \frac{\partial F_3}{\partial a/W} d\delta_{pl} \tag{2.50}$$

These results Equation (2.49 and (2.50) are analogous to Equation (2.22) and (2.23) and so upon comparison we note that the first three terms coincide with the result of [36], which was obtained for a very small remaining ligament b. The last term can be

thought of as a correction term which takes into account the fact that b is comparable with other dimensions. Obviously this term tends to zero as a/W tends to 1, and in general, as was mentioned before, F_3 is expected to be a weak dependent function on a/W.

The analysis is continued as with Equation (2.24) through (2.29), hence:

$$dJ = dG + \left\{ F - \frac{1}{b} \frac{\partial F_3}{\partial \delta_{pl}/b} \cdot \delta_{pl} - \frac{b}{W} \frac{\partial F_3}{\partial a/W} \right\} d\delta_{pl}$$

$$+ \left\{ \frac{2}{W} \int_0^{\delta_{pl}} \frac{\partial F_3}{\partial a/W} \, d\delta_{pl} + \frac{1}{b^2} \int_0^{\delta_{pl}} \frac{\partial F_3}{\partial \delta_{pl}/b} \, \delta_{pl} d\delta \right. \qquad (2.51)$$

$$\left. - \frac{b}{W} \int_0^{\delta_{pl}} \frac{\partial^2 F_3}{\partial \delta_{a/W^2}} \, d\delta_{pl} \right\} da$$

and

$$J = G + \int_0^{\delta_{pl}} \left(F_3 - \frac{1}{b} \frac{\partial F_3}{\partial \delta_{pl}/b} \, \delta_{pl} - \frac{b}{W} \frac{\partial F_3}{\partial a/W} \right) d\delta_{pl}$$

$$+ \int_{a_o}^{a} \left(\frac{2}{W} \int_0^{\delta_{pl}} \frac{\partial F_3}{\partial a/W} \, d\delta + \frac{1}{b^2} \int_0^{\delta_{pl}} \frac{\partial F_3}{\partial \delta_{pl}/b} \, d\delta_{pl} \right. \qquad (2.52)$$

$$\left. - \frac{b}{W} \int_0^{\delta_{pl}} \frac{\partial^2 F_3}{\partial a/W^2} \, d\delta_{pl} \right) da$$

and

$$dP = -F_3\,da + \frac{b}{W}\frac{\partial F_3}{\partial a/W}\,da + \frac{F_3}{\partial \delta_{pl}/b}\,d\delta_{pl} - \frac{1}{b^2}\,\frac{\partial F_3}{\partial \delta_{pl}/b}\,\delta_{pl}\,da \tag{2.53}$$

or

$$da = \frac{\dfrac{\partial F_3}{\partial \delta_{pl}/b}\,d\delta_{pl} - dP}{F_3 - \dfrac{b}{W}\dfrac{\partial F_3}{\partial a/W} + \dfrac{1}{b}\dfrac{\partial F_3}{\partial \delta_{pl}/b}\,\delta_{pl}} \tag{2.54}$$

where

$$T_{mat} = \frac{E}{\sigma_o^2}\frac{dJ}{da}$$

As before, if Equations (2.49) through (2.54) are applied to center crack or double edge notch specimen where little or no bending is present, terms containing $\partial^2 F_3/\partial(a/W)^2$ in (2.49) and (2.50) can be neglected and the influence of the $\partial F_3/\partial a/W$ term in the denominator will be small in some circumstances for certain computations. Thus a simplification of these equations for some practical cases is possible. Moreover, in such cases, experimental procedures very much like those suggested in the preceding section on determination of F_1 and its derivatives for compact specimens are appropriate. However, that analysis and subsequent experimental procedures are so similar to the preceding discussion they are not repeated here.

2.11 THE EXTERNALLY NOTCHED ROUND BAR IN TENSION

For deeply externally notched round bar of radius R, leaving a circular neck of radius r, subjected to an applied centered tension force P, the displacement between load points is [36].

$$\frac{\delta}{r} = f_4\left(\frac{P}{r^2}\right) \tag{2.55}$$

Now if the assumption of deep crack is removed and plasticity is assumed to be confined to the remaining ligament, a functional relationship similar to Equation (2.19) holds

$$\frac{\delta_{pl}}{r} = f_4\left(\frac{P}{r^2},\ a/W\right) \tag{2.56}$$

or inverting

$$P = r^2\, F_4\left(\frac{\delta_{pl}}{r},\ r/R\right) \tag{2.57}$$

So repeating the analysis in Equation (2.12) through (2.19),

$$J = G + \frac{1}{2\pi r}\int_0^{\delta_{pl}} \left(\frac{\partial P}{\partial r}\right)_{\delta_{pl}} d\delta_{pl} \tag{2.58}$$

$$J = G + \frac{1}{2\pi}\left\{3\int_0^{\delta_{pl}} F_4\, d\delta_{pl} - F_4\delta_{pl} + \frac{r}{R}\int_0^{\delta_{pl}} \frac{\partial F_4}{\partial r/R}\, d\delta_{pl}\right\} \tag{2.59a}$$

$$\text{or}\quad J = G + \frac{1}{2\pi}\left\{\frac{1}{r^2}\left(3\int_0^{\delta_{pl}} P d\delta_{pl} - P\delta_{pl}\right) + \frac{r}{R}\int_0^{\delta_{pl}} \frac{\partial F_4}{\partial r/R}\, d\delta_{pl}\right\} \tag{2.59b}$$

It is to be noted that J can also be obtained by differentiation and further integration of Equation (2.59a) as was done previously for other configurations, i.e. Equation (2.44) or (2.51). For

this case the crack length increment -dr can be obtained by differentiation of Equation (2.57) giving

$$-dr = \frac{r \frac{\partial F_4}{\partial r/R} d\delta - dP}{2r F_4 - \frac{\partial F_4}{\partial \delta_{pl}/r} \frac{1}{r^2} + \frac{\partial F_4}{\partial r/R} \frac{1}{R}} \tag{2.60}$$

The T_{mat} can be also obtained by differentiation of Equation (2.59a) and combining it with (2.60).

Internally Notched Bar

For the case of a round bar of radius R, with an internal notch of radius r, leaving an annular remaining ligament of width b (b=R-r) the analysis follows in a similar way as for the previous examples, and is not to be repeated here. It can be just mentioned that for this case the load can be expressed better as

$$P = b^2 F_5\left(\frac{\delta_{pl}}{b}, \frac{b}{R}\right) \tag{2.61}$$

which gives

$$J = G + \frac{b}{2\pi r}\left\{3\int_0^{\delta_{pl}} F_5 d\delta_{pl} - F_5\delta_{pl} + \frac{1}{R}\int_0^{\delta_{pl}} \frac{\partial F_5}{\partial b/R} d\delta_{pl}\right\} \tag{2.62a}$$

$$\text{or} \quad J = G + \frac{1}{2\pi r}\frac{3}{b}\int_0^{\delta_{pl}} P d\delta_{pl} - \frac{P\delta_{pl}}{b} + \frac{1}{R}\int_0^{\delta_{pl}} \frac{\partial F_5}{\partial b/\partial R} d\delta_{pl} \tag{2.62b}$$

The crack extension, -db, can be obtained by differentiation of Equation (2.61), giving

$$da = -db = \frac{b \dfrac{\partial F_5}{\partial \delta_{pl}/b} d\delta_{pl} - dP}{2bF_5 \dfrac{\partial F}{\partial \delta_{pl}/b} \delta_{pl} + b \dfrac{\partial F}{\partial b/R}} \qquad (2.63)$$

2.12 APPLIED TEARING MODULUS

As has been shown, dimensional analysis can be used to provide functional relations between load P, displacement δ and crack length a, and these relations may then be used to derive formulae for obtaining the material's tearing modulus T_{mat}, from a load-displacement record. A similar approach may be used to calculate the externally applied tearing modulus T_{app}. As was mentioned before, in this analysis stability will be considered with the total load point displacement δ_{tot} held fixed to

$$T_{app} = \frac{E}{\sigma_o^2} \frac{\partial J}{\partial a}\Bigg)_{\delta_{tot}}$$

Deeply Cracked Bend Specimen

As was mentioned previously (Section 2.6) the pure bending specimen has the special characteristic that the elastic and plastic parts of the angle of rotation, θ_{el} and θ_{pl}, may be expressed in terms of the same (and unique) non-dimensional variable M/b^2. Thus, it follows [36] that the total angle θ can also be expressed in terms of M/b^2, or inverting gives,

$$M = b^2 H(\theta) \tag{2.64}$$

and then

$$J(a,\theta) = 2b \int_0^{\theta} H d\theta \tag{2.65}$$

To calculate T_{app}, the total differential of J is required from Equation (2.65), which is to be divided by the increment of crack length da. A condition upon this computation relates da and $d\theta$, so that the total angle of rotation θ_{tot} is held constant.

$$\frac{dJ}{da} = -\frac{J}{b} + 2bH\frac{d\theta}{da} \tag{2.66}$$

The condition is

$$\theta_{tot} = C_M dM + \theta = \text{constant} \tag{2.67}$$

or

$$d\theta_{tot} = C_M dM + d\theta = 0$$

where C_M is the compliance of the testing machine. Differentiating Equation (2.64) gives

$$dM = -2bHda + b^2 H' d\theta. \tag{2.68}$$

Solving Equations (2.67) and (2.68) for $d\theta/da$ gives the relationship of da and $d\theta$ as:

$$\frac{d\theta}{da} = \frac{2bH}{C_M^{-1} + b^2 H'} \tag{2.69}$$

Finally, substituting Equation (2.69) into Equation (2.66) results in

$$T_{app} = \frac{E}{\sigma_o^2}\frac{dJ}{da}\Big)_{\theta_{tot}} = -\frac{J}{b} + \frac{4b^2H^2}{C_M^{-1} + b^2H'} \qquad (2.70)$$

The Three Point Bend Specimen

The three point bend specimen is an example of a configuration in which J is better calculated by separating its elastic and plastic parts.

If as usual δ_{el} is given by

$$\delta_{el} = PC \qquad (2.71)$$

then let the F_1 function be used for the plastic part of the displacement, δ_{pl}, assuming that it does not depend on a/W. The expression for the load becomes

$$P = \frac{b^2}{W} F_1\left(\frac{\delta_{pl}}{W}\right) \qquad (2.72)$$

Therefore for this case

$$J = G + \frac{2b}{W}\int_0^{\delta_{pl}} F_1 d\delta_{pl} \qquad (2.73a)$$

or

$$J = G + \frac{2}{b}\int_0^{\delta_{pl}} P d\delta_{pl} \qquad (2.73b)$$

Differentiating (2.73b) leads to

$$\frac{dJ}{da} = \frac{\partial G}{\partial a} - \frac{J_{pl}}{b} + \frac{\partial G}{\partial \delta_{el}} \frac{d\delta_{el}}{da} + \frac{2b}{W} F_1 \frac{d\delta_{pl}}{da} \qquad (2.74)$$

For use in Equation (2.74) $d\delta_{el}/da$ and $d\delta_{pl}/da$ can be obtained by differentiating Equation (2.71) and (2.72) combining these results with the boundary condition $d\delta_{tot} = 0$, gives

$$\frac{d\delta_{el}}{da} = \frac{PC'}{W} + C \frac{dP}{da} \qquad (2.75)$$

and

$$\frac{d\delta_{pl}}{da} = \frac{1}{(b/W)^2 \frac{\partial F}{\partial \delta_{pl}/W}} \left[\frac{dP}{da} + \frac{2b}{W} F_1\right] \qquad (2.76)$$

Furthermore:

$$d\delta_{tot} = d\delta_M + d\delta_{el} + d\delta_{pl} = 0$$

which leads to

$$\frac{PC'}{W} + \frac{dP}{da}(C+C_M) + \left[\frac{2b}{W} F_1 + \frac{dP}{da}\right] \frac{1}{(\frac{b}{W})^2 \frac{\partial F_1}{\partial \delta_{pl}/W}} = 0 \qquad (2.77)$$

From the set of Equations (2.75) through (2.77) $d\delta_{el}/da$ and $d\delta_{pl}/da$ may be obtained and so dJ/da can be evaluated from Equation (2.74).

The Compact Specimen

As another example, the T_{appl} can be obtained for the compact specimen by using an approach similar to the previous example. For the compact specimen case the F_1 function keeps the dependence in a/W, and so additional terms in equations (2.72) and (2.73) must be included.

As before the elastic part of the displacement δ_{el} is given by

$$\delta_{el} = PC \tag{2.78}$$

For this case the load, P, may be expressed as

$$P = \frac{b^2}{W} F_1\left(\frac{\delta_{pl}}{W}, \frac{a}{W}\right) \tag{2.79}$$

Then, J is given by

$$J = G + \frac{2b}{W} \int_0^{\delta_{pl}} F_1 d\delta_{pl} - \frac{b^2}{W^2} \int_0^{\delta_{pl}} \frac{\partial F_1}{\partial a/W} d\delta_{pl} \tag{2.80}$$

and

$$\frac{dJ}{da} = \frac{\partial G}{\partial a} + \frac{\partial G}{\partial \delta_{el}} \frac{d\delta_{el}}{da} - \frac{J_{pl}}{b} + \frac{2b}{W^2} \int_0^{\delta_{pl}} \frac{\partial F_1}{\partial a/W} d\delta_{pl}$$

$$- \frac{b}{W^2} \int_0^{\delta_{pl}} \frac{\partial^2 F}{\partial a/W^2} d\delta_{pl} + \frac{2b}{W} F_1 - \frac{b^2}{W^2} \frac{\partial F_1}{\partial a/W} \frac{d\delta_{pl}}{da} \tag{2.81}$$

It can be noted that usually the F_1 function is weakly dependent on a/W, and so the term involving the second derivative is small compared with the others. Presuming it can be neglected gives

$$\frac{dJ}{da} = \frac{\partial G}{\partial a} + \frac{\partial G}{\partial \delta_{el}} \frac{d\delta_{el}}{da} - \frac{J_{pl}}{b} + \frac{2b}{W^2} \int \frac{\partial F_1}{\partial a/W} d\delta_{pl} +$$

$$+ \frac{2b}{W} F_1 - \frac{b^2}{W^2} \frac{\partial F}{\partial a/W} \frac{d\delta_{pl}}{da} \qquad (2.82)$$

Following the analysis of the previous section, a set of three equations can be obtained by differentiating Equations (2.78) and (2.79) and the condition $d\delta_{tot} = 0$, giving

$$\frac{d\delta_{el}}{da} = \frac{PC'}{W} + C \frac{dP}{da} \qquad (2.83)$$

$$\frac{d\delta_{pl}}{da} = \frac{1}{(\frac{b}{W})^2 \frac{\partial F_1}{\partial \delta a/W}} \left[\frac{dP}{da} + \frac{2b}{W} F_1 - (\frac{b}{W})^2 \frac{\partial F_1}{\partial a/W} \right] \qquad (2.84)$$

and

$$\frac{PC'}{W} + \frac{dP}{da} (C+C_M) + \left[\frac{dP}{da} + \frac{2bF_1}{W} - (\frac{b}{W})^2 \right] \frac{\partial F_1}{\partial a/W} \frac{1}{(\frac{b}{W})^2 \frac{\partial F_1}{\partial \delta_{pl}/W}} = 0 \qquad (2.85)$$

As before from the set of Equations (2.83) through (2.85) $d\delta_{el}/da$ and $d\delta_{pl}/da$ can be obtained and so Equation (2.82) can be used for obtaining T_{appl}. For the other specimens the T_{app} can be obtained in a similar way thus the details are not presented here.

3. THEOREMS ON CONDITIONS FOR SEPARABILITY

3.1 INTRODUCTION

In the previous chapter, exact formulae have been presented for J, Δa, T_{mat} and T_{app}, for different configurations and arbitrary a/W and material constitutive law. It is apparent that any simplification of those formulae (still on an exact basis), would be of great interest, and so an exploration of possibilities of simplification and/or conditions under which those are possible, is needed.

The first consideration is whether the functions F involved are separable into multiplicative functions of displacement δ, and a/W, with the consequent simplification on the final results. In this chapter, a detailed discussion on necessary and sufficient conditions for separating variables is provided. At the same time, Turner's η [51], is introduced and conditions for its existence are also presented. Moreover, separability of J, itself, as multiplicative functions of δ and a/W is a special case.

3.2 J INTEGERAL SEPARABILITY

In this section sufficient conditions for J integral separability are presented. Use is made of the Illyushin theorem [40,41], on conditions for having a state of so called "simple loading". If that is the case, it follows that J is separable.

The Illyushin theorem shows that if certain conditions are met, the state of stress (or strains) is that of simple loading (straining), or, in other words, the principal directions of the

stress-strain tensors do not change during the deformation process. The proof is as follows.

If the conditions for simple loading are met, i.e.:

(1) Surface loads are proportional to a single parameter t, with no body forces present.

(2) The material is incompressible, i.e., $\varepsilon = 0$, where $\varepsilon = \varepsilon_{ii}$, is the unit volume change.

(3) The stress and strain intensities T and Γ are related by a monomial power expression

$$t = A.\Gamma^n \qquad A,\ n > 0 \qquad (3.1)$$

with

$$t = (s_{ij}\ s_{ij})^{1/2} \quad \text{and} \quad \Gamma = (e_{ij}\ e_{ij})^{1/2}$$

where s_{ij} and e_{ij} are the components of the stress and strain deviatoric tensors respectively.

Then, it follows that the state of stresses is that of simple loading, or in other words, at any point

$$\sigma_{ij} = t\sigma^o_{ij} \quad (x,y \text{ geometry})$$

and

$$\varepsilon_{ij} = t^{1/n}\ \varepsilon^o_{ij} \quad (x,y \text{ geometry}) \qquad (3.2)$$

where σ^o_{ij} and ε^o_{ij} are a particular stress-strain field solution.

Proof

Assume that for a body with a crack length to width ratio a/W, σ^{o}_{ij} and ε^{o}_{ij} are a stress-strain field solution of the problem. This means that σ^{o}_{ij} and ε^{o}_{ij} satisfy:

a) equilibrium

$$\frac{\partial \sigma_{ij}}{\partial x_i} = 0 \tag{3.3}$$

b) boundary conditions

$$p^k_j = \sigma_{ij} n_i \tag{3.4}$$

where p^k_j is the jth component of the kth load and n_i is the i-th component of the normal vector.

c) compatibility

$$\frac{\partial^2 \varepsilon_{xx}}{\partial y^2} + \frac{\partial^2 \varepsilon_{yy}}{\partial x^2} = \frac{\partial^2 \varepsilon_{xy}}{\partial x \partial y} \tag{3.5}$$

$$\frac{\partial^2 \varepsilon_{xx}}{\partial y \partial z} = \frac{\partial}{\partial x}\left(- \frac{\partial \varepsilon_{yz}}{\partial x} + \frac{\partial \varepsilon_{xz}}{\partial y} + \frac{\partial \varepsilon_{xy}}{\partial z} \right)$$

and the corresponding cyclic permutation of indexes.

d) equations of deformation theory

$$\sigma_{ij} = \frac{\varepsilon}{3k} \delta_{ij} + 2g(\Gamma) e_{ij} \tag{3.6}$$

where k is the bulk modulus and $g(\Gamma)$ is the modulus of plasticity [40]

$$g(\Gamma) = \frac{t}{\Gamma}$$

noting that for this case

$$\varepsilon = 0 \text{ and } g(\Gamma) = A^{n-1} .$$

Equation (3.6) becomes

$$\sigma_{ij} = 2A\Gamma^{n-1} e_{ij} . \tag{3.7}$$

Now Equation (3.3) through (3.5) are homogeneous degree one in the stresses and strains, this implies that if σ^o_{ij}, ε^o_{ij} is a solution of the problem, $\lambda\sigma^o_{ij}$ and $\beta\varepsilon^o_{ij}$ will be also. But in Equation (3.6) the right-hand side is homogeneous degree n in the strains and the left-hand side is homogeneous degree one in the stresses. So $\lambda\sigma^o_{ij}$ and $\beta\varepsilon^o_{ij}$ is a solution provided

$$\beta = \lambda^{1/n} \quad \text{or calling} \quad \lambda \equiv t.$$

$$\sigma_{ij} = t\sigma^o_{ij} \text{ and } \varepsilon^o_{ij} = t^{1/n} \varepsilon^o_{ij} \tag{3.8}$$

is a solution of the problem for any value of the parameter, t.

It can also be noted that Equation (3.8) can be restated as

$$\sigma_{ij}^{o} = \beta^{n}\,\sigma_{ij}^{o} \quad \text{and} \quad \varepsilon_{ij} = \beta\varepsilon_{ij}^{o} \tag{3.9}$$

Thus it can be concluded that:

1) If the loads are proportional to a single parameter t (and also the rest of the conditions: (1) through (3) hold), at any point the stress tensor components are proportional to that single parameter

$$\sigma_{ij} = t\sigma_{ij}^{o}$$

and the strain tensor components are (3.10)

$$\varepsilon_{ij} = t^{1/n}\,\varepsilon_{ij}^{o}$$

2) At the same time, if displacements are prescribed as boundary conditions, being proportional to a single parameter β then a situation of simple straining results where

$$\varepsilon_{ij} = \beta\varepsilon_{ij}^{o}$$

and (3.11)

$$\sigma_{ij} = \beta^{n}\,\sigma_{ij}^{o}$$

The results of the above analysis are used to determine the conditions of J integral separability. These conditions are expressed in the following theorem.

READEX FICHE

Theorem #1 If a state of simple loading (straining) is present in a cracked body, J is separable into multiplicative functions of displacement and crack length

$$J(\delta/W, a/W) = R(a/W) \cdot S(\delta/W) \tag{3.12}$$

Proof

From the definition (1.13)

$$J = -\frac{dU}{da}$$

where U is the potential energy of the body given by [10]

$$U = \int_A W_s \, dxdy - \int_{S_T} \bar{T} \cdot u \, ds \tag{1.14}$$

If displacements are specified on the boundaries and are proportional to a single parameter $\beta(\delta \propto \beta)$ the potential energy U reduces to the strain energy stored in the body

$$U = \int W_s \, d\, A \tag{3.13}$$

and so

$$J = -\frac{dU}{da} \tag{3.14}$$

Now at a certain point (x,y), the strain energy density W_s is

$$W_s = \int_0^{\varepsilon_{mn}} \sigma_{ij}\, d\varepsilon_{ij} \qquad (3.15)$$

and using Equation (3.9)

$$W_s = \sigma^o_{ij}\, \varepsilon^o_{ij} \int_0^{\beta} \beta^n\, d\beta$$

$$= \sigma^o_{ij}\, \varepsilon^o_{ij}\, \frac{\beta^{n+1}}{n+1} = \beta^{n+1}\, h(x,y,a/W \text{ geom}) \qquad (3.16)$$

And the total strain energy is

$$U = \int_A \beta^{n+1}\, h(x,y,a/W,\text{geom})$$

$$U = \beta^{n+1}\, \bar{h}(a/W, \text{ geom}) \qquad (3.17)$$

and putting Equation (3.17) into Equation (3.14) gives

$$J = -\frac{dU}{da} = \beta^{n+1}\, \frac{\bar{h}'}{W}\,(a/W)$$

Noting that $\frac{\bar{h}'}{W} = R(a/W)$ and $\beta \alpha \delta$ then

$$J = R(a/W) \cdot S(\delta/W) \qquad (3.18)$$

q.e.d.

3.3 P SEPARABILITY

The conditions under which the load P is separable into multiplicative functions of displacement and a/W is also of

interest. The implied form is

$$P = g(a/W)\ H(\delta/W) \tag{3.19}$$

The conditions for this separation of P are presented in the following theorem.

Theorem #2

J is separable if and only if P is separable.

Proof

1) P is separable => J is separable. If P is separable then it can be written as

$$P = g(a/W)\ H(\delta/W)$$

and so using the definition of J (1.15), gives

$$J = -\int_0^{\delta} \frac{\partial P}{\partial a}\, d\delta = \frac{g'(a/W)}{W} \int_0^{\delta} H\, d\delta$$

And so J can be written as

$$J = R(a/W) \cdot S(\delta/W) \tag{3.20}$$

where for this case

$$R(a/W) = \frac{g'}{W} \quad \text{and} \quad S(\delta/W) = \int_0^{\delta} H\, d\delta$$

q.e.d.

2) J is separable => P is separable. If J is separable then it can be written as

$$J = -\int_0^{\delta} \frac{\partial P}{\partial a}\, d\delta = R(a/W) \cdot S(\delta/W) \qquad (3.21)$$

Now defining r(a/W) and s(δ/W) so that

$$r = -\int_0^{\delta} R\, da \quad \text{or} \quad \frac{\partial r}{\partial a} = -R$$

and (3.22)

$$s = \frac{\partial S}{\partial \delta} \quad \text{or} \quad \int_0^{\delta} s\, d\delta = S$$

and replacing in Equation (3.21), J takes the form

$$J = -\frac{\partial r}{\partial a}\int_0^{\delta} s\, d\delta \,.$$

As ∂r/∂a is not a function of δ it can be put into the integral to give

$$J = -\int_0^{\delta} \frac{\partial r}{\partial a}\, s\, d\delta$$

Conversely, as s is not a function of a/W it can be introduced inside the derivative with respect to a/W, giving

$$J = -\int_0^{\delta} \frac{\partial rs}{\partial a}\, d\delta = -\int_0^{\delta} \frac{\partial P}{\partial a}\, d\delta$$

or taking the last equality

$$\int_0^{\delta} \frac{\partial rs}{\partial a}\, d\delta - \int_0^{\delta} \frac{\partial P}{\partial a}\, d\delta = 0$$

Now regrouping under the integral sign gives

$$\int_0^{\delta} \frac{\partial}{\partial a} (rs-P) = 0 \qquad (3.23)$$

but this implies

$$P = r(a/W) \cdot s(\delta/W)$$

and so P is separable into multiplicative functions of a/W and displacement. q.e.d.

3.4 EXISTENCE OF THE η-FACTOR

As was mentioned before Sumpter and Turner [51] introduced a non-dimensional factor, η, for convenience in their numerical calculations.

$$\eta(a/w) \equiv \frac{Jb}{A} \qquad (3.24)$$

where A is the area under the load displacement record and b is the remaining ligament. In this section attention is devoted to the conditions for existence of the η factor. By existence is meant here, that η is a function of a/W only, not of the displacement δ.

$$\eta = \eta(a/W). \tag{3.25}$$

These conditions are presented in the following theorem.

Theorem #3

The η-factor exists (in the sense $\eta = \eta(a/W)$) if and only if J is separable. For proving the theorem use has to be made of the following lemma.

Lemma If $u(xy)$ and $v(x,y)$ are two well behaved functions of the variables x and y, non constant and non zero in any of the variables, the ratio

$$\frac{\int_0^y u\, v\, dy}{\int_0^y u\, dy} = w$$

cannot be a function of x only. That is

$$w = w(x,y)$$

Proof

Let us assume the contrary

$$\frac{\int_0^y u\, v\, dy}{\int_0^y u\, dy} = w(x)$$

so

$$\int_0^y u\,v\,dy = w(x)\int_0^y u\,dy = \int_0^\delta w(x)\,u\,dy$$

$$\int_0^y u(v-w)dy = 0 \quad \text{for all } (x,y)$$

But this is only possible if and only if

$$v \equiv w \quad \text{for any } (x,y)$$

and that would imply $w = w(x,y)$ (as $v = v(x,y)$), which contradicts the initial assumption $w = w(x)$ so w cannot be a function of x only. q.e.d.

Now the Theorem #3 can be proven

η exists <=> J is separable.

Proof

1) J is separable => η exists

If J is separable then P is separable (as proven in Theorem #2) but then

$$P = g_o(a/W)\quad H(\delta/W)$$

$$J = -\int \frac{\partial P}{\partial a}\,d\delta = -\frac{g_o'}{W}\int H\,d\delta = \tag{3.26}$$

$$= -\frac{g_o'}{Wg_o}\int P\,d\delta = -\frac{1}{b}\,\frac{g_o'}{g_o}\,\frac{b}{W}\int P\,d\delta$$

and so

$$J = \frac{\eta}{b} \int_0^{\delta} P \, d\delta$$

with (3.27)

$$\eta = -\frac{g'}{g} \frac{b}{W} = \eta(a/W).$$

q.e.d.

2) η exists => J is separable.

Lets suppose J is not separable => P is not separable (by Theorem #2) => $P = H(a/W, \delta/W)$ nonseparable

or $\frac{1}{H} \frac{\partial H}{\partial a/W} = v$ is still a function of δ and a/W

so $$\frac{\partial H}{\partial a/W} = H(a/W, \partial/W) \cdot v(a/W, \delta/W). \tag{3.28}$$

Now applying the definition

$$J = -\int_0^{\delta} \frac{\partial P}{\partial a})_{\delta} \, d\delta = -\frac{1}{W} \int_0^{\delta} \frac{\partial H}{\partial a/W})_{\delta} \, d\delta = -\frac{1}{W} \int_0^{\delta} H(\frac{\delta}{W}, \frac{a}{W}) \, v(\frac{\delta}{W}, \frac{a}{W}) \, d\delta$$

and

$$\frac{\eta}{b} = \frac{J}{\text{Area}} = \chi \equiv -\frac{1}{W} \frac{\int_0^{\delta} H \, v d\delta}{\int_0^{\delta} H d\delta} \tag{3.29}$$

but using the previous lemma χ cannot be a functon of a/W only so η is not a function of a/W only and so it does not exist (in the sense defined above), which contradicts the original assumption. So J must be separable.

q.e.d.

3.5 SUMMARY

In this chapter the following conditions have been shown:

1) If $T = A\Gamma^n$ and the conditions (1) and (2) of Section (3.1) hold, the state of stresses is that of simple leading.

2) If the state of stresses is that of simple loading (straining) => J is separable.

3) J is separable if and only if P is separable.

4) The η-factor exists if and only if J is separable.

4. AN APPROACH TO DEVELOPMENT OF PLASTIC WORK FACTORS

4.1 INTRODUCTION

In Chapter 3, necessary and sufficient conditions were presented for the existence of the η-factor, as being a function of crack length only. It was shown that, for its existence, the J-integral (or the load P) has to be separable, or the state of stresses has to be that of simple loading. Under those conditions, it followed that η exists on exact basis.

Here a somewhat different approach to development of η-factors will be presented. As was shown before J is separable if stresses and strains are related by a monomial power law; nevertheless it has become common [31,32,34], to separate the plastic part of J, J_{pl}, when the stresses and plastic displacements follows a monomial power law. If this is the case, it can be proven just following the theorems of the previous chapter (applied to the plastic part of the displacements only), that

a) J_{pl} is separable if and only if P is separable (as a function of δ_{pl} and a/W).

b) The pastic η-factor, η_{pl}, exists if and only if J_{pl} is separable, where by definition

$$\eta_{pl} = \frac{J_{pl}\, b}{\int_0^{\delta_{pl}} P d\delta_{pl}} \qquad (4.1)$$

As was mentioned above the separability of J_{pl} or P cannot be regarded as an exact result, since the stresses and plastic strains are never

exactly related by a power law, but it has proven to be accurate enough for many situations.

Finally, as will be discussed in this chapter, the separability of the load P into multiplicative function of plastic displacement, δ_{pl}, and crack length a, may be tested experimentally, and if that is so (to within satisfactory accuracy), it follows (Theorems II and III, Chapter 3) that J_{pl} is separable and η_{pl} does exist.

4.2 THE ELASTIC η-FACTOR

The linear-elastic displacement, δ_{el}, can always be written in terms of the elastic compliance, C, as

$$\delta_{el} = PC \tag{4.2}$$

Moreover, G can also always be written in terms of the compliance derivative, $\frac{\partial C}{\partial a}$, as

$$J_{el} = G = \frac{P^2}{2}\frac{\partial C}{\partial a} \tag{4.3}$$

The elastic work (per unit thickness), W_{el}, is defined as the work recovered by linear elastic unloading (with the crack length fixed) from any point on an elastic-plastic load-displacement record. Therefore,

$$W_{el} = \frac{P\delta_{el}}{2} \tag{4.4}$$

Making use of Equation (4.2) to eliminate δ_{el} in Equation (4.4) and rearranging it to substitute for P^2 in Equation (4.3) gives

$$J_{el} = \frac{1}{C}\frac{\partial C}{\partial a} W_{el} \tag{4.5}$$

Now defining the elastic η-factor by the relation [82],

$$J_{el} = \eta_{el} \frac{W_{el}}{b} \tag{4.6}$$

where b is taken to be the uncracked ligament ahead of the crack. Comparing Equations (4.5) and (4.6), it is noted that η_{el} may always be written

$$\eta_{el} = \frac{b}{C}\frac{\partial C}{\partial a} = -\frac{b}{P}\frac{\partial P}{\partial a}\bigg|_{\delta_{el}} \tag{4.7}$$

This relationship, Equation (4.7), shows that η_{el} always exists for converting the elastic work, W_{el}, directly into J_{el} by Equation (4.6).

Moreover, it is pointed out that stress intensity factor, K, formulas may be used to compute C and $\frac{\partial C}{\partial a}$ as follows. Noting that $G = K^2/E'$ may be combined with Equation (4.6), then

$$\frac{\partial C}{\partial a} = \frac{2(K/P)^2}{E'} \tag{4.8}$$

This may be integrated to give

$$C = C_{NC} + \int_0^a \frac{2(K/P)^2}{E'}\, da \tag{4.9}$$

where C_{NC} is the elastic compliance with no crack present. Thus Equations (4.8) and (4.9) combined with Equation (4.9) show that η_{el} can be found directly from no more information than elastic stress intensity factor formulas, as an alternative to making use of Equation (4.9) directly through experimental determinations. Values of η_{el} for some configurations appear in Table 1.

4.3 PLASTIC η-FACTORS

In order to develop the plastic η-factor, η_{pl}, it is appropriate to begin by refering to the last term of Equation (2.18) J_{pl}, and its definition there. In order to evaluate J_{pl}, the functional relationship for load, P, in terms of crack size, a; plastic displacement, δ_{pl}; and other dimensional lengths, L, W, B, etc. must be known. Since in addition only the material's stress-strain properties also influence that functional relationship, as was discussed in Section (2.2), Equation (2.21) lead to

$$\frac{PW}{b^2} = F_1\left(\frac{\delta_{pl}}{W}, \frac{a}{W}, \frac{L}{W}, \frac{B}{W}, \text{ etc.}\right) \qquad (4.10a)$$

$$\frac{P}{b} = F_2\left(\frac{\delta_{pl}}{W}, \frac{a}{W}, \frac{L}{W}, \frac{B}{W}, \text{ etc.}\right) \qquad (4.10b)$$

$$\frac{P}{b} = F_3\left(\frac{\delta_{pl}}{b}, \frac{a}{W}, \frac{L}{W}, \frac{B}{W}, \text{ etc.}\right) \qquad (4.10c)$$

In addition, other alternative forms may be produced but F_1 and F_3 will later be seen here to be most appropriate for predominately bending and predominately tension, respectively, of the remaining uncracked ligament b.

Table 1. ELASTIC η-FACTORS FOR DIFFERENT CONFIGURATION

a/W	3 Point Bending s/W=4	Tension Specimen h/W=4	Tension Specimen h/W=6	Tension Specimen h/W=8	Single Edge Notch h/W=2	Single Edge Notch h/W=4	Single Edge Notch h/W=6	Single Edge Notch h/W=8
.3	1.13	.177	.119	.090	.808	.431	.294	.223
.4	1.37	.216	.147	.111	1.26	.724	.507	.390
.5	1.61	.247	.170	.130	1.78	1.36	.835	.660
.6	1.77	.270	.190	.147	2.22	1.63	1.29	1.07
.7	1.85	.286	.206	.161	2.45	2.07	1.79	1.58
.8	1.92	.289	.215	.171	2.44	2.28	2.15	2.03
.9	2.04	.267	.210	.172	2.26	2.23	2.20	2.17

s: total span

W: total width for 3PB and SEN and half of the width for Tension Specimen

h: half of the height

Proceeding by substituting Equations (4.10) into the final term of Equation (2.18), noting that db = -da, leads to

$$J_{pl} = \frac{2}{b}\int_0^{\delta_{pl}} P d\delta_{pl} - \frac{b^2}{W^2}\int_0^{\delta_{pl}} \left.\frac{\partial F_1}{\partial \frac{a}{W}}\right|_{\delta_{pl}} d\delta_{pl} \qquad (4.11)$$

$$J_{pl} = \frac{2}{b}\int_0^{\delta_{pl}} P d\delta_{pl} - \frac{b}{W}\int_0^{\delta_{pl}} \left.\frac{\partial F_2}{\partial a/W}\right|_{\delta_{pl}} d\delta_{pl} \qquad (4.12)$$

and

$$J_{pl} = \frac{2}{b}\left\{\int_0^{\delta_{pl}} P d\delta_{pl} - \frac{P\delta_{pl}}{2}\right\} - \frac{b}{W}\int_0^{\delta_{pl}} \left.\frac{\partial F_3}{\partial a/W}\right|_{\delta_{pl}/b} d\delta_{pl} \qquad (4.13)$$

Now in Equations (4.11) to (4.13) the first term of the right side of each contains the plastic work, W_{pl}, (per unit thickness) which is

$$W_{pl} = \int_0^{\delta_{pl}} P d\delta_{pl} \qquad (4.14)$$

Thus, the plastic work, W_{pl}, so defined is the total work, W_{tot}, minus the elastic work, W_{el}, as defined by Equation (4.14). In addition, the plastic η-factor, η_{pl}, is defined in a manner consistent with its elastic counterpart in Equation (4.6) by [51]

$$J_{pl} = \eta_{pl}\frac{W_{pl}}{b} \qquad (4.15)$$

Moreover, it is specified that η_{pl} depends on crack length, a/W, but that it shall not depend on the extent of plastic deformation $\frac{\delta_{pl}}{W}$, by

definition. At this point it is readily seen that Equations (4.11) to (4.13) can be reduced to the form of Equation (4.15) with Equation (4.14) inserted, only if the second integrals on the right sides of Equations (4.11) to (4.12) can be reduced to $\int_0^{\delta_{pl}} P d\delta_{pl}$ forms. Since this reduction will occur only under special additional conditions, as defined here η_{pl} [Equation (4.15)] does not always exist for all structural and/or test piece configuration and material combinations. On the other hand, for many configurations they can exist and thus be of great computational convenience.

In general, the plastic η-factors only exist when the F function can be separated into multiplicative functions of crack length a/W and plastic displacement δ_{pl}/W. Let us assume that this is possible, then

$$F_1\left(\frac{\delta_{pl}}{W}, \frac{a}{W}, ---\right) = H_1\left(\frac{\delta_{pl}}{W}, ---\right) \quad g_1\left(\frac{a}{W}, ---\right) \qquad (4.16)$$

or

$$F_2\left(\frac{\delta_{pl}}{W}, \frac{a}{W}, ---\right) = H_2\left(\frac{\delta_{pl}}{W}, ---\right) \quad g_2\left(\frac{a}{W}, ---\right) \qquad (4.17)$$

Under such conditions, Equations (20) or (21), the second integrals of Equation (4.16) or (4.17) would become:

$$\int_0^{\delta_{pl}} \frac{\partial F_1}{\partial\left(\frac{a}{W}\right)} d\delta_{pl} = \frac{\partial g_1}{\partial\left(\frac{a}{W}\right)} \int_0^{\delta_{pl}} H_1 d\delta_{pl}$$

$$= \frac{\partial g_1}{\partial\left(\frac{a}{W}\right)} \quad \frac{1}{g_1} \int^{\delta_{pl}} F_1 d\delta_{pl}$$

$$= \frac{\partial g_1}{\partial(\frac{a}{W})} \cdot \frac{W}{b^2 g_1} \int_0^{\delta_{pl}} P d\delta_{pl} \qquad (4.18)$$

or (similarly)

$$\frac{\partial F_2}{\partial(\frac{a}{W})} d\delta_{pl} = \frac{\partial g_2}{\partial(\frac{a}{W})} \frac{1}{b g_2} \int_0^{\delta_{pl}} P d\delta_{pl} \qquad (4.19)$$

Substituting Equation (4.18) or (4.19) into Equation (4.11) or (4.12) gives

$$J_{pl} = \frac{1}{b} \int_0^{\delta_{pl}} P d\delta_{pl} \left[2 - \frac{b}{W} \frac{\partial g_1}{\partial(\frac{a}{W})} \frac{1}{g_1}\right] \qquad (4.20)$$

or

$$J_{pl} = \frac{1}{b} \int_0^{\delta_{pl}} P d\delta_{pl} \left[1 - \frac{b}{W} \frac{\partial g_2}{\partial(\frac{a}{W})} \frac{1}{g_2}\right] \qquad (4.21)$$

Finally, comparing these results with Equations (4.14) and (4.15), it is seen that

$$\eta_{pl} = \left[2 - \frac{b}{W} \frac{\partial g_1}{\partial(\frac{a}{W})} \frac{1}{g_1}\right] \qquad (4.22)$$

or

$$\eta_{pl} = \left[1 - \frac{b}{W} \frac{\partial g_2}{\partial(\frac{a}{W})} \cdot \frac{1}{g_2}\right] \qquad (4.23)$$

In addition, other forms may be possible or as noted earlier, it may be that η_{pl} does not exist for some configuration-material combinations. As perplexing as this result may be, let the discussion proceed to cases where η_{pl} clearly does exist and provides useful results.

4.4 A GENERAL CONDITION FOR THE EXISTENCE OF η_{pl}

In general, η_{pl} will exist if a separation of variables can be found of the form of Equations (4.16) or (4.17) (or alternate form). This separation may be viewed as shown in Figure 14.

Now, plotting F_1 or F_2 vs. $\frac{\delta_{pl}}{W}$, if all of the curves for each constant a/W value are of heights F in constant scale to each other, then the separation exists. Further, if this scaling exists for some range of a/W values from $\delta_{pl} = 0$ to some limiting values of δ_{pl}^{limit}, then the separation of variables exist over that region. That is to say, if the condition

$$\frac{F\left(\frac{\delta_{pl}}{W}, \frac{a}{W_i}, \text{---}\right)}{F\left(\frac{\delta_{pl}}{W}, \frac{a}{W_j}, \text{---}\right)} = C_{ij} \text{ (constant)} \qquad (4.24)$$

For any values of $\frac{a}{W_i}$, and $\frac{a}{W_j}$, and for all $\frac{\delta_{pl}}{W}$ values for the region

$$\frac{a}{W_i} \leq \frac{a}{W} \leq \frac{a}{W_j}$$

and

$$0 \leq \frac{\delta_{pl}}{W} \leq \frac{\delta_{pl}^{limit}}{W} \qquad (4.25)$$

then within that region the separation of variables will exist and therefore η_{pl} will exist for the region. It can be seen that the η_{pl} approach will give approximately correct results sufficiently accurate to be practically useful, if the condition is only slightly violated (by small amounts and/or for small parts of the region).

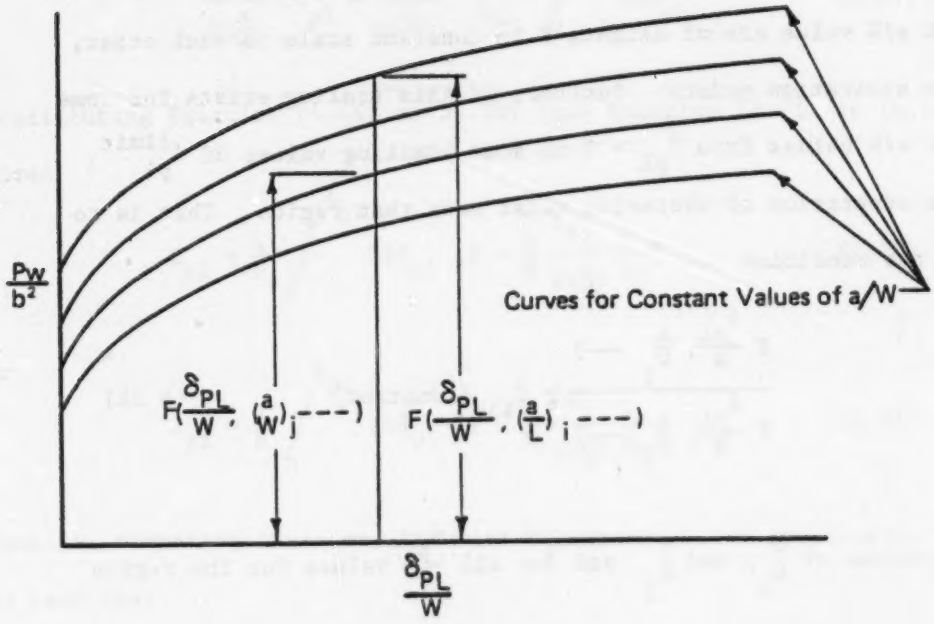

Fig. 14 Proportionality of F - functions for fixed normalized plastic displacement.

Taking a more practical view, the condition of Equation (4.24) for the region (4.25) may be tested experimentally by testing identical configurations with identical material differing only in their $(\frac{a}{W})$ values to produce P vs. δ_{pl} records which can be plotteed as on Figure 14 and tested numerically. Sub-sized (or blunt notch) specimens of the configuration-material combination may be utilized for this purpose which will avoid having crack growth occur prior to the $\frac{\delta_{pl}^{limit}}{W}$ of applicability. In this way the existence of η_{pl} can be directly experimentally determined.

On the other hand Turner [51,82] has observed the existence of the η_{pl} approach through finite element computations. However, subsequent attention here shall be directed to specific conditions for which the η_{pl} approach is possible.

4.5 EXAMPLES OF SPECIFIC CONDITIONS FOR WHICH η_{pl} EXISTS

(a) Power hardening materials

As was shown in Chapter 3 for a pure power hardening material, characterized by

$$\frac{\varepsilon}{\varepsilon_o} = (\frac{\sigma}{\sigma_o})^N$$

Illyushin's theorem may be invoked to show that the condition for existence of η_{pl} through (4.24) with unlimited region (4.25), is met any 2-dimensional configuration. First, the elastic case, N = 1, where it was previously shown that η_{el} always exists, is a limiting case of this proof. Therefore, for nearly elastic behavior, N → 1, including small scale yielding and/or highly hardening materials, the method should be practical for almost all configurations.

Further, for the tendency towards rigid-perfectly-plastic materials, $N = 0$, the other limiting case, η_{pl} always exists. That is to say that for situations where a limit load has been attained considerably prior to a point at which J is to be computed, then the η-factor method should work very well. For moderate amounts of hardening, $0 < N < 1/10$ (or perhaps lower) it is seen that the method should work very well. Indeed power hardening, for all values of N, is usually a fair approximation for developing load-displacement relations whenever displacements are very large, compared to elastic displacements, so existence of η-factors for power hardening shows a strong tendancy toward existence for very many practical cases.

(b) Pure bending of a small remaining ligament

Rice's case [36] of pure bending moment, M, (per unit thickness) on a small remaining ligament, b, ahead of a crack approaching perpendicular to a free boundary is one where η_{pl} can be shown to exist for any elastic-plastic material (with a monotonic stress-strain relation). For such a case dimensional considerations (Section 2.6), lead to

$$\theta = \theta\left(\frac{M}{b^2}\right) \tag{2.30}$$

where θ is the relative work producing rotation of the applied moments, M. Now, θ may be split into its elastic and plastic parts where

$$\theta = \theta_{el} + \theta_{pl} = k\frac{M}{b^2} + f\left(\frac{M}{b^2}\right) \tag{4.26}$$

hence

$$\theta_{pl} = f(\frac{M}{b^2}) \tag{4.27}$$

which may be inverted

$$\frac{M}{b^2} = L(\theta_{pl}) \tag{4.28}$$

This result may be compared indirectly with Equation (4.10a) by noting that it is appropriate to substitute $M = PW$ and $\theta_{pl} = \frac{\delta_{pl}}{W}$, then

$$\frac{PW}{b^2} = F(\frac{\delta_{pl}}{W}, \text{ material properties}) \tag{4.29}$$

where the variables are already separated as in Equation (4.16). Since a/W is absent, or g_1 is simply a constant. Thus refering to Equation (4.22), since $\partial g_1/\partial(\frac{a}{W}) = 0$, then

$$\eta_{pl} = 2 \tag{4.30}$$

and it always exists for arbitrary material properties for this configuration.

Similarly, the elastic parts of Equation (4.26) may be separated and using Equation (4.7), the result is

$$\eta_{el} = 2 \tag{4.31}$$

for this configuration. Also refering to Equations (2.18), (4.6) and (4.15), if $\eta_{el} = \eta_{pl} = \eta$ as in Equations (4.30) and (4.31) for a given configuration, then

$$J = \frac{\eta_{el} W_{el}}{b} + \frac{\eta_{pl} W_{pl}}{b}$$

$$= \frac{\eta}{b} (W_{el} + W_{pl}) = \frac{\eta W_{tot}}{b} \qquad (4.32)$$

where η can now be interpreted as a total work, W_{tot}, η-factor. Of course all of these results were available in Rice, et al. [36], but the repetition gives some new perspective on η-factors.

(c) Deeply cracked beams

For example, for the bending of a deeply cracked beam, where the plasticity is confined to the remaining ligament (uneffected by other boundaries) then it is clear that

$$\eta_{pl} = 2 \qquad (4.33)$$

with the remainder of the beam such as its length and loading arrangement unspecified (except that no appreciable beam shear shall exist at the ligament). Now on the other hand, from Equations (4.7), (4.8) and (4.9), it is clear that η_{el} is not in general equal to 2. However, η_{el} can be altered by simply changing the compliance of the beam away from th cracked section, i.e. C_{NC} changes, so that η_{el} can often be adjusted to 2.

Now, the advantage illustrated above is unusual since from Equation (4.7) and from Equations (4.22) and (4.23) it is clear that η_{el} and η_{pl} are not only usually not equal but indeed both may be dependent on the crack size, a/W. However, specimens could be designed so that η_{el} and η_{pl} exist and are equal at least at one convenient value of crack size, so that very simple relations such as Equation (4.32)

could be used to determine J. It is suggested here that a modified compact specimen might well be specifically designed for optimum J-integral testing convenience.

4.6 PLASTIC WORK FACTORS FOR THE TENSION SPECIMEN

For the case of a ligament, b, (not necessarily small) subjected to tension, a slightly different approach is more suitable for calculations. This approach makes use of the alternative form F_3, Equation (4.10), of the F function, and introduces the μ-factor that, as will be seen, is more convenient than the η_{pl}.

If the F_2 form is used, and assumed to be separable,

$$F_2 = F_2(\frac{\delta_{pl}}{W}, \frac{a}{W}) = g_2(a/W)\ H_2(\frac{\delta_{pl}}{W}) \qquad (4.34)$$

the resultant η_{pl} is

$$\eta_{pl} = (1 - \frac{b}{W}\frac{g_2'}{g_2}). \qquad (4.35)$$

This is not the most convenient form, because the F_2 so defined (or g_2) is still dependent on a/W, even for very deep cracks, and so the term involving $\frac{\partial F_2}{\partial a/W}$ (or $\frac{g_2'}{g_2}$ in the expression for η_{pl}) is not expected to be a small correction. This can be easily seen by comparing the J_{pl} obtained using the F_2, with the plastic part of J for the deeply cracked specimen ($b \to 0$), J_{pldc}, presented by Rice et al. [36].

Using F_2 $$J_{pl} = \frac{2}{b}\int P d\delta_{pl} - \frac{b}{W}\int \frac{\partial F_2}{\partial a/W} \qquad (4.36a)$$

And from Rice et al.

$$J_{pldc} = \frac{2}{b}\int P d\delta_{pl} - \frac{P\delta_{pl}}{b} \qquad (4.36b)$$

This shows that for a very deep crack the last term in (4.36a) tends to

$$\frac{b}{W}\int \frac{\partial F_2}{\partial a/W} + \frac{P\delta_{pl}}{b} = F_2\,\delta_{pl} \qquad (4.37)$$

which is obviously not necessarily small.

An alternate way of treating the tension problem is to make use of the form F_3, Equation (4.10c). In this case J_{pl} is given by Equation (4.13)

$$J_{pl} = \frac{2}{b}\int_0^{\delta_{pl}} P d\delta_{pl} - \frac{P\delta_{pl}}{b} - \frac{b}{W}\int_0^{\delta_{pl}} \frac{\partial F_3}{\partial a/W}\, d_{pl} \qquad (4.38)$$

Now if F_2 is separable, F_3 will be also or

$$F_3 = g_3(a/W)\; H_3\left(\frac{\delta_{pl}}{W}\right) \qquad (4.39)$$

and the last term in Equation (4.38), using Equation (4.10c) can be written as

$$-\frac{b}{W}\int_0^{\delta_{pl}} \frac{\partial F_3}{\partial a/W}\, d\delta_{pl} = -\frac{b}{W}\frac{g_3'}{g_3}\int_0^{\delta_{pl}} F_3\, d\delta_{pl} = -\frac{1}{W}\frac{g_3'}{g_3}\int_0^{\delta_{pl}} P d\delta_{pl} \qquad (4.40)$$

Substituting this result into Equation (4.38) gives

$$J_{pl} = \frac{1}{b}\left(2 - \frac{b}{W}\frac{g_3'}{g_3}\right)\int_0^{\delta_{pl}} P d\delta_{pl} - \frac{P\delta_{pl}}{b} \qquad (4.41)$$

Then, introducing the μ-factor as

$$\mu = \left(2 - \frac{b}{W}\frac{g_3'}{g_3}\right) \qquad (4.42)$$

Equation (4.41) becomes

$$J_{pl} = \frac{\mu}{b}\int_0^{\delta_{pl}} P d\delta_{pl} - \frac{P\delta_{pl}}{b} \qquad (4.43)$$

Comparing this result with that of Rice et al. Equation (4.36b) it is readily seen that, for a very deep crack

$$\mu = \left(2 - \frac{b}{W}\frac{g_3'}{g_3}\right) \to 2 \qquad (4.34)$$

independently of the material behavior, which implies that

$$\frac{b}{W}\quad\frac{g_3'}{g_3} \to 0 \qquad (4.45)$$

and that assures that the last term in (4.38) is a small correction to the total value.

Finally, Equation (4.40) can be written in a different way, under some special conditions. In fact, for the special case when the load P and the plastic displacement, δ_{pl}, are related by a monomial power law (to within the accuracy required).

$$P = D\ (a/W,\ n)\ \delta_{pl}^{N} \tag{4.46a}$$

the area plastic is

$$\int_0^{\delta_{pl}} P d\delta_{pl} = \frac{P\delta_{pl}}{1+N} = P\delta_{pl}\frac{n}{n+1} \tag{4.46b}$$

Also after some manipulations of (4.46b) the following relation can be obtained

$$\int_0^{\delta_{pl}} P d\delta_{pl} = \frac{2n}{n-1}\left[\int_0^{\delta_{pl}} P d\delta_{pl} - \frac{P\delta_{pl}}{2}\right] \tag{4.46c}$$

Thus, replacing Equation (4.46c) in the last term of Equation (4.40) gives

$$-\frac{b}{W}\frac{g_3'}{g_3}\int_0^{\delta_{pl}} P d\delta_{pl} = -\frac{b}{W}\frac{g_3'}{g_3}\frac{2n}{n-1}\left[\int_0^{\delta_{pl}} P d\delta_{pl} - \frac{P\delta_{pl}}{2}\right] \tag{4.47}$$

Then, Equation (4.38) becomes

$$J_{pl} = \frac{1}{b}\left(2 - \frac{2n}{n-1}\frac{b}{W}\frac{g_3'}{g_3}\right)\left\{\int P d\delta_{pl} - \frac{P\delta_{pl}}{2}\right\} \tag{4.48}$$

Defining

$$\rho = 2\left(1 - \frac{n}{n-1}\frac{b}{W}\frac{g_3'}{g_3}\right) \tag{4.49}$$

Then

$$J_{pl} = \frac{1}{b}\rho\left\{\int P d\delta_{pl} - \frac{P\delta_{pl}}{2}\right\} \tag{4.50}$$

As can be noted by comparing Equation (4.50) with J_{pldc} of Equation (4.36b), for a deep crack, the parameter ρ tends to

$$\rho = 2\left(1 - \frac{n}{n-1}\frac{b}{W}\frac{g_3'}{g_3}\right) \to 2 \qquad \text{for all values of } n \qquad (4.51)$$

that assures that the last term in (4.45) is a small correction to the total value, and also becomes independent of n as a/W increases. The disadvantage of this parameter ρ, is that it is not defined for $n \to 1$ (elastic case), and so the whole picture ($n = 1 \ldots n \to \infty$) is not complete.

Hutchinson et al. [34] calculated values of J_{pl}, for this configuration using finite elements. They also calculated ratios of the J_{pldc} of Equation (4.36b) and their value of J_{pl}. As it can be seen using Equations (4.49) and (4.50) this corresponds to $2/\rho$.

$$\frac{J_{pldc}}{J_{pl}} = \frac{2}{\rho} = \frac{1}{\left(1 - \frac{n}{n-1}\frac{b}{W}\frac{g_3'}{g_3}\right)} \qquad (4.52)$$

This ratio was found to be within 3% of unity for $n \geq 5$ when $a/W = .75$ and $n \geq 7$ when $a/W = .5$. These results give some indication as to the values of a/W and n needed for the deeply-cracked analysis to prevail, and also gives support to the analysis above, regarding showing the term $\frac{n}{n-1}\frac{b}{W}\frac{g_3'}{g_3}$ in Equation (4.51) as a small correction.

As discussed above, μ appears to be the most suitable parameter to be used for the tension specimen. As a consequence, values of the μ-factor were obtained, after some manipulation from the data presented by Hutchinson et al. [34]. They appear in Table 2 and in Figure 15.

Table 2. TENSION SPECIMEN μ-FACTOR FROM HUTCHINSON ET AL [34]

a/W \ n	1	1.5	2	3	5	7	10
.25	8.092	5.841	4.716	3.617	2.772	2.437	2.216
.50	4.376	3.379	2.892	2.427	2.112	2.025	1.990
.75	3.118	2.543	2.298	2.097	2.008	2.019	2.032

with $\lim_{a/W \to 1} \mu = 2$ for all n

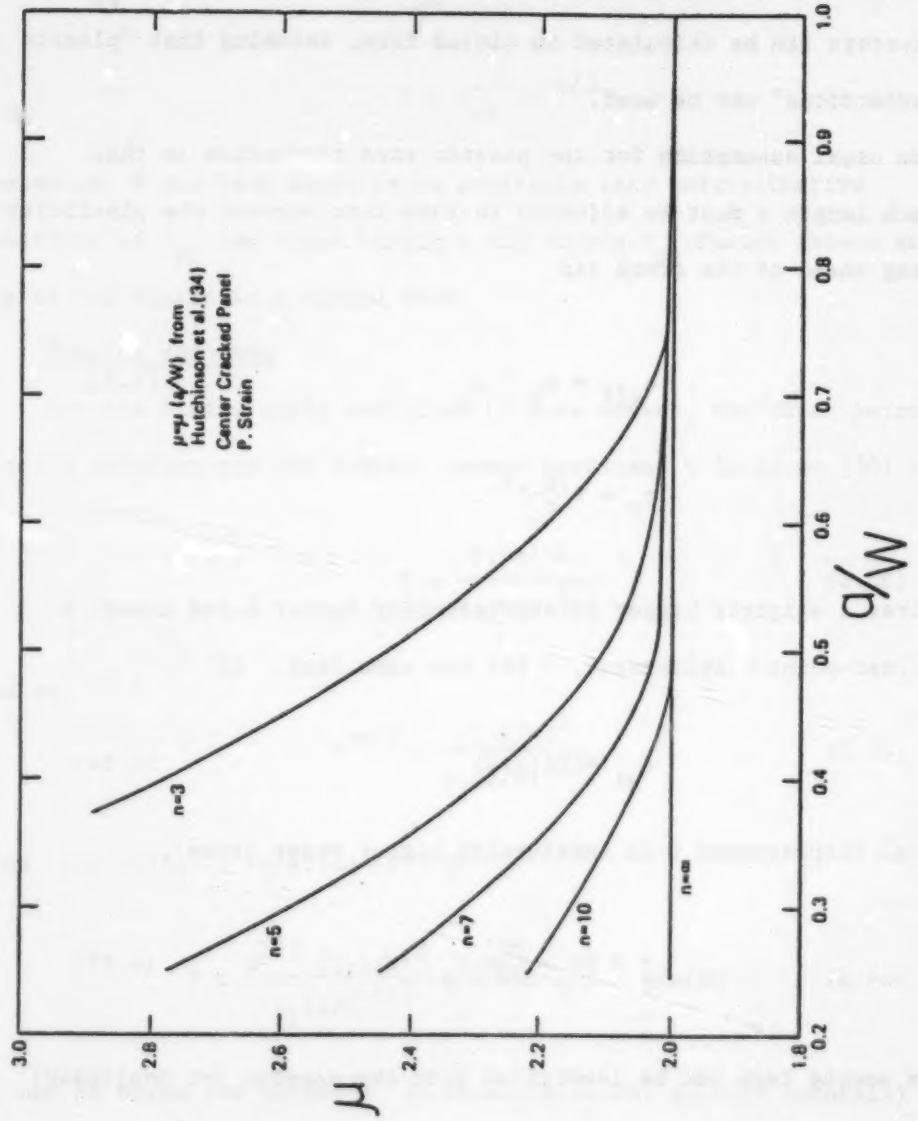

Fig. 15 Tension specimen. μ - factor from Hutchinson el al 34 .

4.7 THE η- AND μ-FACTORS IN THE SMALL SCALE YIELDING SITUATION

For the small scale yielding situation (ssy) [57,60], plasticity is confined to a small region ahead of the crack tip, and the η_{pl} and μ-factors can be calculated in closed form, assuming that "plastic zone corrections" may be used.

The usual assumption for ssy plastic zone correction is that the crack length a must be adjusted to take into account the plasticity occurring ahead of the crack tip

$$a_{eff} = a_o + r_y \tag{4.53}$$

where

$$r_y = \gamma \left(\frac{K}{\sigma_o}\right)^2 .$$

This gives a slightly bigger stress intensity factor K and though a bigger load-point displacement, δ for the same load. If

$$\delta_{el} = PC(a/W) \tag{4.54}$$

the total displacement δ is (neglecting higher order terms),

$$\delta = PC + \frac{PC'}{W} r_y \tag{4.55}$$

Now the second term can be identified with the plastic (or nonlinear) part of the displacement

$$\delta_{pl} = \frac{PC'}{W} r_y \propto PC'K^2 \tag{4.56}$$

or using $K = \frac{P}{B\sqrt{W}} V(a/W)$ and $C' \alpha V^2$

Then $$\delta_{pl} \alpha P^3 V^4$$

or

$$P \alpha \delta_{pl}^{1/3} V^{-4/3} \tag{4.57}$$

Therefore, P has been shown to be separable into multiplicative functions of δ_{pl} and crack length a and so the η_{pl}-factor exists and can be calculated in a closed form.

Bending specimen

For the finite strip subjected to pure moment, the three point bending specimen and the compact tensor specimen, V is given [30] by

$$V \alpha \frac{P_1(a/W)}{(1-a/W)^{3/2}} \tag{4.58}$$

and so

$$V^{-4/3} \alpha \frac{(1-a/W)^2}{P_1(a/W)^{4/3}} \tag{4.59}$$

thus, replacing in Equation (4.57)

$$P \alpha \frac{\delta^{1/3} (1-a/W)^2}{P_1(a/W)^{4/3}} = b^2 H(\frac{\delta_{pl}}{W}) \cdot g(a/W) \tag{4.60}$$

As can be noted the factor b^2 in Equation (4.60) appears naturally as in Equation (2.21a) so

$$F_1 = H(\frac{\delta_{pl}}{W}) \cdot g(a/W) \tag{4.61}$$

From Equation (4.60)

$$g(a/W) \alpha p_1(a/W)^{-4/3} \tag{4.62}$$

Therefore, from Equation (4.22) the η_{plssy} can be calculated as

$$\eta_{plssy} = (2 - \frac{b}{W}\frac{g_1'}{g_1}) = (2 - \frac{4}{3}\frac{b}{W}\frac{p_1'}{p_1}) \tag{4.63}$$

The values of p(a/W) for the different bending configurations can be obtained from [30]. Values of η_{plssy} for these configurations appear in Table 3 and in Figure 16.

Tension Specimen

A similar procedure can be used for the center cracked specimen subjected to tension. For this configuration [30]

$$V \alpha \frac{(a/W)^{1/2} p_2(a/W)}{(1-a/W)^{1/2}} = \frac{q(a/W)}{(1-a/W)^{1/2}} \tag{4.64}$$

so

$$V^{-4/3} \alpha \frac{(1-a/W)^{2/3}}{q(a/W)^{4/3}} \tag{4.65}$$

Substituting these results into Equation (4.57) gives

$$P \alpha \delta_{pl}^{1/3} \frac{(1-a/W)^{2/3}}{q(a/W)^{4/3}} \alpha \frac{\delta_{pl}^{1/3}}{W^{1/3}} \frac{b}{q(a/W)^{4/3}(b/W)^{1/3}}$$

$$= b\, H_2(\frac{\delta_{pl}}{W}) \cdot g_2(a/W) \tag{4.66}$$

Table 3. Bending Configuration η_{plssy} Factor

a/W	Pure Bending	3PB	Compact
.25	1.47	1.44	2.72
.30	1.66	1.61	2.42
.35	1.76	1.71	2.23
.40	1.81	1.79	2.14
.45	1.85	1.84	2.10
.50	1.88	1.88	2.10
.55	1.91	1.92	2.11
.60	1.94	1.95	2.13
.65	1.97	1.97	2.14
.70	1.99	1.98	2.14
.75	2.01	1.98	2.13
.80	2.02	1.98	2.10
.85	2.02	1.98	2.08
.90	2.02	1.98	2.05
.95	2.01	1.99	2.02
1.00	2.00	2.00	2.00

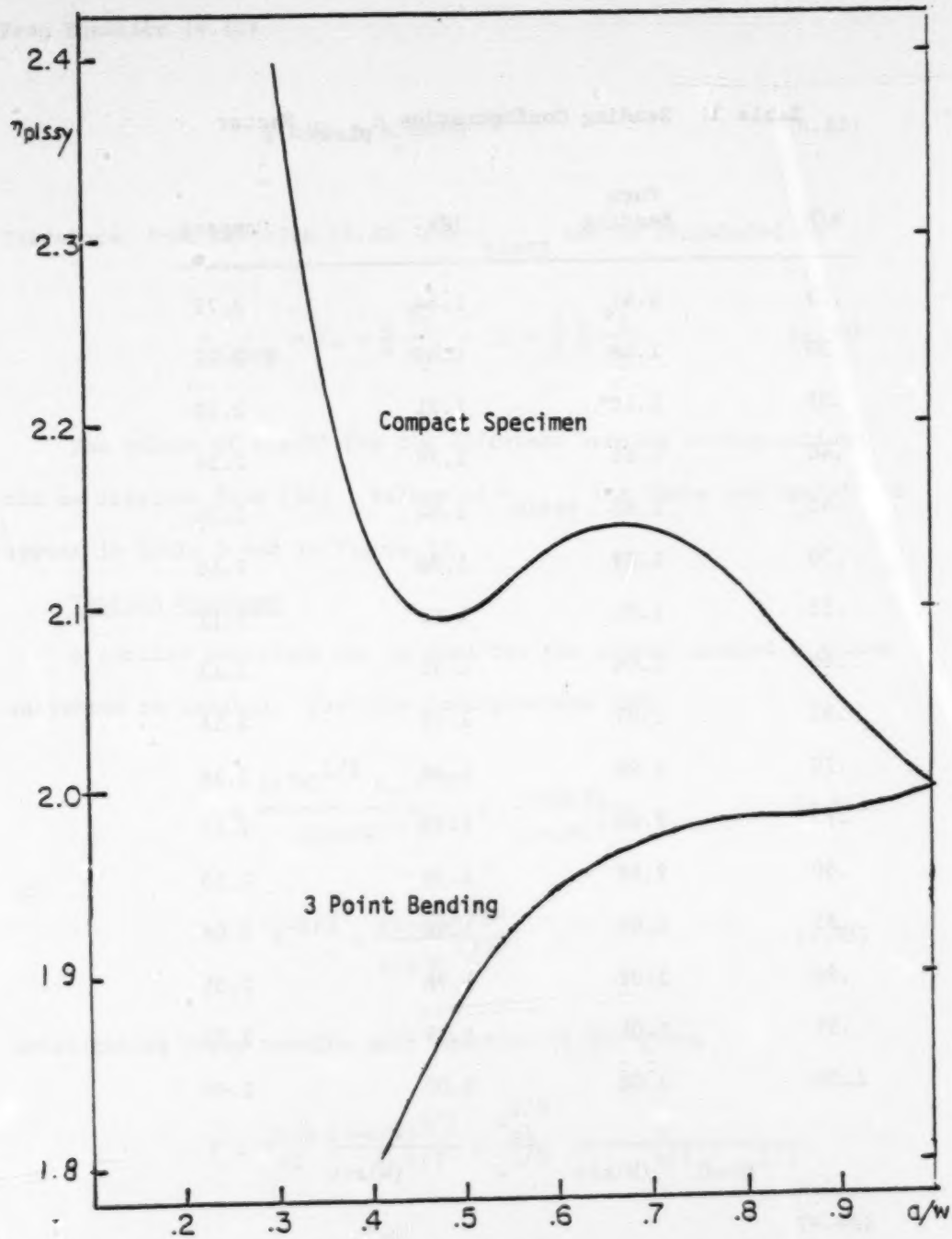

Fig. 16 The η_{plssy} factor for Bending Configurations.

As can be noted the factor b appears naturally in Equation (4.66), as in Equation (2.21b) so

$$F_2 = H_2\left(\frac{\delta_{pl}}{W}\right)\, g_2(a/W) \tag{4.67}$$

Then,

$$g_2(a/W) \propto \left[\frac{1}{q(a/W)^4 b/W}\right]^{1/3} \tag{4.68}$$

Again the η_{plssy}, for the tension case, is

$$\eta_{plssy} = \left(1 - \frac{b}{W}\frac{g_2'}{g_2}\right) \tag{4.69}$$

Therefore, it can be calculated using Equation (4.68) and results in [30] in a closed form. Values of η_{plssy} appear in Table 4 and Figure 17.

The μ-factor

As was discussed in section 4.6 another convenient way to treat the tension problem, is by means of the F_3 function Equation (4.39) and the μ-factor, Equation (4.44). Rewritting Equation (4.66), referring to Equations (4.39) and (4.44),

$$P \propto \delta_{pl}^{1/3}\, \frac{b}{q^{4/3} b^{1/3}} = \frac{\delta_{pl}^{1/3}}{b^{1/3}}\, b\, \frac{1}{q^{4/3}}$$

$$= b\, H_3\left(\frac{\delta_{pl}}{b}\right)\, g_3(a/W) = b\, F_3 \tag{4.70}$$

Therefore

$$g_3 \propto \frac{1}{q^{4/3}} \tag{4.71}$$

Table 4. TENSION SPECIMEN η_{pl}, μ AND ρ-FACTOR FROM SMALL SCALE YIELDING

a/W	η_{plssy}	μ_{ssy}	ρ_{ssy}
.3	1.92	3.25	5.75
.35	1.71	3.04	5.12
.40	1.52	2.85	4.55
45	1.32	2.65	3.95
80	1.21	2.54	3.62
55	1.12	2.45	3.35
60	1.04	2.37	3.11
65	.99	2.32	2.96
70	.93	2.26	2.78
75	.88	2.21	2.63
80	.84	2.17	2.51
85	.79	2.12	2.36
90	.75	2.08	2.24
95	.71	2.04	2.12
1	.67	2.00	2.00

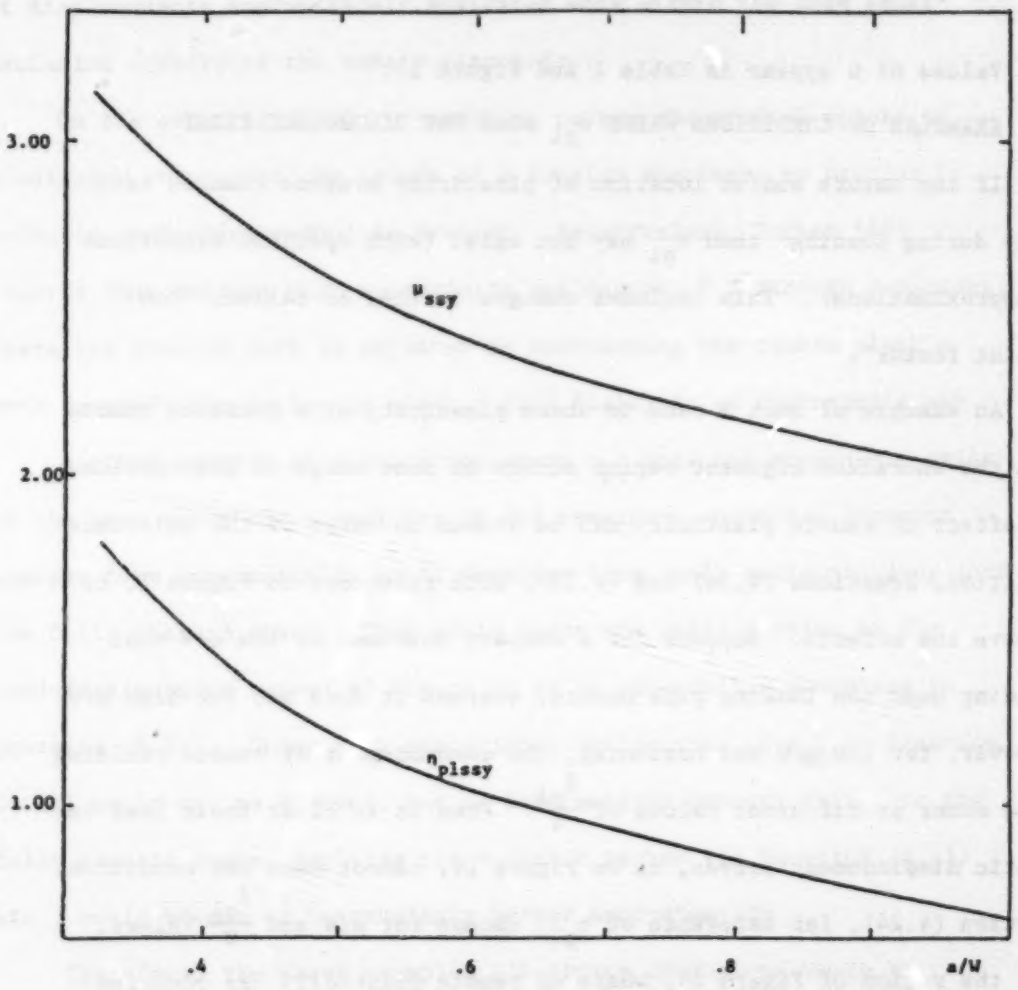

Fig. 17 The η_{plssy} and the μ- factors for the tension case.

Then μ can be calculated as

$$\mu = (2 - \frac{b}{W}\frac{g_3'}{g_3}) = (2 - \frac{4}{3}\frac{b}{W}\frac{q'}{q}) \qquad (4.72)$$

Values of μ appear in Table 4 and Figure 17.

4.8 EXAMPLES OF CONDITIONS WHERE η_{pl} DOES NOT RIGOROUSLY EXIST

If the nature and/or location of plasticity present changes radically during loading, then η_{pl} may not exist (with specific exceptions or approximations). This includes changes in the, so called, "constraint factor".

An example of such a case is where plasticity at a location remote from the uncracked ligament region occurs at some stage of deformation. The effect of remote plasticity can be viewed in terms of the existence condition, Equations (4.24) and (4.25), with reference to Figure 10 to observe the effects. Suppose for a compact specimen or low a/W that yielding near the loading pins occurs, whereas it does not for high a/W. Moreover, for low a/W and hardening, the commencement of remote yielding would occur at different values of $\frac{\delta_{pl}}{W}$. Then it is clear their load vs. plastic displacement curves, as on Figure 14, cannot meet the condition, Equation (4.24), for existence of η_{pl}, except for a/W and $\frac{\delta_{pl}}{W}$ values, i.e. the region of Figure 14, where no remote plasticity has occurred. Therefore, in general the η-factor method should not be used where plasticity has occurred remote from the uncracked ligament region, except where further justification is given.

However, from a practical point of view, if the effects of the remote plasticity can be removed, then an η_{pl} may be found for computation of J_{pl} from plastic work, W_{pl}, as in Equation (4.15). For

example, for a long uniaxially loaded tension specimen, if plasticity at loading pins (or grips) occurs, gage length points between the pins and cracked location can be selected (remote from both) so that measurement of displacements appropriately evaluates work within the gage length excluding effects of the remote plasticity.

On the other hand, where hardening causes the gradual spread of plasticity throughout the length of a tension specimen, no precise η-factor evaluation method is present. Nevertheless, Turner [82] reports some success with approximate evaluation of J through η-factors, where the plastic work is adjusted by subtracting the remote plastic work (outside the perfectly plastic slip field) in an approximate way.

Another example of a situation where η_{pl} does not rigorously exist is the case where the plasticity at the remaining uncracked ligament changes form substantially as it develops from small scale yielding into the fully plastic state. This would cause the early portion of the load-displacement curves of Figure 14 to be non-similar according to Equation (4.24). Under such conditions, evaluations of J_{pl} by Equation (4.15) would not be correct, but as deformations proceed well into the fully plastic state, applying the η-factor method via Equation (4.15) etc., would become an increasingly better approximation.

Therefore, the above examples illustrate conditions where the η-factor method is not strictly or rigorously applicable, but it is also made clear that certain modifications or approximations may be possible to permit practical evaluations of J by the η-factor method for some special cases in violation of rigorous conditions for applicability.

4.9 SUMMARY AND DISCUSSION

The existence of the η-factor method is not necessary for the evaluation of J, which alternately can be found by other means directly from its definitions, Equation (2.12). However, the η-factor method is a great simplification in finding J, both in test pieces and in structural components for circumstances where it is applicable either in a rigorous or approximate way.

Indeed, though the previous discussion here has been formulated on the basis of computations of J using equations employing η-factors such as Equation (4.15) which were written as if no crack growth has occurred, they can be easily adapted for growing cracks. However, a correct method for determining J for any point on Figure 13a ia to take the load-displacement record with no crack growth for the a/W which passes through the point and make the computation according to Equation (4.15) etc. The computation will be correct provided that the point is in the region of applicability of η-factors, Equations (4.24) and (4.25) and if the conditions for "strict deformation theory" apply [49]. Therefore, the η-factor method can be adopted whether or not crack growth occurs.

Finally, some examples of configuration material combinations and conditions have been given here where the η-factor method is rigorously applicable or approximately applicable. On the other hand, some combinations and conditions have been identified where η_{pl}, as defined here, does not exist.

5. EXPERIMENTAL RESULTS

5.1 INTRODUCTION

In the previous chapters, a general method, applicable to all configurations (2D) was presented. This method of analysis of load-displacement records allows obtaining J-R curves from single test specimens. In chapter 2 the analysis presented is exact from an analytical viewpoint. In chapters 3 and 4, the possibility of simplification of the method was explored and the conditions under which this simplification is possible, were set.

In this chapter the results of application to actual P-δ records are presented. In these applications, different configurations are considered as well as different materials.

It is to be noted, that the analysis of section 5.2 was done with the method in an early state of development, although, the results are presented for a historical reason. Nevertheless, the records were reanalyzed with the method fully developed and the analysis appears in section 5.5.

5.2 AN INITIAL EXPERIMENTAL INVESTIGATION OF TEARING INSTABILITY THEORY

Since application of the tearing instability theory [71,72], seems relevant for certain fully-plastic plane-strain situations of practical interest (such as reactor vessels at operating temperatures with low upper shelf Charpy materials), it is of special importance to experimentally verify the analysis for these situations, where no other instability analysis has as yet been formulated. For that

reason a simple testing program was elected, which could be performed quickly using a material which was pedigreed and would exhibit fully-plastic plane-strain behavior (in the J-integral tearing sense) in reasonably sized samples.

The material selected was Ni-Cro-Mo-V supplied by Westinghouse Research, which has been subjected to extensive testing by them previously [17]. This material has flow properties and and J-integral and R-curve properties (J_{IC} and $\frac{dJ}{da}$) for tearing) for temperatures well above the transition temperature which make it quite convenient for crack instability tests. Convenience is gained by being able to select reasonable test specimen proportions requiring moderate test loads and usual instrumentation while being able to change from stable to unstable results from test to test due to simple modifications of test variables.

The test configuration was selected to be a 3-point bend specimen of full span, s, of 8" with a specimen depth of 1", fatigue precracked to various crack size to specimen depth ratios, a/W. A schematic diagram of the test configuration is shown in Figure 18.

In the tests stability was affected mainly by varying the a/W of the test specimen and/or the effective or equivalent elastic span of the test specimen. The method of adjusting the effective elastic span was by inserting an elastic spring bar in the test arrangement of adjustable span for a variable spring constant.

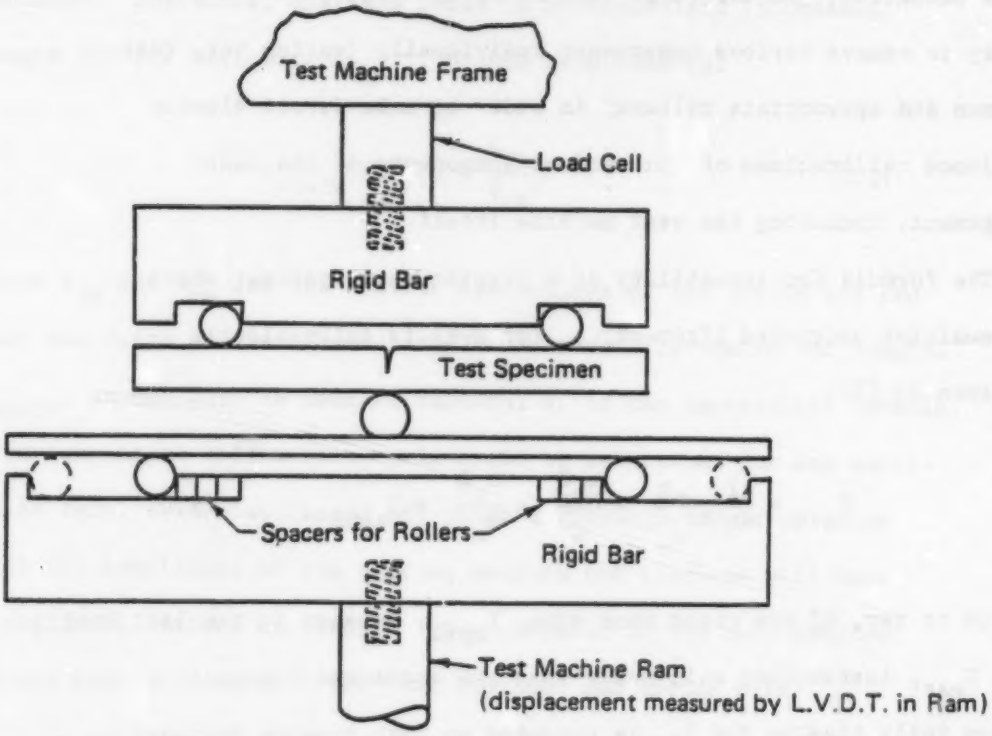

Fig. 18 Testing Machine.

The testing arrangement as shown in Figure 18 also permitted measuring load, from a load cell, and displacement, from the ram displacement, in a usual M.T.S. servo-hydraulic testing machine to produce a load displacement record for analysis of the stability of the situation. An important feature of the arrangement was the ability to remove various components individually (spring bar, test specimen and appropriate rollers) in order to make direct elastic compliance calibrations of the various components of the test arrangement, including the test machine itself.

The formula for instability of a 3-point bend specimen where the remaining uncracked ligament, b, (or W-a) is fully plastic was given in [71]

$$T_{mat} = \frac{dJ}{da}\frac{E}{\sigma_o^2} = \frac{2b^2 s}{W^3} - \frac{\theta_c E}{\sigma_o} = T_{appl} \qquad (5.1)$$

That is to say, if the right hand side, T_{appl}, exceeds in the left hand side, T_{mat}, instability will occur when the uncracked ligament becomes fully plastic <u>and</u> J_{IC} is exceeded so that tearing begins. This formula assumes a rigid testing machine (fixed displacements) and rigid test fixtures. On the other hand, the driving energy or force for instability comes from the elastic unloading of the bend specimen as the limit load diminishes due to crack extension. Thus T_{app} contains these influences through specimen proportions s, b and W, but in addition it is affected by the bend angle, θ_c, of the cracked section of the test specimen.

Now s as a factor in the above formula for T_{app} appears due to elastic compliance of the test specimen with no crack present. Adding compliance to the test arrangement by using in addition a spring bar is equivalent to adding compliance to the uncracked test specimen. Therefore, analysis leads to an equivalent (increased) length for the test bar, s_{equiv}, by the relationship,

$$s_{equiv} = s\left[1 + \frac{\delta_{SB}}{\delta_{TB}}\right] \qquad (5.2)$$

where δ_{SB} and δ_{TB} and the elastic deflections of the spring bar and test bar (with no crack) under the same load. The equivalent length, L_{equiv}, should then be used to replace, s, in the instability formula. From compliance calibrations this could be determined for any particular test. The compliances are given in Table 5 and it is noted that the compliance of the testing machine and fixtures will have a negligible effect on results (when compared to the much smaller spring constants of both the test specimen and spring bars).

In addition, θ_c, can be analyzed for any point on a load displacement record by subtracting elastic displacements for the uncracked test bar and spring bar from compliance calibration information and thus obtaining the displacement due to the crack That includes both the elastic and plastic deformations of the uncracked ligament sections. Then θ_c is obtained directly from geometry

$$\theta_c = \frac{4\delta_c}{s} \qquad (5.3)$$

Table 5. Instability Test Component Stiffnesses

Component	Size	Spring Constant
A) Test machine and fixtures	-	320,000 lbs/in
B) Test machine fixtures and spring bar	s_{SB} = 8"	30,047 lbs/in
	s_{SB} = 11"	13,035
	s_{SB} = 12"	10,000
	s_{SB} = 14"	6,472
	s_{SB} = 15 3/4"	4,638
C) Test bars	no crack	100,000 lbs/in
(s = 8")	a/W = 0.4	90,000
	a/W = 0.5	50,397
	a/W = 0.6	36,570
	a/W = 0.7	19,217

Thus all factors in T_{app} can be obtained directly from specimen dimensions, compliance calibrations and a given point on the load displacement record.

On the other hand, T_{mat} can be evaluated in a quite different manner. Following the definition

$$T_{mat} = \frac{\Delta J}{\Delta a} \frac{E}{\sigma_o^2} \tag{5.4}$$

where in this case J has been evaluated from the usual Rice et al. [36] pure bending analysis,

$$J = \frac{2}{bB} \text{Area} \tag{5.5}$$

where the "area" is the area under the load displacement record. And so the J was taken as

$$\Delta J = \frac{2}{bB} \Delta(\text{Area}) \tag{5.6}$$

On the other hand changes in crack length are less easy to evaluate. However, if limit load is assumed to be reached prior to beginning of crack extension (i.e., the J_{IC} point) then crack extension can be evaluated from the reduction in limit load due to crack growth. So, if the limit load is expressed as

$$P_L = \frac{4}{L} Ab^2 B\sigma_o \tag{5.7}$$

where A is a constant, differentiating for crack extensions gives

$$\Delta a = -\frac{b}{2}\frac{\Delta P_L}{P_L} \qquad (5.8)$$

Thus upon reaching limit load, Δa can be evaluated from one point to the next simply from the ligament size, b, and the change in limit load to, ΔP_L, and the limit load, P_L, itself. Hence substituting Equations (5.6) and (5.8) in (5.4) the T_{mat} was determined.

In all computations the original ligament size was used which implies that the analysis is limited to small crack extensions compared to the ligament size.

Moreover, the J-integral method itself becomes suspect if substantial crack extension occurs so that restriction to small crack extension was already implied.

RESULTS OF THE TESTING PROGRAM

The testing program is enumerated on Table 6. Test specimens were machined from a single piece of material which was originally cut from a rotor forging as a blank for a 4-T compact specimen of ASTM-A471 steel (i.e., Ni-Cr-Mo-V from Westinghouse Research as mentioned earlier). The cracking plane and direction was as intended in the 4-T blank so that results can be compared.

Specimens are numbered according to a positive location system. First slabs A, B, and C were removed from the blanks starting with the side opposite to the notch location in the 4-T blank. They were then sliced into specimens 1 through 6 for each slab, dividing the thickness dimension of the 4-T blank. Therefore, each test

Table 6. Tests and Results

Test No	a or a/W	Test Temp °C	s_{spring} Bar (in)	$s_{equivalent}$ (in)	$T_{matl.}$	$T_{appl.}$	Physical Stability	J_{Ic} in-lb/in^2
A-1	0.513	130	8.0	12.9	36.2	4.6	stable	700.0
A-2	0.516	130	8.0	12.9	40.8	5.8	stable	840.0
A-3	0.313	130	8.0	(did not reach P_{limit})			stable	-
A-4	0.411	130	8.0	(did not reach P_{limit})			stable	-
A-5	-	-	-	(broken in precracking)			-	-
A-6	0.411	130	12.0	34.0	34.5	41.5	unstable	720.0
B-1	0.427	230	12.0	34.0	35.5	51.5	unstable	600.0
B-2	0.518	130	11.0	27.1	33.0	18.7	stable	800.0
B-3	0.510	130	14.0	51.6	32.0	45.4	unstable	750.0
B-4	0.513	130	12.0	34.0	33.7	29.4	stable	725.0
B-5	0.510	130	13.0	42.1	34.9	33.2	unstable	850.0
B-6	0.510	130	0	8.0	41.0	-2.2	stable	650.0
C-1	0.502	230	13.0	42.1	36.5	35.6	(marginal)	720.0
C-2	0.516	230	14.0	51.6	38.5	45.2	unstable	750.0
C-3	0.505	230	12.0	34.0	34.6	26.6	stable	750.0
C-4	0.713	130	15.75	76.0	34.1	19.7	stable	600.0
C-5	0.620	130	15.75	76.0	40.8	40.1	unstable	600.0
C-6	0.706	130	13.0	42.1	35.5	7.5	stable	840.0

$T_{mat.}$ (average) = 36.1

Other dimensions of the 3 point bend specimens

depth, W = 1"
thickness, B = 1/2"
span, s = 8"

specimen is numbered with a letter and number identifying its location in the 4-T blank. Though care was taken in identifying with location, no effect of location was necessarily anticipated, nor was any found in test results to be described further here.

The test bars were machined with notches 0.2" deep and fatigue precracked to give crack depths, a, from 0.313" to 0.713" (the same as a/W values since W = 1"). Precracking loads were applied in the same testing fixtures but with the spring bar removed to give tension-tension loading of the notched side with maximum fatigue loads less than 1/2 the maximum (limit) load in each stability test.

Test temperatures were chosen to be 130°C and 230°C so that each is at least 100°C above the transition temperature of the material to avoid cleavage and thereby examine upper-shelf tearing instability behavior as intended here. Occasionally at 130°C some minor pop-in was noted, which was entirely absent at 230°C. However, tearing instability results of these tests show no substantial difference for the two temperatures, as may be noted later.

The next columns in Table 6 give the length of the spring used in each test and the equivalent span of the test specimen, as determined from Equation (5.2) and compliance calibration information on Table 5.

The equivalent span and other test information from load displacement records were then used to determine independently T_{mat} and T_{app} as described in the preceding section. Thus the columns for T_{mat} and T_{app} may be compared to determine according to the theory if unstable behavior is expected, i.e., if $T_{mat} \leq T_{app}$.

These results can be compared with the column of Table 6 marked stability where the actual physical state of stability observed in each test is listed. Such a comparison is shown in Figure 19. For each test a point is plotted from its T_{mat} vs T_{app} values. Lying on one or the other side of the 45° theory line is a theoretical prediction of stable or unstable as noted. On the other hand, actual physical behavior is noted for each point as solid points, stable and open points, unstable (and one half shaded points as marginal). It is noted that the agreement between physical behavior and theory is very good. Only two points exhibiting adjudged unstable physical behavior lie on the stable side but very close to the theory line. Moreover, the data on Figure 19 shows that T_{mat} is reasonably constant for a wide variety of variables (temperature and also a/W, s_{equiv}, etc., as the effective T_{app}). Thus this is felt to be a strong verification of the theory for a single type of specimen, the bend test.

Discussion of the Results

Physical behavior can be clarified and better understood by a more specific discussion of load-displacement records from the testing program. Furthermore, it is of special interest to make these observations for a sequence of tests, where temperature and test specimen dimensions including a/W are held constant and only the elastic compliance of the testing system is varied by varying only the spring bar length. Referring to Table 6 for a set of tests, where the temperature is 130°C and a/W is about 0.510 to 0.518), it is seen that test A-2 (s_{SB} = 8.0), B-2 (s_{SB} = 11.0), B-4 (s_{SB} = 12.0), B.5 (s_{SB} = 13.0) and B-3 (s_{SB} = 14.0) is such a set of tests.

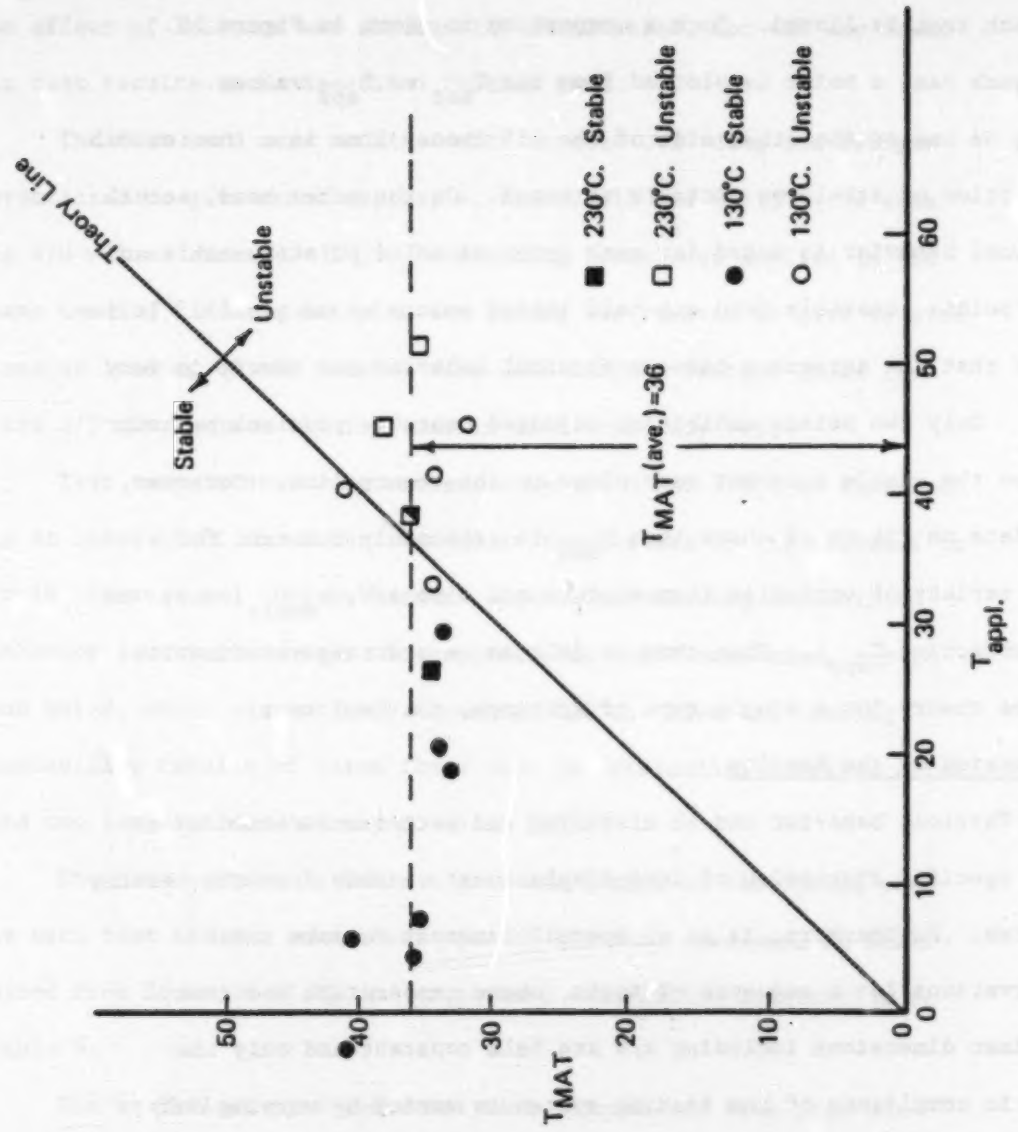

Fig. 19 T_{app} *vs* T_{mat} *for three point bending specimens.*

Figures 20 through 24 show load displacement records from these particular tests in the same respective order.

Tearing stability or instability depends on the character of the descending part of the load displacement records beyond the point of beginning of tearing.

As noted from Figures 20 and 24, as elastic compliance, i.e., spring bar length, is added, the descending portion of the records becomes steeper. Since the testing system is in displacement control as measured by an LVDT in the hydraulic ram, when sufficient elastic compliance is added to cause the descending load displacement record to be vertical, unstable behavior ensues. Noting the sequence of behaviors with added compliance in Figures 20 through 24, it is judged that Figures 23 and 24 are substantially unstable and that Figure 22 shows substantially stable behavior (though a short segment of vertical record occurs just after maximum load).

Moreover, when observing the test, unstable behavior as described above is occasioned by a sudden increase in crack size and deformation. It is by these observations and analysis of test records, such as Figure 20 through 24, that the "physical instability" was judged and recorded in the column entitled in Table 6.

It is relevant to observe here and emphasize that as described above and in the more general analysis [71,72], tearing instability is a system behavior, not only involving the local fracture characteristics of a test specimen (or structural component) but also the elastic compliance of the overall test specimen and loading system. Perhaps cleavage fracture instability is a local material instability

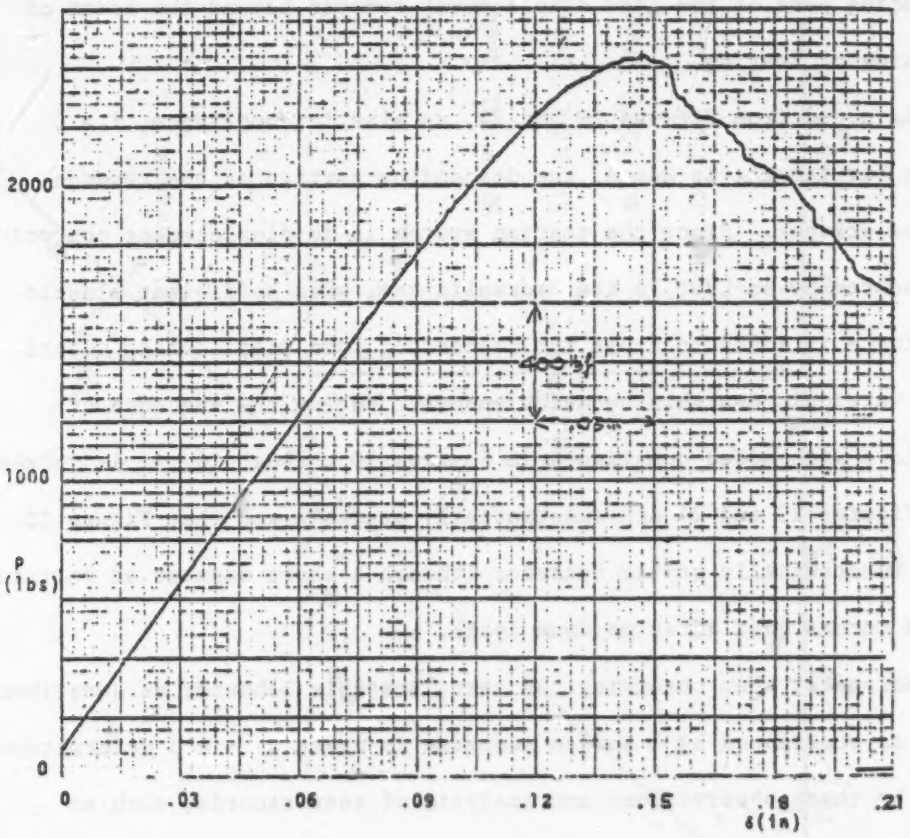

Fig. 20 P - δ Record for Test A-2 with s_{SB} = 8''

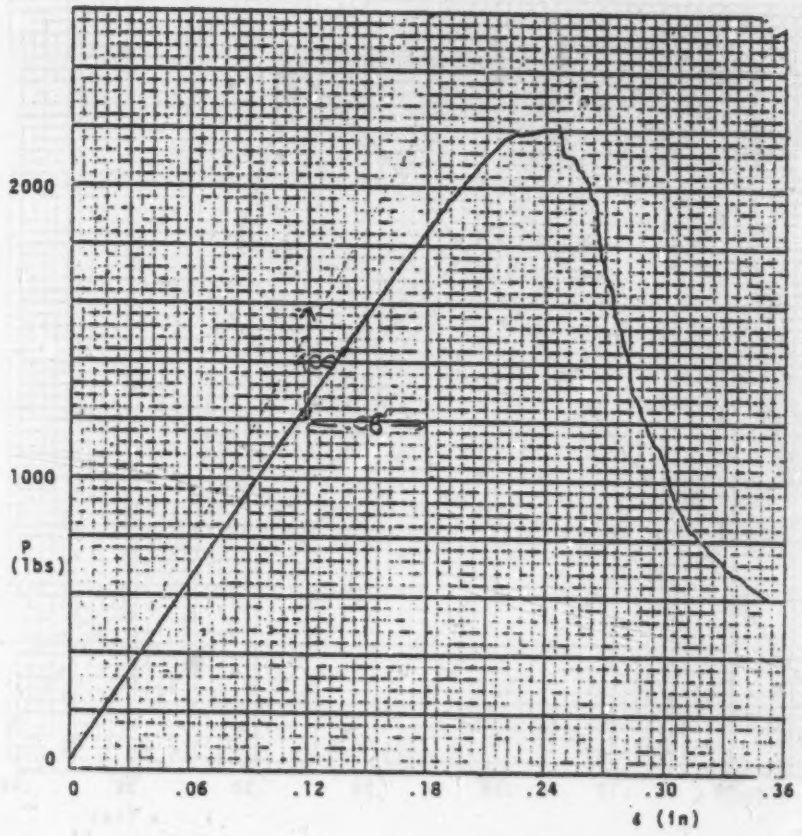

Fig. 21 P- δ Record for Test B-2 with s_{SB} *= 11".*

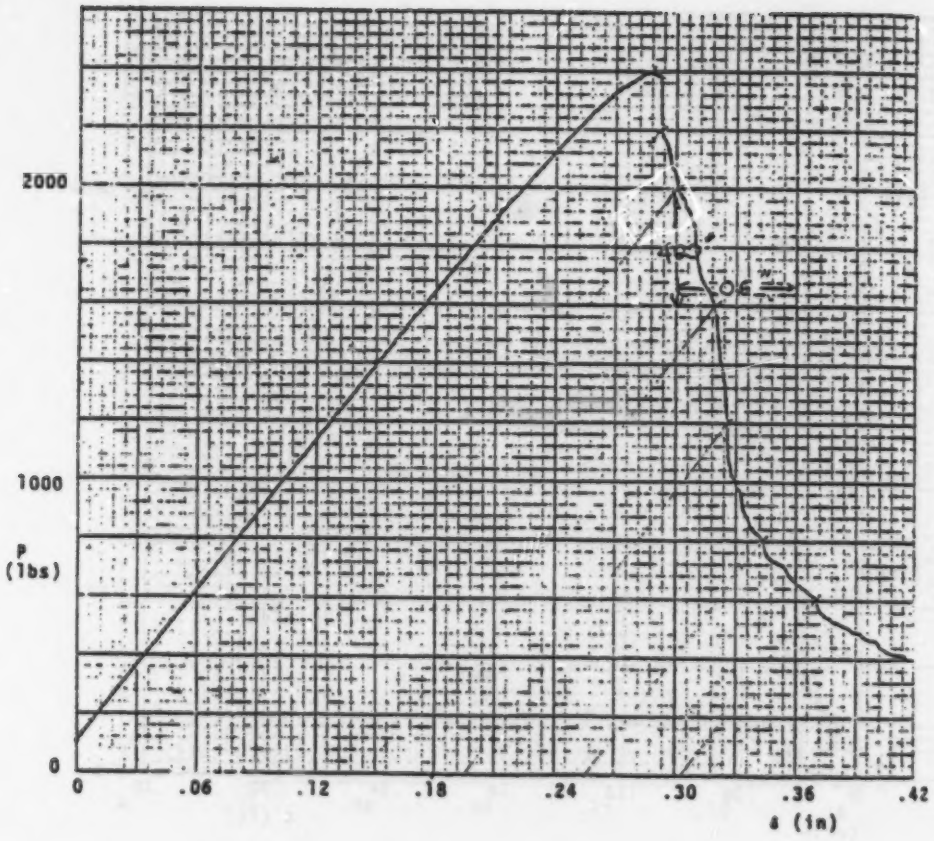

Fig. 22 P- δ Record for Test B-4 with s_{SB} = 12".

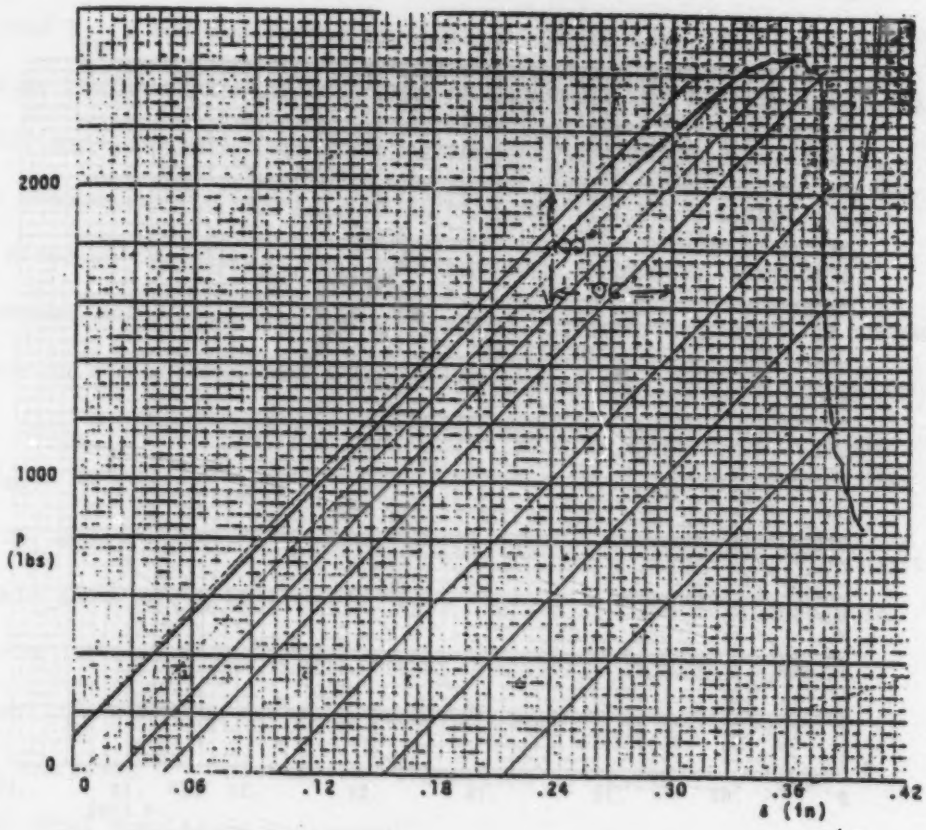

Fig. 23 P- δ Record for Test B-5 with e_{SB} = 13".

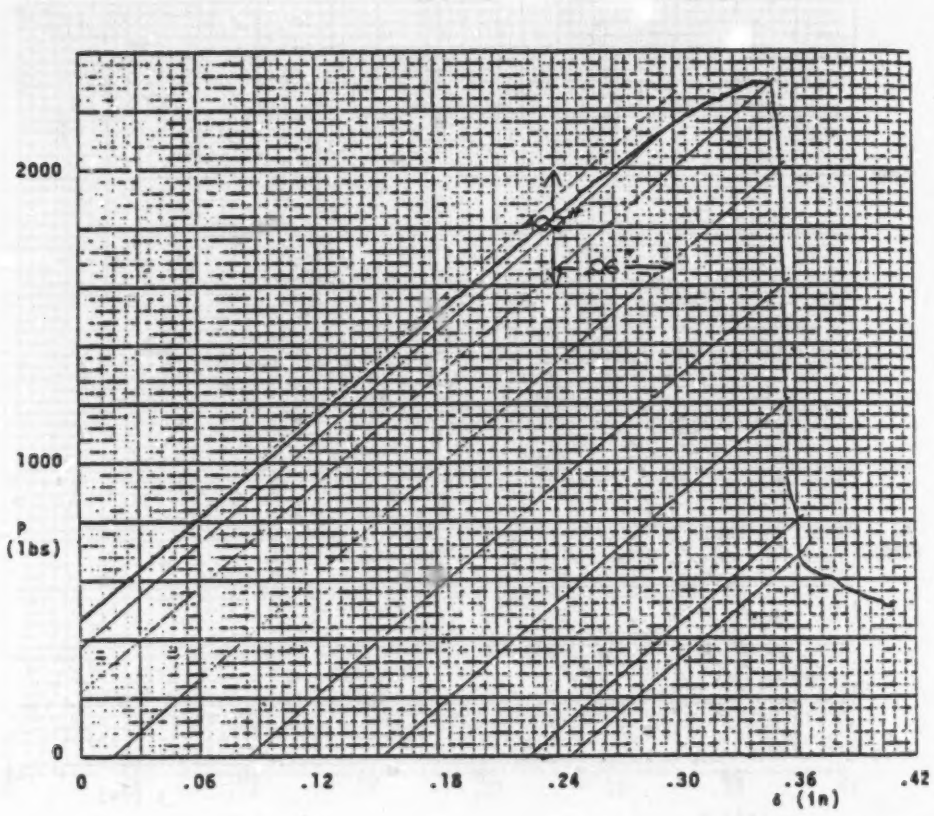

Fig. 24 P-δ Record for Test B-3 with s_{SB} = 14".

phenomenon, but it is clear here that tearing instability is a general system type of instability. Moreover, this testing program where in Table 6 and Figure 19 stability is judged by theory, comparing T_{mat} and T_{app}; and separately by physical instability behavior, clearly verifies the general approach taken by the theory of tearing instability [71,72] and especially that tearing instability is not treatable as a local phenomenon (in the J_{IC}, local critical field intensity, sense).

Although the tearing instability theory is seen as a system phenomenon, where transition from stable to unstable behavior is caused by varying the system compliance, other transitions caused by varying local test specimen dimensions are observed from the data in the test program.

For example, with other conditions identical, a switch from unstable behavior is observed in test C-6 and B-5 due to a change in a/W from 0.706 to 0.510 respectively; see Table 6. Since b = W-a, the implied effect is noted in Equation (5.1) as an increase in b which increases T_{app} causing the transition to instability (even though total compliance increases).

Two other pairs of specimens B-4 and A-6 and also C-3 and B-1 each exhibit a switch from stable to unstable due to a change in a/W from about 0.5 to 0.4. Both of these pairs were tested with spring bar lengths of 12", but one pair was at 130°C and the other at 230°C. Thus it was shown that the switching of behavior from stable to unstable was not appreciably effected by this temperature change, even though switching was induced by a relatively small change in a/W.

Again, these results were expected from the theory, Equation (5.1) and the fact that temperature changes on the upper shelf only weakly effect J-integral R-curve tearing behavior [17] (specifically, dJ/da) and flow stress, σ_o, and modulus, E. Therefore, the results in Table 6 verify the theory even more strongly than the conclusions drawn in the previous section herein.

Conclusions of the Initial Investigation of Tearing Instability

(1) Tearing instability in three point bend tests was shown to occur under fully-plastic plane-strain conditions.

(2) The tests demonstrated the systems aspects tearing instability by transition from stable to unstable behavior through changes in loading system compliance.

(3) The tests demonstrated the effect of local cracked section geometry on the tearing instability by transition from stable to unstable behavior through changes in a/W (i.e., remaining ligament size effect).

(4) A temperature change of 100°C (within upper shelf Charpy behavior range) was shown to not effect tearing instability behavior appreciably for the material tested, ASTM-A471 (Ni-Cr-Mo-V) rotor steel.

(5) All test behavior patterns observed tended to support the theory of "instability of the tearing mode of elastic plastic crack growth" as developed in [71] and its approach to the phenomenon.

5.3 ANALYSIS OF COMPACT TENSION SPECIMENS HY 130 NONGROWING CRACKS

As discussed before (section 2.1), the method presented here is exact under the assumptions of strict deformation theory. Although, the question still remained on how good the actual results obtained are, compared with those obtained from another exact method. Thus, values of J were compared with the so called J definition, J_{DEF} (section 1.4), obtained by the Begley and Landes multispecimen technique [14] for nongrowing cracks. This method is also exact on the basis of strict deformation theory.

Analysis of Data

In this section results are presented of values of J obtained by the present analysis and compared with those from other techniques, including the J_{DEF}.

In 1977, Landes et al. [54], presented a report of an experimental program conducted to evaluate the accuracy of some estimation techniques on J, by comparing them with the usual Begley and Landes [14] multi-specimen J-integral tests, or J-definition, J_{DEF}. Results were presented for compact three point bend, and center cracked tension specimens, covering a wide range of a/W, were machined, with a blunt notch, in order to eliminate any crack growth during the tests. The material used was HY 130 steel whose mechanical properties appear in Table 7.

Here, the P-δ records for the compact tension specimen are analyzed using the method presented in the previous chapters.

The analysis is done as follows:

1) In every P-δ record (for each particular a/W), the elastic part of the displacement was substracted, i.e., every point in the

Table 7. Mechanical and Chemical Properties of HY130 Steel Used by Landel et al. [54]

Mechanical Properties:

0.2% Yield Strength	(904.2 MN/m^2)	141.4 ksi
Ultimate Strength	(956.6 MN/m^2)	151.0 ksi
Percent Elongation	20.0%	
Reduction in Area	66.5%	
Room Temperature Charpy Energy	(107.4 J)	79 ft-lbs

Chemical Composition (Weight Percent)

C	Mn	P	S	Si	Ni	Cr	Mo	V	Al
0.12	0.79	.004	.005	.35	4.96	0.57	0.41	0.057	0.059

record was shifted to the left by an amount of P.C, where P is the load, and C is the compliance of the specimen

$$\delta - P\,C = \delta_{pl}$$

obtaining though the P vs δ_{pl} record.

2) Each record was then normalized in order to plot the F_1 function

$$\frac{PW}{b^2} \equiv F_1 \text{ vs } \frac{\delta_{pl}}{W}$$

the different curves obtained appear in Figure 25.

3) From the F_1 curves, it was noted that the ratio of any pair of them, was independent of the particular δ_{pl}, to within satisfactory accuracy (see section 4.4). So it was concluded that separability applied and then the F_1 function is

$$F_1\left(\frac{\delta_{pl}}{W}, \frac{a}{W}\right) = g_1\left(\frac{a}{W}\right) \quad H\left(\frac{\delta_{pl}}{W}\right) \tag{5.9}$$

Then

$$\frac{\partial F_1}{\partial a/W} = g_1'(a/W)\ H\left(\frac{\delta_{pl}}{W}\right) = \frac{g_1'}{g_1}\ F_1 \tag{5.10}$$

and so replacing Equation (5.10) in the expression for J, Equation (2.23) gives

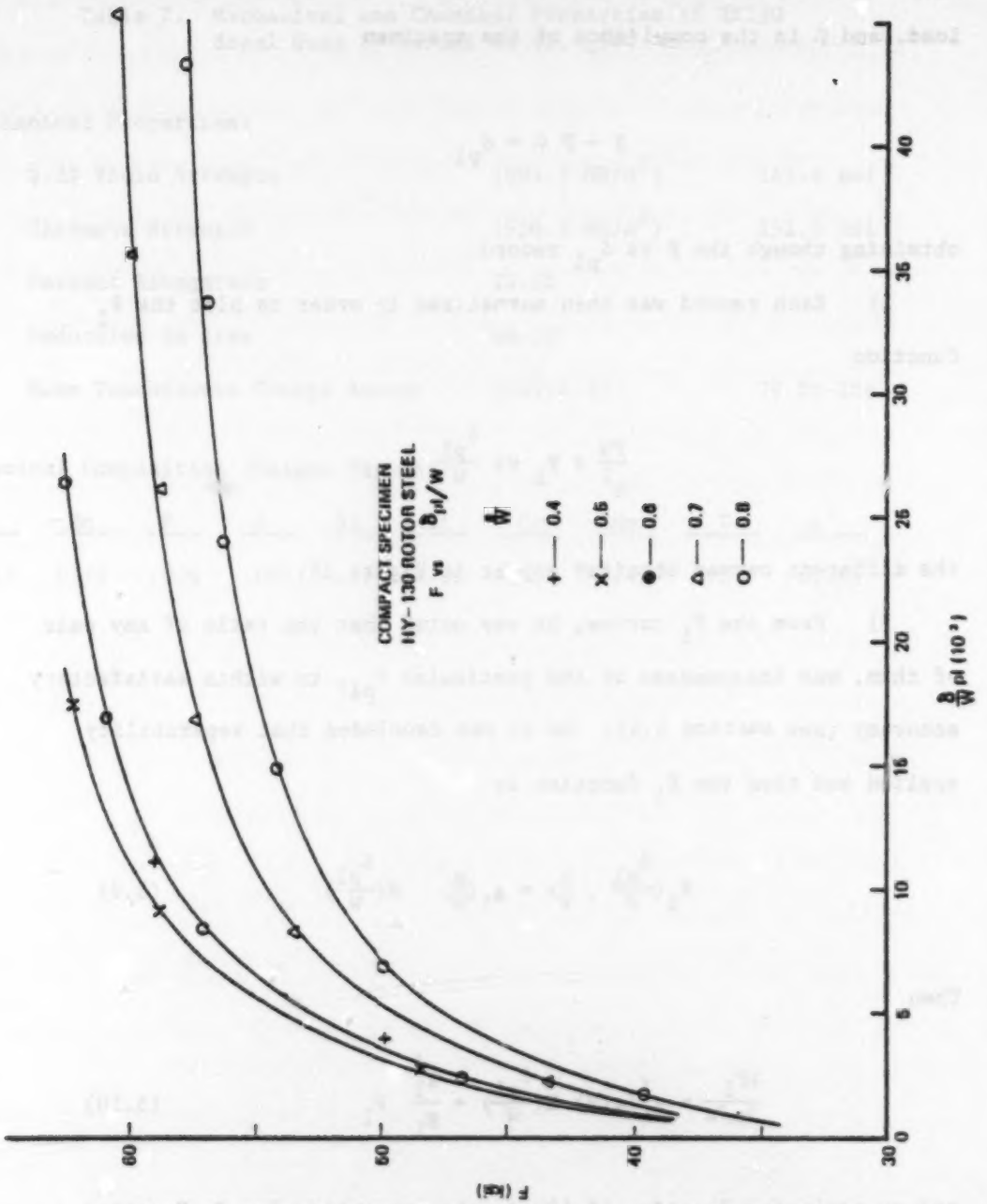

Fig. 25 F- function vs normalized displacement for HY 130 compact specimens.

$$J = G + \frac{2}{b}\int_0^{\delta_{pl}} P d\delta_{pl} - \frac{b^2}{W^2}\frac{g_1'}{g_1}\int_0^{\delta_{pl}} F_1 d\delta_{pl}$$

or

$$J = G + \frac{1}{b}\left(2 - \frac{b}{W}\frac{g_1'}{g_1}\right)\int_0^{\delta_{pl}} P d\delta_{pl} \qquad (5.11)$$

Thus the term $\frac{g_1'}{g_1}$ was evaluated at $\delta_{pl} = 40.10^{-3}$ inches and the J value was obtained using Equation (5.11).

4) Values of J were also obtained by calculating the η_{pl} of Equation (5.12),

$$J = G + \frac{\eta_{pl}}{b}\int_0^{\delta_{pl}} P d\delta_{pl} \qquad (5.12)$$

from the small scale yielding analysis, η_{plssy} (Table 3).

In Table 8 the results of the present analysis J_{CC} as in Equation (5.11), J_{est} using η_{plssy}, in Equation (5.12) and the five different values of J (including J_{DEF}) appearing in [54] are shown.

Discussion of the Results

As it can be seen from Table 8 the values of J obtained by the present method J_{CC} and those obtained by using the η_{plssy}, J_{est}, come the closest to J_{DEF}.

Of the other estimation techniques, the closest to J_{DEF} is the simplified Merkle-Corten (MC)[67] value J_{SMC}. Now, the J_{SMC} is obtained by neglecting the potential energy ($\int_0^{\delta} \delta\, dP = 0$). This means that a flat P-δ record is assumed. Obviously there is no physical explanation on why this type of behavior gives a better result than the real one (actual P-δ record).

Table 8. Comparison of J From Different Techniques
(J in (in lb/inch^2) Deflection (10^3 inches)

a/W		20	40	60	80	100	120	140
.4	J_{DEF}	523	1595	2996				
	J_2	366	1351	2680				
	J_{SMC}	423	1562	3099				
	J_{MC}	503	791	3432				
	J_5	507	1736	3287				
	J_{CC}	507	1715	3118				
	J_{est}	510	1771	3313				
.5	J_{DEF}	322	1219	2375	5045			
	J_2	277	1060	2143	3357			
	J_{SMC}	313	1200	2427	3801			
	J_{MC}	350	1310	2596	4000			
	J_5	308	1256	2462	3728			
	J_{CC}	322	1195	2343	3579			
	J_{est}	322	1202	2369	3635			
.6	J_{DEF}	235	892	1800	2823	3858		
	J_2	209	799	1637	2590	3569		
	J_{SMC}	231	880	1811	2865	3948		
	J_{MC}	245	936	1891	2959	4052		
	J_5	247	919	1829	2879	3957		
	J_{CC}	234	888	1794	2809	3846		
	J_{est}	234	887	1788	2794	3822		

Table 8 (continued)

a/W		20	40	60	80	100	120	140
.7	J_{DEF}	163	615	1270	2025	2762	3571	4373
	J_2	146	565	1162	1823	2555	3267	4002
	J_{SMC}	157	609	1254	1967	2757	3526	4319
	J_{MC}	152	585	1201	1898	2635	3360	4125
	J_5	166	628	1279	2022	2828	3718	4613
	J_{CC}	I68	643	1306	2032	2831	3607	4408
	J_{est}	167	670	1296	2010	2794	3557	4342
.8	J_{DEF}	90	381	790	1228	1733	2175	2642
	J_2	92	353	717	1135	1590	2038	2492
	J_{SMC}	97	371	754	1194	1673	2144	2622
	J_{MC}	103	389	784	1231	1714	2188	2667
	J_5	102	383	780	1234	1731	2275	2865
	J_{CC}	105	401	808	1270	1770	2261	2759
	J_{est}	105	399	799	1249	1734	2210	2693

$$J_{DEF} = -\frac{1}{B}\frac{dU}{da} \qquad J_2 = \frac{2A}{Bb} \qquad J_{SMC} = \frac{1+\alpha}{1+\alpha^2}\,\frac{2A}{Bb}$$

$$J_{MC} = G + \frac{2}{Bb}\,\frac{1+\alpha}{1+\alpha^2}\,A_{pl} + \frac{2}{b}\,\alpha\,\frac{(1-2\alpha-\alpha^2)}{(1+\alpha^2)^2}\int_0^{P/B} \delta_p\, d\,\frac{P}{B}$$

$$J_5 = \frac{K_I^2}{E} \quad \text{secant offset} \qquad J_{CC} = G + \frac{2}{bB}\,A_{pl} - \frac{b^2}{W^2}\int_0^{\delta_{pl}} \frac{\partial F}{\partial (a/W)}\,.$$

$$J_{est} = G + \frac{(2+\varepsilon)}{bB}\,A_{pl} \text{ with } \varepsilon \text{ from ssy.}$$

On the other hand, it is interesting to note the good agreement between the J_{est} and the J_{DEF}.

This matter needs further exploration but the results seem to indicate that for bending configurations the approach works very well. This agreement is possibly related to the fact that for bending configurations, η does not vary very much with n. In fact for the pure bending case Rice's analysis [36] gives $\eta = 2$ for all n ($n = 1...\infty$). Thus the η from ssy, η_{plssy}, may represent a good estimation for η, giving though a very good result for J.

At the same time, this agreement may explain, at least for bending, the success of McCabe's tangent offset method [52].

Note that the value of J obtained with this approach J_{est},

$$J_{est} = G + \frac{(2+\varepsilon)}{b} \int_0^{\delta_{pl}} P d\delta_{pl} \qquad (5.13)$$

is not just J for ssy. But rather the small correction term ε in Equation (5.13), is taken from the ssy analysis.

Finally, in Figure 26, values of η_{plssy} are shown, as well as η_{pl} factors obtained from the simplified (see above) MC analysis [67]. It can be noted that both parameters coincide for values of a/W above .7, but for smaller values of a/W, the η_{plssy} are smaller giving though smaller values of J. This result is consistent with the results of Table 8, where it can be seen that the simplified MC analysis overestimates J for values of a/W below .7.

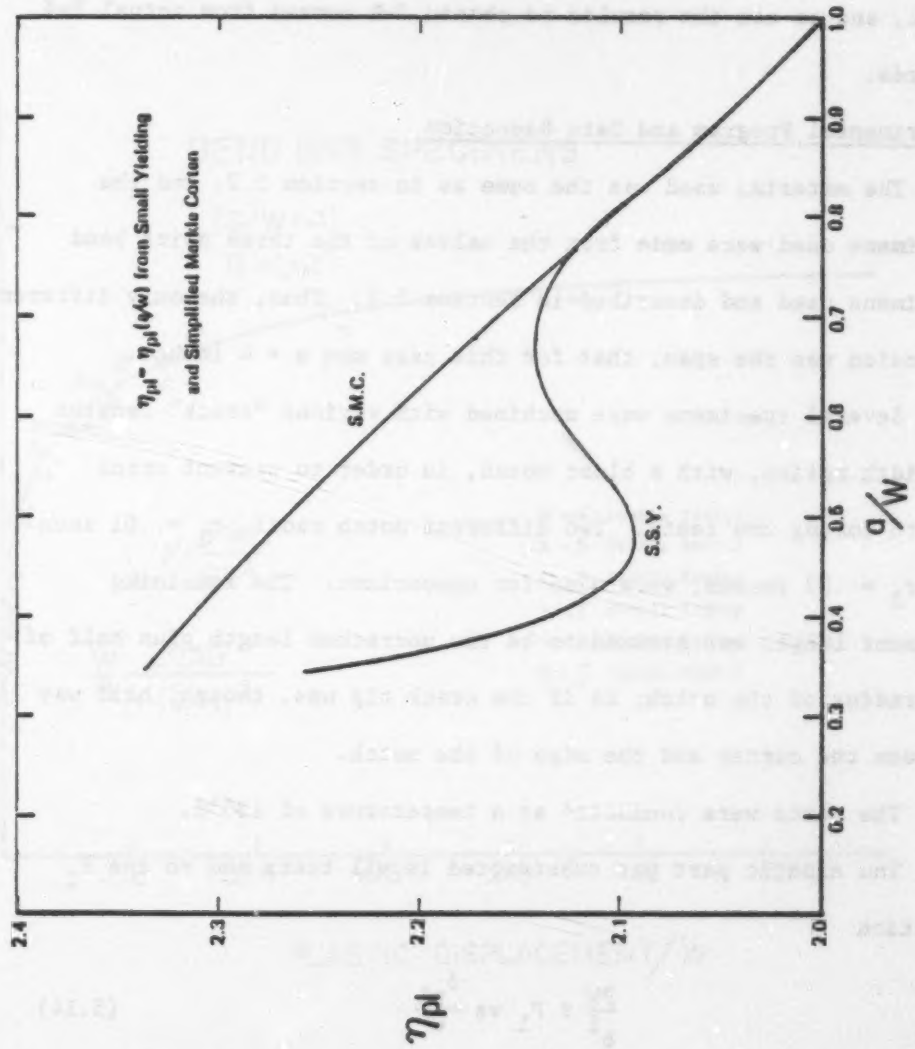

Fig. 26 The η_{pl} factor from small scale yielding and simplified Merkle Corten analysis [67] .

5.4 ANALYSIS OF THREE POINT BEND SPECIMENS s/W = 4

Ni-Cr-Mo-V ROTOR STEEL

The aim of this experimental program was to determine F_1 functions for the three point bend specimens of a Ni-Cr-Mo-V rotor steel, and to use the results to obtain J-R curves from actual P-δ records.

Experimental Program and Data Reduction

The material used was the same as in section 5.2, and the specimens used were made from the halves of the three point bend specimens used and described in section 5.2. Thus, the only different dimension was the span, that for this case was s = 4 inches.

Several specimens were machined with various "crack" lengths to width ratios, with a blunt notch, in order to prevent crack growth during the tests. Two different notch radii, r_1 = .01 inch and r_2 = .02 inches, were used for comparison. The remaining ligament length was assumed to be the uncracked length plus half of the radius of the notch; as if the crack tip was, though, half way between the center and the edge of the notch.

The tests were conducted at a temperature of 130°C.

The elastic part was substracted in all tests and so the F_1 function

$$\frac{PW}{b^2} \equiv F_1 \text{ vs } \frac{\delta_{pl}}{W} \tag{5.14}$$

was obtained for all a/W. They are shown in Figure 27. As it can be seen, the F_1 function is independent of a/W (to within the accuracy required).

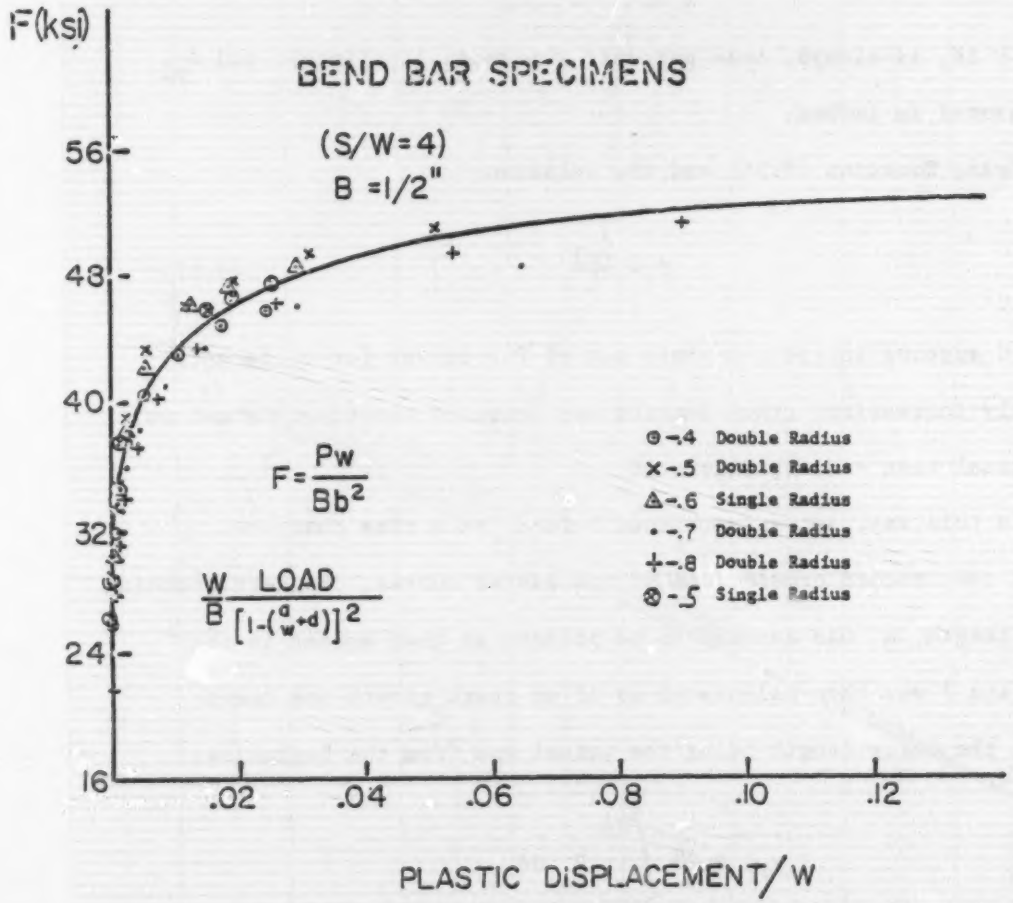

Fig. 27 F- function vs. Normalized Plastic Displacement for Ni-Cr-Mo-V 3P Bending Specimen (s/W = 4).

The curve was fitted with a usual numerical technique, giving the expression

$$\frac{PW}{b^2} = F = 63000 \left(\frac{\delta_{pl}}{W}\right)^{.08} \tag{5.15}$$

and so

$$P = \frac{b^2}{W} 63000 \left(\frac{\delta_{pl}}{W}\right)^{.08} \tag{5.16}$$

where P is, as always, load per unit thickness (lbs/inch), and δ_{pl} is measured in inches.

Using Equation (5.16) and the relation

$$P = \frac{\delta_{el}}{C} \tag{5.17}$$

where C appears in [30], a whole set of P-δ curves for different, slightly increasing, crack lengths was obtained and superimposed on the actual test record, Figure 28.

In this way, as was mentioned before, each time that the actual test record crossed one of the master curves, the corresponding crack length, a, was assumed to be present at that moment in the test, and J was then calculated as if no crack growth had taken place; the crack length being the actual one from the beginning.

$$J = G + \frac{2b}{W} \int_0^{\delta_{pl}} F_1 \, d\delta_{pl}$$

or (5.18)

$$J = G + \frac{2}{b} \int_0^{\delta_{pl}} P d\delta_{pl}$$

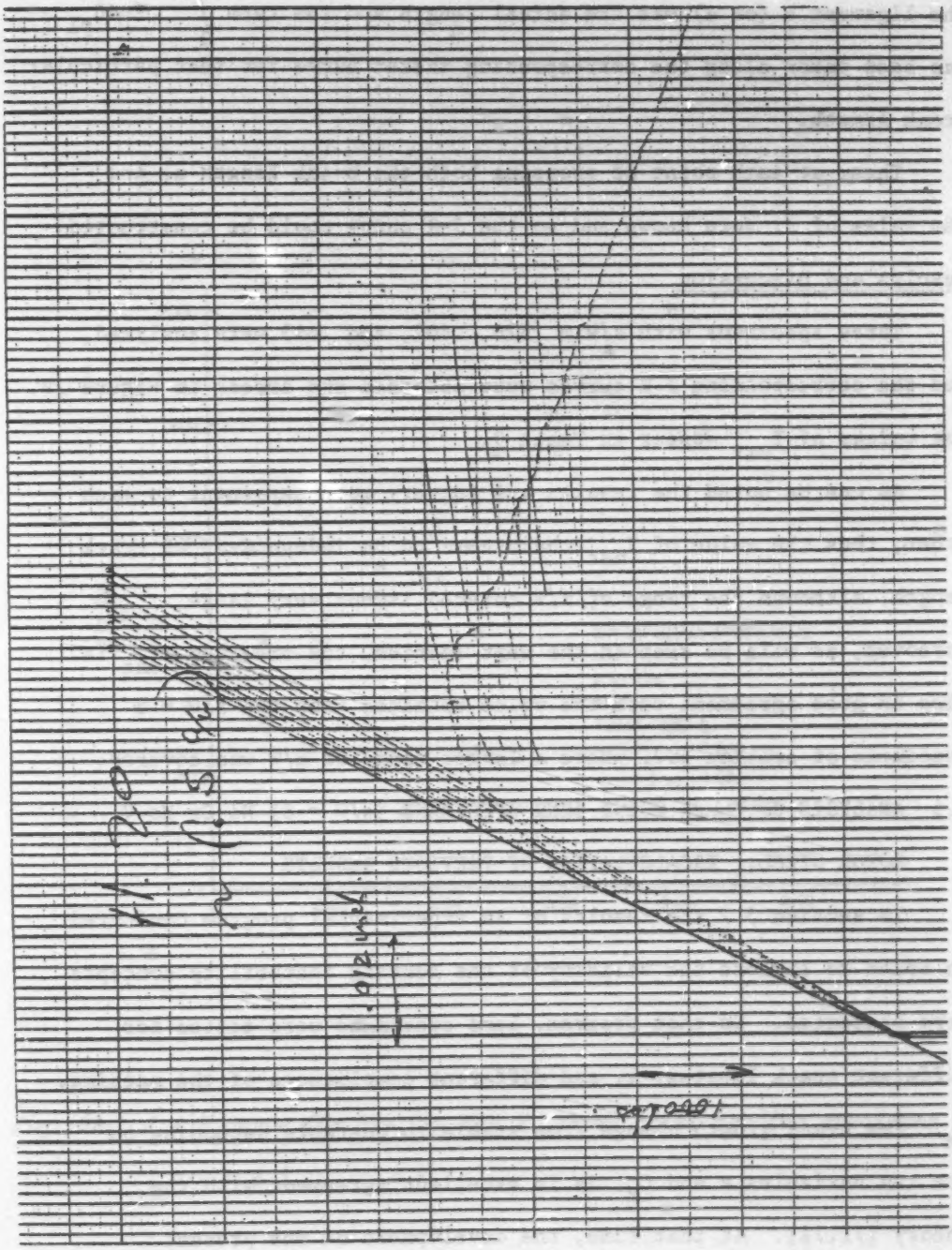

Fig. 28 P - δ record for Test H. 20

The ligament b (or a) was the actual length and the term $\int_0^{\delta_{pl}} P \, d\delta_{pl}$ has been taken along the corresponding master curve for that particular crack length.

Thus, at each point of crossing both the crack length a, and the value of J, were known and so the J-R curve could be constructed.

Results and Discussion

Three specimens with a/W = .526, .602, and .643 were analyzed, and the corresponding J-R curves were obtained and appear in Figure 29. The values of T_{mat} appear in Table 9.

As can be noted the results are in very good agreement to each other, thus the value of T_{mat} that seems to be independent of crack length, although the range of a/W covered is not very large. Moreover, as will be seen in the next section, the observed T_{mat} is also in good agreement with the value obtained from the s/W = 8 specimens of section 5.2, where a larger range of a/W was covered.

5.5 ANALYSIS OF THREE POINT BEND SPECIMENS (s/W = 8) Ni-Cr-Mo-V ROTOR STEEL. RECALCULATION OF PREVIOUS RESULTS

In section 5.2 the results of an experimental program conducted in order to explore the validity of the tearing instability concepts were presented. In that program, bend specimens were tested for different crack lengths, a, and different compliances of the machine, C_M. The crack growth change from stable to unstable depending on the two variables a and C_M, is in excellent agreement with the theory [71,72]. At that time, the development of the present method was in an early stage and some approximations were made (e.g., Equation (5.8)).

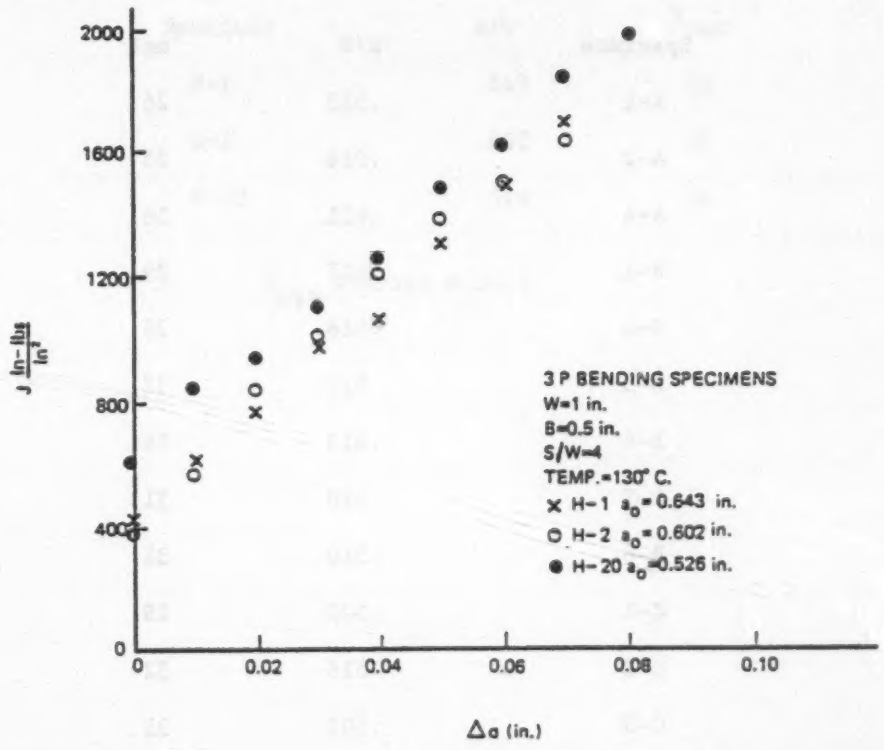

Fig. 29 J - R curve for Ni- Cr- Mo- V three point bending specimens (s/W = 4).

Table 9. T_{mat} Values Ni-Cr-Mo-V Rotor Steel
3 Point Bending Specimens

s/W = 8

Specimen	a/W	T_{mat}
A-1	.513	26
A-2	.516	25
A-6	.411	36
B-1	.427	29
B-2	.518	28
B-3	.510	32
B-4	.513	26
B-5	.510	31
B-6	.510	31
C-1	.502	29
C-2	.516	32
C-3	.505	31
C-4	.713	25
C-5	.620	31
C-4	.706	26

T_{mat} average = 29.2

Table 9. (continued)

s/W = 4

Specimen	a/W	T_{mat}
H-1	.643	29
H-2	.602	31
H-20	.526	34

T_{mat} average = 31.3

Consequently, here the 15 P-δ records were reanalyzed using the method as fully developed.

Analysis and Experimental Program

In section 5.4, the F_1 function obtained for the three-point bend specimen (3PB) s/W = 4, was

$$\frac{PW}{b^2} \equiv F_1\left(\frac{\delta_{pl}}{W}\right) = 63000\left(\frac{\delta_{pl}}{W}\right)^{.08} \qquad (5.19)$$

However, this result can be modified for the 3PB specimens described in section 5.2 (all dimensions the same, except for the span s = 8). The modification involves replacing W with s in Equation (5.19) so that Ps is then directly related to the moment applied to the cracked section, and δ_{pl}/s is directly related to the plastic angle imposed.

The result is:

$$\frac{Ps}{b^2} = F_{1s}\left(\frac{\delta_{pl}}{s}\right) = 281556\left(\frac{\delta_{pl}}{s}\right)^{.08} \qquad (5.20)$$

This form of the F function, in terms of s instead of W is more general and allows the span to be variable.

Once the F_1 function was obtained, the analysis proceeded in the same way as in the previous section. A whole set of P-δ records, for slightly different crack lengths (increased by equal steps), was obtained using Equation (5.20) and the given relation between P and δ_{el} for this particular configuration [30]. The set was again superimposed on the test record and as before, each time

that the actual P-δ record crossed one of the master curves, that particular a was assumed to be the current crack length at the moment, and J was calculated by

$$J = G + \frac{2b}{W} \int_0^{\delta_{pl}} F_1 d\delta_{pl}$$

or

$$J = G + \frac{2}{b} \int_0^{\delta_{pl}} P d\delta_{pl} \qquad (5.21)$$

were, as before, in Equation (5.21), the crack length (or remaining ligament) was taken as the current value and the $\int_0^{\delta_{pl}} P d\delta_{pl}$ term was evaluated along the particular master curve.

Results

The results of the experimental program appear in Table 9. As can be noted the average value of 29.2 of T_{mat}, is in good agreement with the value of 36.1 obtained previously (section 5.2, Table 6), using a simplified version of the method. Also the average T_{mat}, 29.2, is in excellent agreement with the value 31.3 obtained for 3PB specimen s/W = 4 of section 5.4.

So far T_{mat} values were obtained for a wide range of a/W and for 3PB configurations with two different spans obtaining basically the same result.

At the same time it must be emphasized the fairly good agreement of the T_{mat} of section 5.2, 36.1 and the average value obtained in this program and in section 5.4 of 30.2. Taking into account the much simplified version of the method used.

5.6 ANALYSIS OF H.Y. 130 STEEL COMPACT SPECIMENS

In the previous sections, the calibration function method has been applied to different situations. First values of J have been obtained for nongrowing crack type tests, (section 5.3), and then comparison of J values were made with other methods. Further, J-R curves were obtained for different kinds of 3PB specimens (section 5.4 and 5.5), and in this study of bending the F function obtained from one configuration was used to analyze another.

In order to extend these previous results, this method will be used to determine J-R curves directly from the load-displacement records reported previously by Gudas et al [83] on H.Y. 130 steel.

The H.Y. 130 Test Records for Analysis

A set of 11 load- displacement records for tests of H.Y. 130 steel 1 T compact specimens was furnished by NSRDC from their experimental program [83]. The specimens covered a range of a/W from .533 to .790 and the face grooving was 0 to 12.5 percent (see Table 10). The records obtained were not the usual simple P vs δ plots, but instead they were normalized and given as functions of the variables

$$\frac{PW}{b_o^2} \text{ vs } (\delta - PC_o)/W = \delta^* \qquad (5.22)$$

where P is, as usual load per unit thickness, and C_o is the value of the compliance for the initial crack length. Note that δ^* represents the normalized plastic displacement, δ_{pl}/W, only for points on the record prior to initiation of crack growth. For points beyond that, that δ_{pl}/W is given by

$$(\delta - PC)/W = \delta_{pl}/W \qquad (5.23)$$

where C is to be taken for the current crack length.

Step By Step Analysis of the Records

The analysis proceeded as follows:

1) The normalized records were compared, in order to get the degree of dependence of the F function on a/W. This dependence could not be determined, the trend being masked by normal (small) experimental error (this includes error from instrumentation, material variability, etc.). Thus, it was decided to neglect this dependence, since its effect must be quite small in any event.

2) Points of initiation of crack growth were identified by comparing the particular record, as mentioned above, with others of longer initial crack lengths. Crack growth was observed to start when the curves deviated from each other.

3) The records from tests with longer initial crack lengths served to establish the initial part of the F function. But a longer (to higher δ_{pl}/W values) F plot was needed. Consequently the initial part was extended by fitting a monomial power law relation to the normalized load and the normalized displacement (see sections 5.4 and 5.5), and in this in order to extrapolate them.

4) Once the F function was obtained the analysis proceeded as in the previous sections. Curves were scaled after eliminating the linear relationship $\delta_{el} = PC$ to fit the expression for the plastic part of the displacement

$$P = \frac{b^2}{W} F(\delta_{pl}/W) \qquad (5.24)$$

Thus a whole set of PW/b_o^2 vs $(\delta - PC_o)/W$ master curves was obtained and superimposed on an actual test record.

5) As was done before, every time that the actual test record crossed one master curve, the particular crack length for that master curve was assumed to be present in the actual test at the moment.

6) The J-integral was calculated for each point as

$$J = G + \frac{2}{b}\int_0^{\delta_{pl}} P \, d\delta_{pl} \qquad (5.25)$$

$$= G + 2\,\frac{b}{W}\int_0^{\delta_{pl}} F \, d\delta_{pl}$$

where, as usual, b was taken as the current remaining ligament, and the integral was evaluted along the particular corresponding master curve.

Discussion of the Method

At this point, some further discussion of the method is appropriate. Equation (5.24) was obtained by assuming that the F function is independent of a/W. This assumption appeared to have an almost negligible effect on the scaling of the curves. Thus in fact, F is, at most, very weakly dependent on a/W and so the scaling is reasonably accurately given by

$$P_1 = P_o \left(\frac{b_1}{b_o}\right)^2 \quad \text{(at any constant } \delta_{pl}) \qquad (5.26)$$

Consequently the values of the crack lengths, a (or Δa), obtained are not seriously in error because of this assumption. On the other hand, for the values of J, the approximations made above, do have some impact.

In fact, by neglecting the dependence of F on a/W, the third term in Equation (2.23), i.e.

$$-\frac{b^2}{W^2}\int_0^{\delta_{pl}} \frac{\partial F}{\partial a/W}\, d\delta_{pl}$$

is neglected. For a/W of 0.533 this error is estimated to be 7% of the plastic part of J, J_{pl}, and it will diminish with higher a/W.

Results

The results of the analysis of H.Y. 130 compact specimens appear in Table 10. As can be seen, the final crack extension values obtained with this method, Δa_{CC}, are in very good agreement with heat tinting measurement, Δa_{HT}. The results seem to be even better than those obtained by unloading compliance, Δa_{UC}.

The values of T_{mat} obtained are, in general, smaller by a factor of about 2, than those presented by Gudas et al in [83]. However, Gudas did not correct J values for the effects of crack extension. On the other hand, the J_{IC} values agree well with those in [83] as would be expected.

It is also to be noted, that for the face grooved specimens, T_{mat} values were also smaller by a factor of about 2, but in this case the J_{IC} values are lower than those in [83]. This leaves the desirability of face grooves an ambiguous matter. It will be discussed further later.

Table 10. Experimental Results on HY130 Steel Compact Tension Specimen

Specimen	a/W	F.G%	Cal Curve Method J_{IC}	Cal Curve Method dJ/da	Cal Curve Method T_{mat}	Gudas et al. [83] J_{IC}	Gudas et al. [83] dJ/da	Gudas et al. [83] T_{mat}	Δa_{UC}	Δa_{HT}	Δa_{CC}
T 3	.554	0	982	7925	12	976	14632	22	55	89	82
T 4	.652	0	1015	8305	13	998	18497	28	53	70	71
T 7	.788	0	734	11637	18	797	27510	42	43	61	71
T19	.539	12.5	813	6086	9	921	12369	19	52	55	57
T20	.533	12.5	828	11229	17	835	15938	24	53	41	39
T 8	.652	12.5	834	7928	12	934	16344	25	54	57	50
T12	.646	12.5	725	8227	13	823	13664	21	101	104	*
T21	.647	12.5	862	5261	8	919	12011	20	58	62	58
T 2	.786	12.5	608	6343	10	844	12084	19	49	52	57
T 5	.781	12.5	675	5867	9	832	15132	24	59	57	73
T28	.790	12.5	669	6710	10	802	15399	25	49	49	54

Δa_{UC} = Δa from Unloading Compliance

Δa_{HT} = Δa from Heat Limiting

Δa_{CC} = Δa from Calibration Curve Method

*Test Record Incomplete

5.7 ANALYSIS OF HY.130 STEEL COMPACT SPECIMENS BY AN EXPERIMENTALLY OBTAINED CALIBRATION FUNCTION

To test the validity of the proposed calibration function approach, a program was conducted by Joyce Ernst and Paris [76]. The experiments were performed at the U.S. Naval Academy. The objective of this work was to experimentally develop for HY.130 steel compact specimens an F-function and to use this experimental function to obtain J-R curves from available P-δ records.

Eight 1/2 T compact specimens with crack lengths from a/W = 0.59 to 0.94 were used to generate a series of load displacement records which were assembled in a computer file as the calibration function for geometrically similar compact specimens of this steel. Using this file, J-resistance curves (J-R curves) for 1T compact specimens were then obtained directly from the load displacement records and compared with unloading compliance J-R curves obtained for the same specimens.

Analysis

In section 2.2, the total displacement δ, was separated into its elastic and plastic parts giving though two expressions for P

$$P = \frac{\delta_{el}}{C}$$

and using F_1 (5.27)

$$P = \frac{b^2}{W} F_1\left(\frac{\delta_{pl}}{W}, \frac{a}{W}\right)$$

Consequently the expression for J is

$$J = G + 2\frac{b}{w}\int_0^{\delta_{pl}} F_1 d\delta_{pl} - \frac{b^2}{w^2}\int_0^{\delta_{pl}} \frac{\partial F}{\partial a/W}\, d\delta_{pl} \qquad (5.28)$$

The advantage of this approach, as discussed previously is that the first two terms can be accurately determined, and is only the last term that is less than 10% of the total value, which has to be evaluated by some numerical procedure. This implies that even a rather big error in the procedure results in a very small one in the total value of J. Also, because of the way the function F_1 is defined, a weak dependence of F_1 on a/W is expected and separability of the function remains as a possibility (sections 4.3 and 4.4).

In this work a somehow different approach was taken. Instead of separating δ into δ_{el} and δ_{pl}, a total displacement variable was used, giving so only one expression for the load P

$$P = \frac{b^2}{w} F\left(\frac{\delta}{W}, \frac{a}{W}\right) \qquad (5.29)$$

and consequently the expression for J is

$$J = \frac{2b}{W}\int_0^{\delta} F d\delta - \left(\frac{b}{W}\right)^2 \int_0^{\delta} \frac{\partial F}{\partial a/W}\, d\delta \qquad (5.30)$$

With this approach, the F function is not in general separable but as an advantage, no separation of δ, into elastic and plastic parts during the analysis of the test is needed.

Now differentiation of Equations (5.29) and (5.30) gives

$$dJ = \left(\frac{2b}{W} F - \frac{b^2}{W^2} \frac{\partial F}{\partial a/W}\right) d\delta +$$

$$+\left[-\int_o^\delta \frac{2}{W} F \, d\delta + \int_o^\delta \frac{4b}{W^2} \frac{\partial F}{\partial a/W} \, d\delta - \int_o^\delta \frac{b^2}{W^2} \frac{\partial^2 F}{\partial a/W^2} \, d\delta \right] da \tag{5.31}$$

and

$$da = \frac{\left(\frac{b}{W}\right)^2 \frac{\partial F}{\partial a/W} d\delta - dP}{\frac{2b}{W} F - \left(\frac{b}{W}\right)^2 \frac{\partial F}{\partial a/W}} \tag{5.32}$$

Using Equations (5.31) and (5.32) the T_{mat} can be calculated at each point, by the expression

$$T_{mat} = \frac{dJ}{da} \frac{E}{\sigma_o^2}$$

As another possibility, discrete versions of Equations (5.31) and (5.32) can be written, obtaining thus a continuous J-R curve, and from there the T_{mat} can be calculated. This will follow later.

Experimental Program

The experimental program was conducted at the U.S. Naval Academy. HY.130 plate supplied in 25 mm thickness was used for all tests. The chemical composition of the plate and the mechanical properties are presented in Table 11.

Table 11. Mechanical and Chemical Properties of HY130 Steel Used by Joyce et al. [76]

	Components (Weight Percent)												
Code	C	Mn	P	Si	Ni	Cr	Mo	V	S	Cu	Al	Co	Ti
FKS	0.11	0.76	0.005	0.03	5.00	0.42	0.53	0.043	0.004	0.022	0.021	0.02	0.008

Tensile Mechanical Properties of HY130 Steel

Code	0.2% YS MPa	UTS MPa	Elongation %in 2-inches	Reduction of Area %
FKS	937	978	21	55

Modified 1/2 T compact specimens were produced according to Figure 30, all with crack planes oriented in the T-L orientation. All specimens were machined from the center section of the 25 mm plate. A total of eight specimens were fatigue precracked to crack lengths between 0.59 and 0.94 a/W.

All tests were carried out at ambient temperature using computer data acquisition. A standard fracture mechanics clip on displacement gage was mounted on the knife edges in the load-line of each specimen. Using the computer interactive system for unloading compliance J-R curve determination described by Joyce and Gudas [84] the initial specimen compliance was carefully measured at loads below 1/2 the expected limit load. Then starting from zero load, a load displacement record was run to a final displacement of 0.1 in. In order to obtain as smooth a curve as possible no unloadings were taken and no attempt was made to determine when crack extension initiated in these specimens. A uniform crosshead speed of 5×10^{-3} in/min. was maintained throughout each test. Data points were taken approximately every 0.8×10^{-3} in of displacement and the load displacement file was stored on magnetic tape. After testing each specimen was heat tinted at 370°C for 20 min. and broken open in liquid nitrogen and the fatigue crack length was measured using a nine point average technique.

Function Assembly

The digital load-displacement records for each of the eight sub-size specimen tests were sent to the U.S. Naval Academy Honeywell

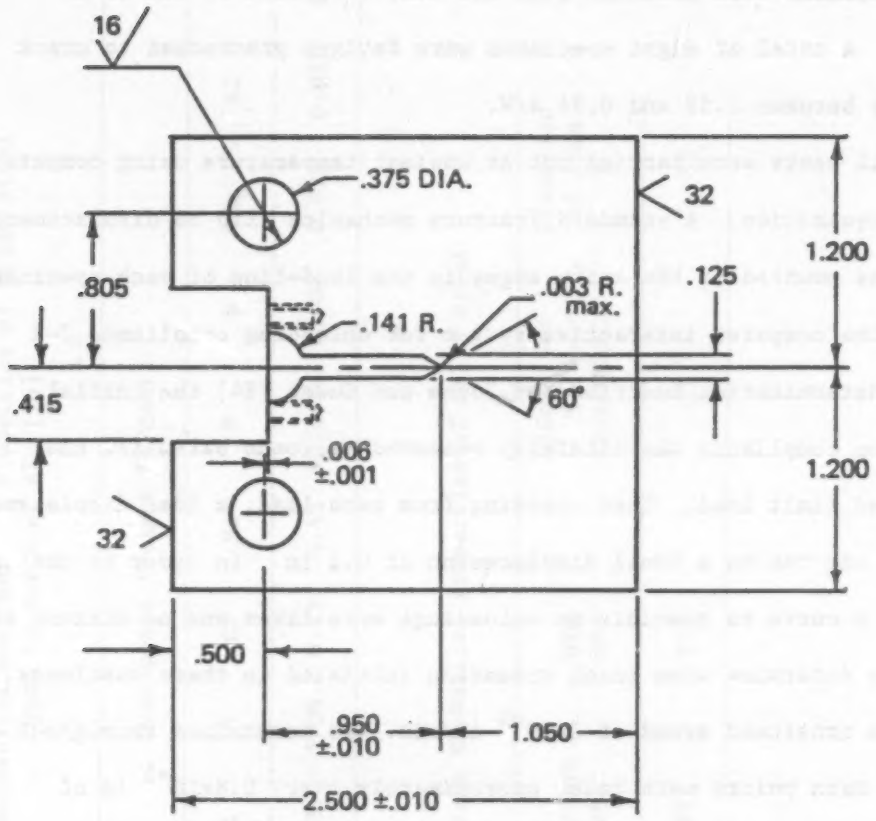

Fig. 30 Modified compact specimen.

6060 Time Sharing System. For each file the load and displacement were normalized to give:

$$P' = \frac{PW}{b^2}$$

$$\delta' = \frac{\delta}{W}$$

The displacement scale was then smoothed and reduced by an incerpolation routine to contain evenly spaced displacement valves at $5x10^{-4}$ in. intervals, to facilitate numerical differentiation. The eight separate files were then assembled into an f-function file on x, y, z triples where

$$x = \frac{\delta}{W}$$

$$y = \frac{a}{W}$$

$$z = \frac{PW}{Bb^2}$$

or

$$\frac{PW}{Bb^2} = F\left(\frac{\delta}{W}, \frac{a}{W}, C_1, C_2, C_3 \ldots\right)$$

where B is the specimen thickness, b is the uncracked ligament, δ is the total crack opening (load line) displacement and C_1, C_2 etc., are constants terms which are assumed to be identical for the 1/2 T

calibration specimens and the 1T specimens test specimens to which the analysis is to be applied. Geometrical similarity and material similarity were controlled as closely as possible between the two specimen size to assure that the F function of Equation (5.29) applies to both 1/2 T and 1T compact specimens.

It was noticed that for this material configuration, F is only a weak function of a/W, falling off approximately linearly, for a fixed δ/W. Terms of Equation involving $\partial F/\partial a/W$ are then constants depending on δ/W but not on a/W, and $\partial^2 F/\partial a/W^2 = 0$. The F function was not used beyond $\delta/W = .05$ because the load was approaching the maximum load in the shortest cracked specimens at this value of load line displacement implying the crack extension was imminent or even occurring in these specimens. This cutoff limits the maximum load line crack opening displacement to 0.1 in. for a 1T specimen but this is adequate in the material tested here to produce a J-R curve.

Application of the F Function

An application of the experimental F function to the determination of J-R curves directly from load displacement records was done by an analysis of data reported previously by Gudas, Joyce, and Davis [83] on this same HY.130 steel. In that work J-R curves for a matrix of specimens with a/W from 0.54 to 0.81 for 12% and + 25% face grooves and non-face grooved specimens had been obtained using the computer interactive unloading compliance technique. Digital load displacement records were obtained for all of these specimens and recorded on computer files.

The unloading compliance J-R curves results had shown that the average J_{IC} for all geometries 870 in lb/in^2 $\pm$ 10%. The apparent tearing modulus, T_{mat}, was shown to be distinctly lower for face grooved specimens than for non-face grooved specimens. The tearing modulus was independent of a/W for face grooved specimens. For non-face grooved specimens, the apparent T_{mat} was larger by a factor of 2 for specimens with a/W = 0.81 compared to specimens with a/W = 0.54. It was noted that the unloading compliance method underestimated crack extension when compared to a nine point average of measured values obtained after heat tinting and breaking open the specimens.

To obtain J-R curves directly from the load displacement curves of these specimens discrete versions of Equations (5.31) and (5.32) were written, namely:

$$\Delta J_n = \left[\frac{2b}{W} F_n - \frac{b^2}{W} \frac{F^*}{(a/W)_n}\right] \Delta\delta_n + \left[-\frac{2}{W} \sum_{i=1}^{n} F_i \Delta\delta_i + \frac{4b}{W^2} \sum_{i=1}^{n} \frac{\partial F^*}{\partial (a/W)_i} \Delta\delta_i\right] \Delta a_n \tag{5.33}$$

$$\Delta a_n = \frac{\frac{b^2}{W^2} \frac{\partial F^*}{\partial (\delta/W)_n} \Delta\delta_n - \Delta P_n}{\frac{2b}{W} F_n - \frac{b^2}{W^2} \frac{\partial F^*}{\partial (a/W)_n}} \tag{5.34}$$

At each point, n, on the load displacement record of a specimen the total J and a are:

$$J = \sum_{n=1}^{m} \Delta J_n \tag{5.35}$$

$$\Delta a = \sum_{n=1}^{m} \Delta a_n \tag{5.36}$$

In the above equations the terms without asterisks are evaluated from the specimen load displacement curve. The terms with asterisks are evaluated from the F calibration curve file. For the small amounts of crack extension considered here the remaining uncracked ligament b was assumed to remain constant.

A small computer program was written on the U.S. Naval Academy Time Sharing System which evaluates Equations (5.35) and (5.36) generating for each point on the specimen's digital load displacement record a Δa-J pair on a J-R curve for the specimen. Each point, n, of the load displacement record gives F_n and P_n directly. The specimen's measured crack length obtained by a heat tint 9 point average measurement technique and the δ/W at each point of the specimen's load displacement record locates a position on the F calibration function for the material. Numerical differentiation techniques are used about this point to determine

$$\frac{\partial F}{\partial (a/W)_n} \quad \text{and} \quad \frac{\partial F}{\partial (\delta/W)_n}$$

These values are used to give Δa_n from Equation (5.34) and subsequently a ΔJ_n from Equation (5.41). Summation of these by Equation (5.35) and (5.36) gives running totals of J and a. Stepping through complete load displacement curves, ignoring all data points on the unloadings, gives J-R curves like those shown in Figures

Discussion of Results

On Figures 31-33 the J-R curves resulting from the present analysis are shown with the previous J-R curve result from the unloading compliance method. Also shown on the figures are the final measured crack extensions plotted at J_{RICE} values where

$$J_{RICE} = \frac{2A}{Bb}$$

is the value of J from the area under the load displacement record A without an additional Merkle-Corten [67] correction. Final Merkle-Corten corrected J values are also shown on the J-R curve records. The critical J for the new analysis is reasonable compared to the previous results. The tearing moduli from the new analysis are smaller than the unloading compliance results but show much less variation with specimen geometry. The new analysis also predicts the final measured crack length very accurately, predicting at each point of the load displacement record more crack extension than that predicted by the unloading compliance method. J values resulting from the new analysis are lower than the Merkle-Corten corrected values used for the unloading compliance work. Note that in the present

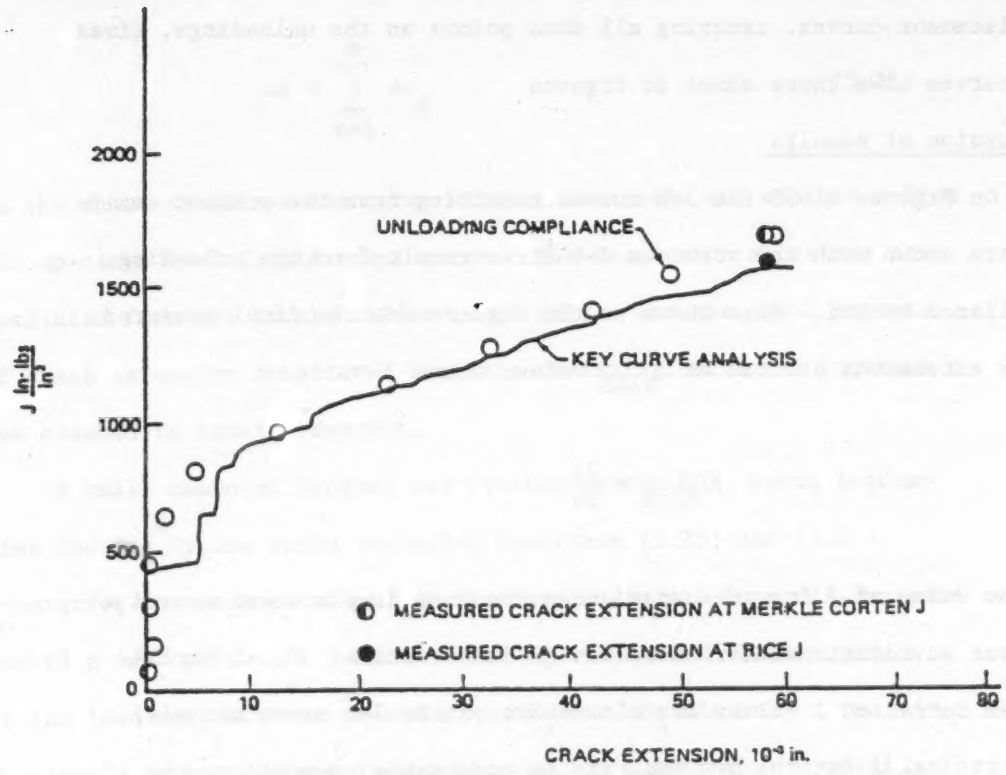

Fig. 31 J- R curve for HY 130 compact specimen a/W = .8

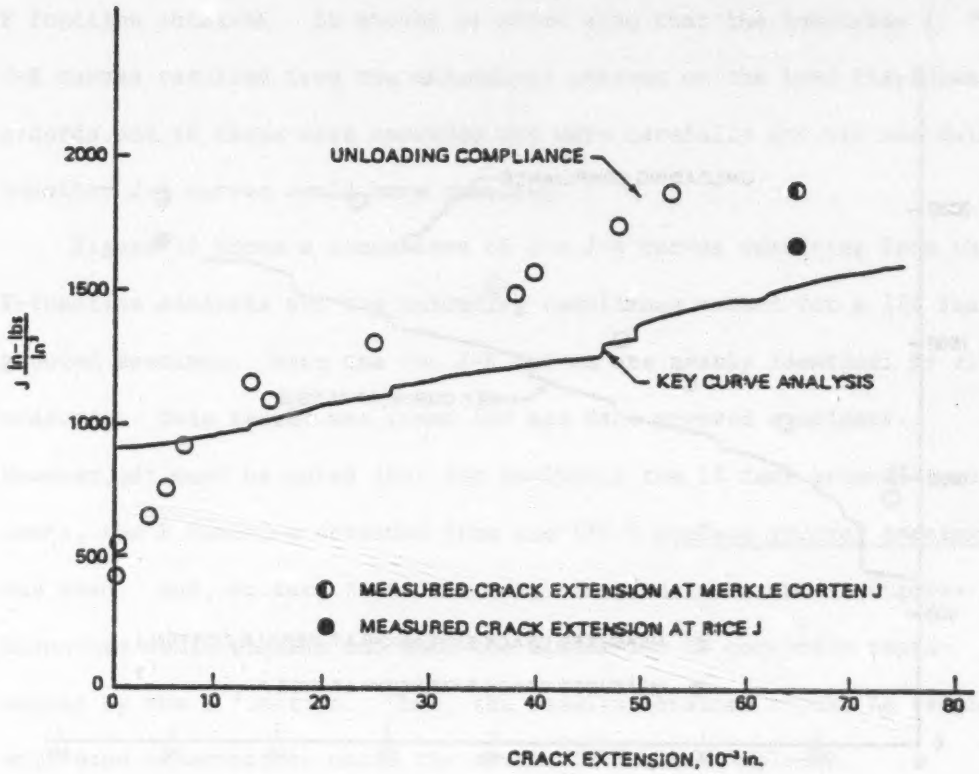

Fig. 32 J- R curve for HY 130 compact specimen a/W = .55

READEX FICHE

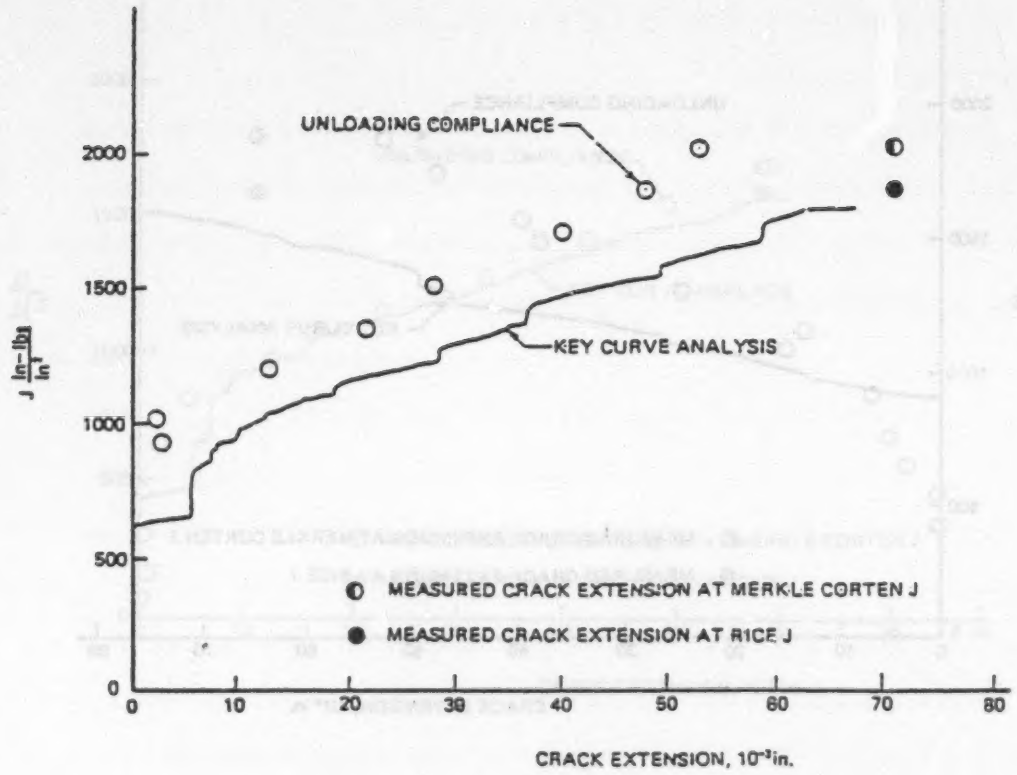

Fig. 33 J- R curve for HY 130 compact specimen a/W = .67 .

analysis $\partial F/\partial(a/W)$ was taken as a constant, implying that this correction for this material is fairly independent of crack length. This result is not intuitively satisfying but is justified by the F function obtained. It should be noted also that the lumpiness in the J-R curves resulted from the unloadings present on the load displacement records and if these were smoothed out more carefully (or did not exist) smoother J-R curves would have resulted.

Figure 34 shows a comparison of the J-R curves resulting from the F-function analysis and the unloading compliance method for a 12% face grooved specimen. Here the two J-R curves are nearly identical by all measures. This result was found for all face grooved specimens. However, it must be noted that for analyzing the 1T face grooved specimens, the F function obtained from the 1/2 T nonface grooved specimens was used. And, so far, it is not very clear that the two configurations are still similar and that the similarity is correctly represented by the F function. Thus, the results obtained should be taken with some reservations until the matter is further explored.

Also shown on Figure 34 is the result of multispecimen (4) tests on this material, which are plotted here without the Merkle-Corten correction. For these specimens $a/W = 0.72$. The J-R curve made up from these results falls close to the composite point made up of the final J_{RICE} value for the unloading compliance specimen plotted at the 9 point measured crack extension value. Good agreement is also found between the multispecimen curve and the F-function

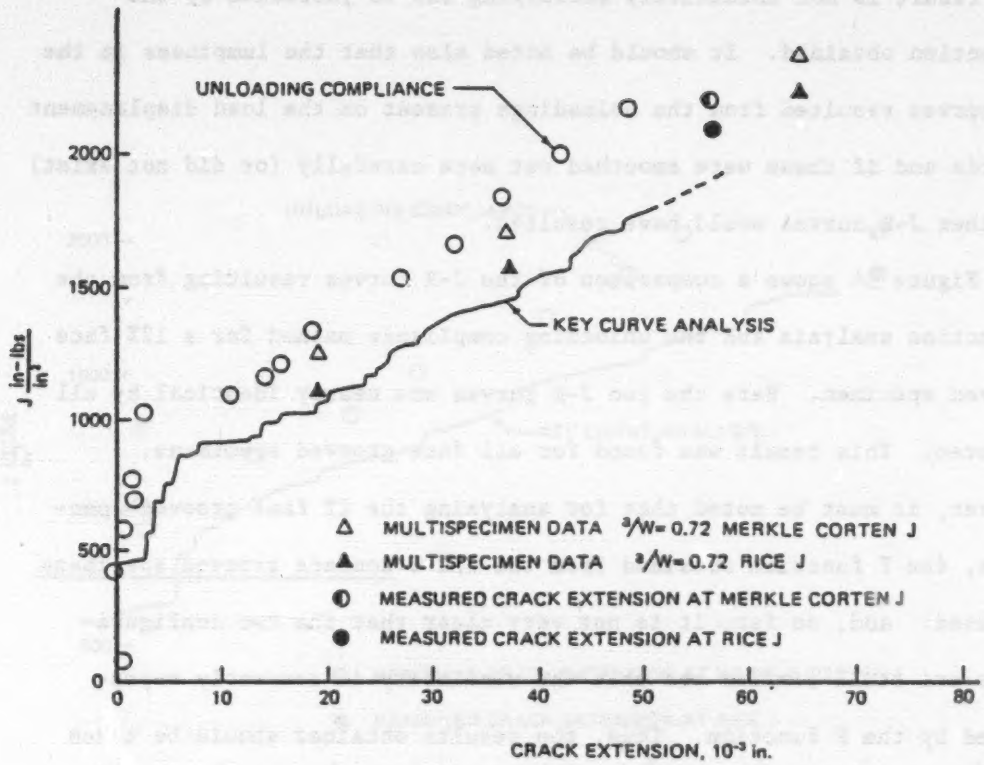

Fig. 34 J - R curve for HY 130 compact specimen a/W = .81 and multispecimen data.

curve analysis for the a/W = 0.81 specimen. The multispecimen line lies slightly above the F-function result but the deviation is less at larger a values.

The method as presented here, may be lengthy, but the resulting J-R curve is a considerable improvement over results obtained by unloading compliance or multispecimen methods. The new method evalutes J accurately without the assumptions of the fully plastic approximation used in the Merkle-Corten [67] analyis. Still, some inaccuracies remain in the experimental evaluation of the F function to obtain quantities used in Equations (5.33) and (5.34) for determining the J-R curve.

The unloading compliance method with face grooved specimens and without the Merkle-Corten correction is shown, in the above work, to correspond very well with the results of the new method. On the other hand, the tearing modulus evaluated by the unloading compliance method with nonface specimens is shown to be considerably different.

Summary

The major conclusions which can be drawn from this work are:

1. An experimental F "calibration function" can be obtained from subsize specimens, assembled in a computer file, and used to determine J-R curves from digitized load displacement records of geometrically similar specimens of the same material including the effects of crack extension. The J-R curves that result from this analysis are complete in that a point on the J-R curve exists for each point on the digitized load displacement record. This is an improvement over previous J-R curves which have contained only a few discrete points through which curves must be fit.

2. The F-function obtainable from fatigue cracked 1/2T compact specimens of this steel was restricted to δ/W values < .05. This allowed analysis of 1TCT specimens to a load line crack opening displacement of 0.1 in. in this HY130 steel which was adequate to obtain 0.06 in. of crack extension.

3. J-R curves resulting from the "calibration function" analysis of the HY130 matrix specimens were much more self-consistent, than those from other methods, with just a slight tendency to lower T values for shorter crack lengths observed. Moreover, tearing modulus values from the F-function method agree well with those obtained for face grooved specimens using the unloading compliance method. However, the adequacy of the use of the F function is as yet not completely clear and the results should be taken with some reservation. Generally, tearing moduli for nonface grooved specimens obtained by the unloading compliance method appear to be high due to the effects of crack tunneling on crack extension estimates.

4. Final crack length predictions from the calibration function method corresponded very accurately with final crack length measurements by heat tinting.

5. The J-R curves found using the F-function analysis agreed well with the results of multispecimen tests done on this alloy.

6. If the calibration function method were to be extended to situations involving large amounts of crack extension, where the crack

extension corrections would become important, it might be necessary to use blunt-notched subscale-specimens in order to have an F function which did not include crack extension effects at the required displacement values.

6. SUMMARY AND CONCLUSIONS

The overall objective of this work has been to develop analysis methods for fracture, in particular crack stability, under fully plastic conditions. The compatibility of these methods with formerly developed methods of linear-elastic fracture mechanics has been regarded as essential. The work has emcompassed further developing the concepts of crack stability. In addition and in particular, methods have been developed which make use of the characteristics of load-displacement relationships for both laboratory material (fracture) property measurements and for analyzing the fracture behavior of structural members. Since work done (or energy absorbed) on a structural member is a highly practical concept for both measurements and intuitive evaluations of circumstances or fracture, a substantial part of the effort has been put into developing relationships between the applied work and rigorous analytical parameters. The emphasis throughout this work has been on first developing a rigorous and complete analytical basis for the analysis of crack stability and then developing simplifications and approximations which make the methods useful in practice. Finally, an evaluation of the usefulness is developed with experimental evidences.

The analytical basis of all of this work adopts Rice's J-integral approach. Consistent with the methods of linear-elastic fracture mechanics, J is viewed as the controlling parameter of the crack tip stress-strain field which is justified under fully established conditions ($\omega >> 1$, $\Delta a << b$). Under these concepts the J-R curve

is the material's response crack length change, Δa, to monotonically increasing applied field intensity, J. This equilibrium is stated by equating the applied field intensity, J_{app} to the material's resistance, J_{mat} or

$$J_{app} = J_{mat} \quad \text{(Equilibrium)}$$

Then, again consistent with L.E.F.M. concepts instability occurs. When,

$$\frac{dJ_{app}}{da} \geq \frac{dJ_{mat}}{da} \quad \text{(Unstable)}$$

or alternately for convenience,

$$T_{appl} = \frac{E}{\sigma_o^2}\frac{dJ_{app}}{da} \geq \frac{E}{\sigma_o^2}\frac{dJ_{mat}}{da} = T_{mat} \quad \text{(Unstable)}$$

Where T is a dimensionless parameter, the tearing modulus. A full discussion of the details and history of these considerations has appeared in Chapter 1.

Formerly, the development of a material's J-R curve in the laboratory and its use were limited by awkward assumptions on methods of computing J and measuring crack length change. The work here proceeds to show that by employing dimensional considerations of the necessary form of load-displacement relationships for a cracked test specimen (or component) that "exact" methods can be developed. The effect of crack growth on J itself. Furthermore, the amount of crack growth, Δa, can also be obtained directly from

load-displacement data, provided that the function form or calibration function, F, of the load-displacement record is known (as a function of displacement and crack size). Methods of determining the F-function are given so that it becomes a practical reality to determine a J-R curve from a single load-displacement record (without other instrumentation or unloading). These methods have been developed in Chapter 2. In addition, it is shown that T_{appl} can also be evaluated from the characteristics of the load-displacement record, the F-function, for abitrary configuration. For both J-R curve development and T_{appl}, the results are specialized for application to common test specimen configurations, the compact specimen, bend specimens and tension specimens.

The "exact" load-displacement record analysis methods are complete as stated above, but require a significant amount of numerical work in order to evaluate a load-displacement record. However, it has been found that if the load-displacement relationships are separable functional forms (so that dependence on displacement and crack size can be separated into products of functions) then substantial additional simplifications ensue. Theorems are developed under which the separations are possible from an "exact" viewpoint in Chapter 3. Nevertheless, working with experimental data and other observations made it clear that conditions for such separations of variables are almost always approximately correct, at least individually for the elastic and plastic parts of the load-displacement relationships. The type of simplifications which ensue are that J becomes directly related to areas of the load-displacement curve, i.e., work done and like

quantities. This observation gives a J-integral analytic basis to Turner's η-factors, i.e., where

$$J = \frac{\eta}{b} \text{ Work}$$

which is most applicable in bending and derives a new μ-factor most appropriate for tension. The assumptions and conditions under which J and work are related thus become greatly clarified. Chapter 4 completes the analytical exposition of this analysis.

Finally, experimental results were produced and some acquired from other researchers to compare with the analytical methods developed. First, a series of 3-point bend bar tests were performed with variable loading systems compliance to clearly demonstrate the "tearing instability theory" for crack stability. Its interdependence of specimen proportions and loading system compliance on T_{appl} and the constant J-R curve control of T_{mat} were shown. The same 3-point bend tests were subjected to reanalysis of their load-displacement records by the single-record method developed to produce consistent J-R curves. Moreover, other 3-point bend tests of the same material with shorter relative spans were run and produced again a consistent J-R curve. Within these other 3-point bend tests blunt notch compact specimen load-displacement records and the calculation methods for J developed here were compared with theirs by reanalysis of their data. The results indicate the new analysis methods are highly accurate (with the scatter of the data itself). On the other hand, for compact specimens with growing cracks, the data of Gudas et al. [83], was

reanalyzed with excellent results. In this case J-R curves were developed from load-displacement record data alone, without the crack length measurement data taken by Gudas. Finally, results of a joint effort are presented where the methods of load-displacement analysis herein were computerized for automated (on-line) data reduction. The resulting J-R curves compare favorably with other methods of their evaluation for these compact specimen tests. Now, the actual methods and degrees of approximation through simplifying assumptions varied in the evaluation of the experimental data. This demonstrates clearly not only the correctness of the method but its adaptability for simplifications with the desired accuracy.

Indeed, it is believed that the methods of load-displacement analysis developed here permit obtaining J-R curves for materials (without separate crack length measurement instrumentation) at least as accurately as former methods. Moreover, the perhaps most important information derived from the J-R curves is the tearing modulus, T_{mat}, which measured in a natural way. That is to say that crack stability depends on the way material properties effect load-displacement relationships, so it is most natural to measure those material properties directly from load-displacement relationships, as was developed here. The additional advantages of not requiring separate crack length measurement schemes also will be of great advantage in adverse environments (e.g., hot cells, high temperature, etc.) as well as for dynamic testing.

ACKNOWLEDGEMENTS

This work was principally supported by the U.S. Nuclear Regulatory Commission Contract NRC 04-78-227 with Washington University. Earlier work and data under contract NRC 03-77-029 provide preliminary effort and background data for this work. Support under both contracts is acknowledged with thanks.

8. BIBLIOGRAPHY

1. Griffith A.A., "The Phenomena of Rupture and Flow in Solids", Transactions Royal Society London, Vol. 221, 1920.

2. Irwin G.R., "Fracture", Handbuch der Physiks, Vol. VI, Springer, Berlin, 1958.

3. Paris P.C. and Sih G.C., "Stress Analysis of Cracks", in Fracture Toughness and its Applications, ASTM STP 381, American Society for Testing and Materials, 1965, pp. 30-83.

4. Rolfe S.T. and Barsom J.M., "Fracture and Fatigue Control in Structures", Prentice Hall, 1977.

5. Paris P.C., "The Mechanics of Fracture Propagation and Solutions to Fracture Arrestor Problems", Boeing document D2-2195, 1957.

6. Wells A.A., "Unstable Crack Propagation in Metals, Cleavage and Fast Fracture", Cranfield Crack Propagation Symposium 1, Sept. 1961.

7. Dugdale D.S., "Yielding of Steel Sheets Containing Slits", Journal of the Mechanics and Physics of Solids, 8, 1960, p. 100.

8. Rice J.R., "A Path Independent Integral and the Approximate Analysis of Strain Concentration by Notches and Cracks", Journal of Applied Mechanics, 35, 1968, pp. 379-386.

9. Paris P.C., "Fracture Mechanics in the Elastic Plastic Regime", Flaw Growth and Fracture, ASTM STP 631, American Society for Testing and Materials, 1977, pp. 3-27.

10. Rice J.R., "Mathematical Analysis in the Mechanics of Fracture", in Fracture Vol. II, H. Liebowitz, Ed., Academic Press, 1968, pp. 191-311.

11. Hutchinson J.W., "Singular Behavior at the End of Tensil Crack in a Hardening Material", Journal of the Mechanics and Physics of Solids, Vol. 16, 1, 1968, pp. 13-31.

12. Hutchinson J.W., "Plastic Stress and Strain Fields at a Crack Tip", Journal of the Mechanics and Physics of Solids, Vol. 16, 5, 1968, pp. 337-347.

13. Rice J.R. and Rosengren G.F., "Plane Strain Deformation Near a Crack Tip in a Power Law Hardening Material", Journal of the Mechanics and Physics of Solids, Vol. 16, 1, 1968, pp. 1-12.

14. Begley J.A. and Landes J.A., "The J integral as a Fracture Criterion", in Fracture Toughness, ASTM STP 514, American Society for Testing and Materials, 1972, pp. 1-23.

15. Landes J.D. and Begley J.A., in Fracture Analysis ASTM STP 560, American Society for Testing and Materials, 1974, pp. 170-186.

16. Clarke G.A., Andrews W.R., Paris P.C. and Schmidt D.W., "Single Specimen Test for J_{IC} Determinations", in Mechanics of Crack Growth, ASTM STP 590, American Society for Testing and Materials, 1976, pp. 27-42.

17. Logdson W.A., "Elastic Plastic Fracture Toughness Values: Their Experimental Determination and Comparison with Linear Elastic Fracture Toughness Values for Five Materials", in Mechanics of Crack Growth, ASTM STP 590, American Society for Testing and Materials, 1976, pp. 43-61.

18. "Fracture Toughness Evaluations by R Curve Methods", ASTM STP 527, American Society for Testing and Materials, 1973.

19. Rice J.R., "Elastic Plastic Fracture Mechanics", The Mechanics of Fracture, F. Erdogan Ed. ASME, 1976.

20. Begley J.A. and Landes J.D., "Serendipity and the J integral", International Journal of Fracture, Vol. 12, 5, 1976.

21. Heyer R.H. and McCabe D.E., "Crack Growth Resistance in Plane Stress Fracture Testing", Engineering Fracture Mechanics 4, 1972, pp. 413-430.

22. McCabe D.E. and Heyer R.H., "R Curve Determination using a Crack-line Wedge Loaded (CLWL) Specimen", ASTM STP 527, American Society for Testing and Materials, Philadelphia, 1973, pp. 17-35.

23. Heyer R.H. and McCabe D.E., "Plane Stress Fracture Toughness Testing using a Crack-line-loaded Specimen", Engineering Fracture Mechanics, 4, 1972, p. 393.

24. "Recommended Practice for R Curve Determinations", ASTM Annual Book of Standards Part 10, American Society for Testing and Materials, Philadelphia, 1975.

25. McCabe D.E., "Determination of R-curves for Structural Materials using Non-linear Mechanics Methods", in Flaw Growth and Fracture, ASTM STP 631, American Society for Testing and Materials, 1977, pp. 245-266.

26. Shih C.F., De Lorenzi H.G., and Andrews W.R., "Studies on Crack Initiation and Stable Crack Growth", Symposium on Elastic Plastic Fracture, Nov. 1977, to appear in ASTM STP 1978.

27. McMeeking R.M., "Path Dependence of the J integral and the Role of J as a Characterizing Parameter of the near Tip Field", in Flaw Growth and Fracture, ASTM STP 631, American Society for Testing and Materials, 1977, pp. 28-41.

28. Paris P.C., Discussion on [14] and [29].

29. Landes J.D. and Begley J.A., "The Effect of Specimen Geometry on J_{IC}", in Fracture Toughness, ASTM STP 514, American Society for Testing and Materials, 1972, pp. 24-39.

30. Tada H., Paris P.C. and Irwin G.R., "The Stress Analysis of Cracks Handbook", Del Research Corp., 1973.

31. Shih C.F. and Hutchinson J.W., "Fully Plastic Solutions and Large Scale Yielding Estimates for Plane Stress Crack Problems", Journal of Engineering Materials and Technology, Vol. 98, 1976, pp. 289-295.

32. Goldman N.L. and Hutchinson J.W., "Fully Plastic Crack Problems: The Center Cracked Strip under Plane Strain", International Journal of Solids and Structures, Vol. II, 1975, pp. 575-591.

33. Amazigo J.C., "Fully Plastic Crack in a Infinite Body under Anti-plane Shear", International Journal of Solids and Structures, Vol. 10, 1974, pp. 1003-1015.

34. Hutchinson J.W., Needleman A. and Shih C.F., "Fully Plastic Problems in Bending and Tension", to be published in the Proceedings of an ONR International Symposium on Fracture Mechanics, Washington, DC, September 1978.

35. Bucci R.J., Paris P.C., Landes J.D. and Rice J.R., "J integral Estimation Procedures", in Fracture Toughness, ASTM STP 514, American Society for Testing and Materials, 1972, pp. 40-67.

36. Rice J.R., Paris P.C., and Merkle J.G., "Some Further Results of J-integral Analysis and Estimates", ASTM STP 536, American Society for Testing and Materials, 1973.

37. Love A.E.H., "A Treatise on the Mathematical Theory of Elasticity", Dover Publications, New York, 1944.

38. Westergaard H.M., "Bearing Pressures and Cracks", Transactions, American Society of Mechanical Engineers, Journal of Applied Mechanics, 1939.

39. Bilby B.A., Cottrell A.H., and Swinden K.H., "The Spread of Plasticity from a Notch", Proceedings Royal Society Series A 272, p. 304, London, 1963.

40. Kachanov L.M., "Fundamentals of the Theory of Plasticity", Mir Ed. 1974.

41. Illyushin A.A., "Plasticité, Deformations Elastico-Plastiques", Eyrolles Ed., 1956.

42. Hayes D.J., "Some Applications of Elastic-Plastic Analysis of Fracture Mechanics", Ph.D. Dissertation, Imperial College, University of London, October 1970.

43. Bilby B.A., Cottrell A.H., Smith E. and Swinden K.H., "Plastic Yielding from Sharp Notches", Proceedings Royal Society Series A 279, p. 1, London, 1964.

44. Carlsson A.J. and Markstrom K.M., "Some Aspects of Non linear Fracture Mechanics", Fracture 1977, Proceedings of the 45th International Conference on Fracture, Ontario, Canada, pp. 683-693.

45. McClintock F.A. and Irwin G.R., "Plasticity Aspects of Fracture Mechanics", in Fracture Toughness Testing and its Applications, ASTM STP 381, American Society for Testing and Materials, 1965, pp. 84-113.

46. Rice J.R., "Elastic-Plastic Models for Stable Crack Growth", in Mechanics and Mechanisms of Crack Growth, M.J. May, Ed., British Steel Corporation 1975, pp. 84-113.

47. Anderson H., "A Finite Element Representation of Stable Crack Growth", Journal of the Mechanics and Physics of Solids, Vol. 21, 1973, pp. 337-356.

48. Shih C.F., "On J Controlled Crack Growth: Evidence, Requirements, and Applications", Seminar offered at Washington University, St. Louis, MO, Dec. 1978.

49. Hutchinson J.W. and Paris P.C., "Stability Analysis of J-controlled Crack Growth", presented at the ASTM Symposium on Elastic Plastic Fracture, Nov. 1977, to appear in ASTM STP 1978.

50. Begley J.A., Landes J.D. and Wessel E.T., "Some Observations of Subcritical Crack Growth in Fracture Toughness Testing", in Mechanics and Mechanisms of Crack Growth, M.J. May, Ed., British Steel Corporation 1975, pp. 40-54.

51. Sumpter J.D.G. and Turner C.E., "Method for Laboratory Determination of J_{IC}", Cracks and Fracture, ASTM STP 601, American Society for Testing and Materials, 1976, pp. 3-18.

52. McCabe D.E. and Landes J.D., "An Evaluation of Elastic-Plastic Methods Applied to Crack Growth", presented at the Symposium on Elastic-Plastic Fracture, ASTM, Atlanta, November 1977.

53. Shih C.F., "J integral Estimates for Strain Hardening Materials in Antiplane Shear Using Fully Plastic Solution", Mechanics of Crack Growth, ASTM STP 590, American Society for Testing and Materials, 1976, pp. 3-26.

54. Landes J.D., Walker H. and Clarke G.A., "Evaluation of Estimations Procedures used in J integral Testing", presented at the Symposium on Elastic Plastic Fracture, ASTM, Atlanta, November 1977.

55. Berger C., Keller H.P. and Munz D., "Determination of Fracture Toughness with Linear-Elastic and Elastic-Plastic Methods", presented at the Symposium on Elastic-Plastic Fracture, ASTM, Atlanta, November 1977.

56. Zahoor A., "Tearing Instability of Elastic-Plastic Crack Growth", Ph.D. Dissertation, Washington University, St. Louis, MO, August 1978.

57. Parsons W.B., "Engineers and Engineering in the Renaissance", Williams and Wilkens, Baltimore, 1939.

58. Irwin G.R., "Analysis of Stresses and Strain Near the End of a Crack Traversing a Plate", Transactions, American Society of Mechanical Engineers, Journal of Applied Mechanics, 1957.

59. Tracey D.M., "On the Fracture Mechanics of Elastic-Plastic Materials using the Finite Element Method", Ph.D. Thesis, Brown University, 1973.

60. Irwin G.R., "Fracture Mechanics", Structural Mechanics, Pergamon Press, New York, NY, 1960.

61. Harrison J.D., Dawes M.G., Archer G.L. and Kamath M.S., "The COD Approach and its Applications to Welded Structures", presented at the ASTM Symposium on Elastic-Plastic Fracture, Atlanta, Nov. 1977.

62. Wells A.A., Engineering Fracture Mechanics, Vol. 1, 1969, p. 399.

63. Sumpter J.D.G., "Elastic Plastic Fracture Analysis and Design using the Finite Element Method", Ph.D. Thesis, University of London, 1974.

64. "Methods for Crack Opening Displacement (COD) Testing", Draft for Development, No. 3, British Standards Institution, 1971.

65. Garwood S.J. and Turner C.E., in Fracture 1977, University of Waterloo, 2 (1977), pp. 279-284.

66. McMeeking R.M. and Parks D.M., "On Criteria for J-dominance of Crack Tip Fields in Large Scale Yielding", presented at the ASTM Symposium on Elastic Plastic Fracture, Atlanta, Nov. 1977.

67. Merkle J. and Corten H., Journal of Pressure Vessel Technology Transactions of ASME, pp. 286-292, 1974.

68. Shih C.F., "Relationships between the J-integral and Crack Opening Displacement for Stationary and Extending Cracks", submitted for publication to the Journal of Mechanics and Physics of Solids, Oct. 1978.

69. Shih C.F. and German M.D., "Requirements for One Parameter Characterization of Crack Tip Fields by the HRR Singularity", submitted for publication to the International Journal of Fracture, Oct. 1978.

70. Clarke G.A., "Tentative Recommendation Procedure for J_{IC} Testing", ASTM E-24 Committee Meeting, Norfolk, Virginia, March 1977.

71. Paris P.C., Tada H., Zahoor A. and Ernst H., "The Theory of Instability of the Tearing Mode of Elastic Plastic Crack Growth", to be published in ASTM STP 668, American Society for Testing and Materials, 1979.

72. Paris P.C., Tada H., Ernst H. and Zahoor A., "An Initial Experimental Investigation of Tearing Instability Theory", to be published in ASTM STP 668, American Society for Testing and Materials, 1979.

73. Ernst H., Paris P.C., Rossow M., and Hutchinson J.W., "Exact Methods for Calculating J-integral and T-modulus Values for Stable Crack Growth", to be published as part of a report to the Nuclear Regulatory Commission, Center for Fracture Mechanics, Washington University, St. Louis, MO, Dec. 1977.

74. Ernst H., Paris P.C., Rossow M. and Hutchinson J.W., "Methods of Exact Analysis for J-integral with Stable Crack Growth", to be published in ASTM, STP 677, American Society for Testing and Materials, 1979.

75. Paris P.C., Ernst H. and Turner C.E., "A J-integral Approach to the Development of η-factors", submitted for publication to the XII Annual Symposium on Fracture Mechanics to be held at Washington University, St. Louis, MO in May 1979.

76. Joyce J.A., Ernst H., and Paris P.C., "Experimental Calibration Function Determination and Application to the Evaluation of J-Resistance Curves Directly from Load-Displacement Records", to be presented at the XII National Symposium on Fracture Mechanics, to be held at Washington University, St. Louis, MO, in May 1979.

77. Garwood S.J., Robinson J.N. and Turner C.E., International Journal of Fracture II (1973), pp. 525-531.

78. Garwood S.J., "The Measurement of Crack Growth Resistance using Yielding Fracture Mechanics", Ph.D. Thesis, University of London, 1976.

79. Garwood S.J. and Turner C.E., "Slow Stable Crack Growth in Structural Steel", International Journal of Fracture 14 (1978) R195-R198.

80. Rice J.R., in The Mechanics of Fracture, AMD 19, American Society of Mechanical Engineers, New York (1976), pp. 25-34.

81. Rice J.R., in Numerical Methods in Fracture Mechanics, University College of Swansea (1978), pp. 434-449.

82. Gudas J.P., Joyce J.A., and Davis D.A., "Investigation of Specimen Geometry Modifications to Determine the Conservative J_I-R Curve Tearing Modulus Using the HY-130 Steel System", ASTM STP 677, 1979.

83. Joyce J.A. and Gudas J.P., in Elastic-Plastic Fracture, J.D. Landes, J.A. Begley, and G.A. Clarke, Eds, ASTM STP 668, 1979, pp. 451-468.

84. "Concepts in Elastic Plastic Fracture Mechanics," Conference held by the Center for Fracture Mechanics, Washington University at St. Louis, MO, June 1978.

85. Garwood S.J., Robinson N. and Turner C.E., "The Measurements of Crack Growth Resistance Curves (R-Curves) using the J-integral," International Journal of Fracture, Vol. 11, Number 3, June 1975.

APPENDIX - ESTIMATES ON J AND T

As was discussed extensively in Chapter 3, the existence of the η-factor:

$$\eta = \eta(a/w) = \frac{b\ J}{\text{Area}} \tag{A1.1}$$

as being independent of the level of applied deformation (load or displacement) is related to the separability of J and/or the load P, into multiplicative functions of displacement and crack length. It was shown that a necessary and sufficient condition for the existence of η is the separability of P as

$$P = H\ (\delta/w)\ g_o(a/w) \tag{A1.2}$$

Moreover, as shown in Chapter 4, this separation may be viewed from another point of view. In fact, plotting load P vs. δ/W, if all the curves for each constant a/W value are of height P in constant scale to each other, then the separation exists. Further, if this scaling exists for some range of a/W values from δ=0 to some limiting value δ^{limit}, then the separation of variables exists over that region. That is to say, if

$$\frac{P(\delta/W\ ,\ a/W_i)}{P(\delta/W\ ,\ a/W_j)} = C_{ij}\ \text{(constant)} \tag{A1.3}$$

$$\text{for} \quad a/W_i \leq a/W \leq a/W_j$$

$$\text{and} \quad 0 \leq \delta \leq \delta^{\text{limit}}$$

then within that region the separation of variables and η will exist for that region.

Nevertheless, it can be readily seen that, in general, the scaling factor doesn't have to be necessarily the same in the linear elastic and in the plastic region. If that is the case it has proven sometimes useful, to separate the displacement into its elastic and plastic parts. By doing so separability is often recuperated, holding now for each particular region. That is

$$P = g_{o_{el}}(a/W) \cdot H_{el}(\delta/W)$$

and (A1.4)

$$P = g_{o_{pl}}(a/W) \cdot H_{pl}(\delta/W)$$

In this case two η factors are defined, i.e. η_{el} and η_{pl} and then the expression for J becomes

$$J = \frac{\eta_{el}}{b} A_{el} + \frac{\eta_{pl}}{b} A_{pl} \qquad (A1.5)$$

where A_{el} and A_{pl} refer to the elastic and plastic parts of the area under the $P \cdot \delta$ record respectively.

Thus, if and only if, the scaling factor is the same throughout the whole region of interest (i.e. elastic and plastic),

$$\eta_{el} = \eta_{pl} = \eta$$

the load can be separated as

$$P = g_o(a/W) \cdot H(\delta/W) \qquad (A1.6)$$

and the expression for J becomes

$$J = \frac{\eta}{b} \int_o^{\delta} P d\delta \qquad (A1.7)$$

Taking a more practical point of view, the conditions (A1.3) and/or (A1.4) can be always tested experimentally, and then the adequate expression for J can be used according to the scaling properties of the P·δ records.

On the other hand if separability does not hold or a better accuracy is required, the complete analysis developed in the previous chapters have to be applied.

On the other hand, it has become common lately, to calculate J for bending configurations using Equation (A1.7). In fact it has been recommended to use that expression taking η as given by the simplified

Merkle-Corten analysis [67] for the compact tension specimen (CT) and taking n=2 for the 3 Point Bend s/W = 4 specimen (3PB4).

Here the consequences of assuming Equation (A1.7) are explored in terms of J, the crack increment da, and the tearing modules T, although no attempt is made to justify the validity of the starting assumption.

J for the Growing Crack

As was mentioned above if J is expressed as

$$J = \frac{\eta}{b} \int_o^\delta P d\delta \qquad \text{(A1.7)}$$

the separability of the load is automatically implied (see Chapters 3 and 4) i.e.

$$P = g_o(a/W) \cdot H(\delta/W)$$

as well as the existence of the scaling factors C_{ij} of Equation (A1.3), for all a/W and δ of interest. Usually is convenient for bending configurations (Chapter 2), to express the load P as

$$P = \frac{b^2}{W} \; g(a/W) \; H(\delta/W) \qquad \text{(A1.8)}$$

Thus applying the definition, the expression for J becomes

$$J = \eta \frac{gb}{W} \int_o^\delta H d\delta = \frac{\eta}{b} \int_o^\delta P d\delta \qquad \text{(A1.9)}$$

$$\text{where} \quad \eta = (2 - \frac{b}{W} \frac{g'}{g}) \qquad \text{(A1.10)}$$

Following the procedure of Chapter 2, the above Equation can be differentiating to give

$$dJ = - \frac{J}{b} (\eta - 1 - \frac{b}{W} \frac{\eta'}{\eta}) \, da + \eta \frac{b}{W} g H d\delta \qquad \text{(A1.11)}$$

And reintegrating

$$J = \tilde{J} - \int_{a_o}^{a} \frac{J}{b} (\eta - 1 - \frac{b}{W} \frac{\eta'}{\eta}) \, da \qquad \text{(A1.12)}$$

where $\tilde{J}$ is J computed as if no crack growth occurred (Section 2.4).

In particular, for the 3PB4 taking $\eta = 2$ Equation (A1.12) gives

$$J = \tilde{J} - \int_{a_o}^{a} \frac{J}{b} \, da \qquad \text{(A1.13)}$$

Crack length increment da

Using as the starting assumption the separability of the load

$$P = \frac{b^2}{W}\, g(a/W)\, H(\delta/W) \qquad \text{(A1.8)}$$

the procedure shown in Chapter 2 can be followed directly. In fact, the crack length increment da can be obtained by differentiating Equation (A1.8).

$$dP = -\frac{b}{W}\, gH\, \eta\, da + \frac{b^2}{W^2}\, gH'\, d\delta$$

and rearranging

$$da = \frac{-dP + \frac{b^2}{W^2}\, gH' d\delta}{\frac{b}{W}\, g\, H\eta} = \frac{b}{\eta}\left(-\frac{dP}{P} + \frac{H'}{H}\,\frac{d\delta}{W}\right) \qquad \text{(A1.14)}$$

In particular for the 3PB4, with $\eta = 2$

$$da = \frac{b}{2}\left(-\frac{dP}{P} + \frac{H'}{H}\,\frac{d\delta}{W}\right) \qquad \text{(A1.15)}$$

Note that, as was mentioned in Section 2.5, the above equations can be further simplified by comparing two points at the same displacement i.e. $d\delta = 0$. In fact, if the reference point is taken as shown in Figure 12, then the crack increment da is

$$da = -\frac{b}{\eta}\frac{dP}{P} \qquad \text{for the CT} \quad \text{and} \qquad \text{(A1.16)}$$

$$da = -\frac{b}{2}\frac{dP}{P} \qquad \text{for the 3PB4} \qquad \text{(A1.17)}$$

where the values of b, η and P are taken at a reference point at the same displacement as the point of interest.

The tearing modulus

The tearing modulus as being the rate of change of J with crack length was defined in Chapter 1 and calculated for different configurations in Chapter 2 extending the ideas presented by Hutchinson and Paris [49]. These expressions can be further simplified if the starting conditions of the previous section are assumed.

In fact, if as before, the load P is separable as

$$P = \frac{b^2}{W} F(a/W\ ,\ \delta/W) = \frac{b^2}{W}\ g(a/W)\ H(\delta/W) \qquad \text{(A1.8)}$$

and then J is

$$J = \frac{\eta b}{W}\, g \int_o^{\delta} H\, d\delta = \frac{\eta}{b} \int_o^{\delta} P d\delta \qquad \text{(A1.9)}$$

the applied and material tearing modulus can be obtained by proper differentiation of the above expressions.

Material tearing modulus T_{mat}

The material tearing modulus T_{mat}, is defined as the rate of change of J with crack length along the actual P-δ record, normalized by the factor $\frac{E}{\sigma_o^2}$. Thus the expression for T_{mat} is

$$T_{mat} = \frac{E}{\sigma_o^2} \left\{ \frac{\partial J}{\partial a} + \frac{\partial J}{\partial \delta} \frac{d\delta}{da} \right\} \tag{A1.18}$$

$$= \frac{E}{\sigma_o^2} \left\{ -\frac{J}{b} \left(\eta - 1 - \frac{b}{W} \frac{\eta'}{\eta}\right) + \eta^2 \frac{F}{W} \frac{1}{\left(\frac{H'}{HW} - \frac{1}{P} \frac{dP}{d\delta}\right)} \right\} \tag{A1.19}$$

where $\partial J/\partial a$ and $\partial J/\partial \delta$ are obtained from Equation (A1.11) and $d\delta/da$ is obtained by rearranging Equation (A1.15). The increment $dP/d\delta$ is to be taken from the actual P-δ record.

For the 3PB4 specimen, with $\eta = 2$, Equation (A1.19) gives

$$T_{mat} = \frac{E}{\sigma_o^2} \left\{ -\frac{J}{b} + \frac{4F}{W} \frac{1}{\left(\frac{H'}{HW} - \frac{1}{P} \frac{dP}{d\delta}\right)} \right\} \tag{A1.20}$$

Applied tearing modulus T_{app}

The applied tearing modulus T_{app} has been defined in Chapter 1, as being the rate of change of J with crack length under the condition that the overall displacement is kept constant. That is

$$T_{app} = \frac{E}{\sigma_o^2} \frac{dJ}{da}\Big)_{\delta_{tot}} = \frac{E}{\sigma_o^2} \left\{ \frac{\partial J}{\partial a} + \frac{\partial J}{\partial \delta} \frac{d\delta}{da} \right\}$$

with the condition $d\delta_{tot} = d\delta + d\delta_M = 0$.

$$\text{or} \qquad d\delta = - d\delta_M = - dPC_M \tag{A1.21}$$

where C_M is the testing machine compliance as defined in Section 2.1.

Again as before, $\partial J/\partial a$ and $\partial J/\partial \delta$ are obtained from Equation (A1.11), and $d\delta/da$ is obtained from Equations (A1.21) and (A1.14) to give

$$T_{app} = \frac{E}{\sigma_o^2} \left\{ - \frac{J}{b} \left(\eta - 1 - \frac{b}{W} \frac{\eta'}{\eta}\right) + \frac{\eta^2 F}{W} \frac{1}{\left(\frac{C_M - 1}{P} + \frac{H'}{HW}\right)} \right\} \tag{A1.22}$$

In particular for the 3PB4 with $\eta = 2$

$$T_{app} = \frac{E}{\sigma_o^2} \left\{ - \frac{J}{b} + \frac{4F}{W} \frac{1}{\left(\frac{C_M - 1}{P} + \frac{H'}{HW}\right)} \right\} \tag{A1.23}$$

NRC FORM 335 (7-77) U.S. NUCLEAR REGULATORY COMMISSION

BIBLIOGRAPHIC DATA SHEET

1. REPORT NUMBER (Assigned by DDC): NUREG/CR-1222

4. TITLE AND SUBTITLE (Add Volume No., if appropriate): Techniques of Analysis of Load-Displacement Records by J-Integral Methods

2. (Leave blank)

3. RECIPIENT'S ACCESSION NO.

7. AUTHOR(S): Hugo A. Ernst, Paul C. Paris

5. DATE REPORT COMPLETED: MONTH November, YEAR 1979

9. PERFORMING ORGANIZATION NAME AND MAILING ADDRESS (Include Zip Code)
Washington University
Campus Box 1124, 405 Urbauer
St. Louis, MO 63130

DATE REPORT ISSUED: MONTH January, YEAR 1980

6. (Leave blank)

8. (Leave blank)

12. SPONSORING ORGANIZATION NAME AND MAILING ADDRESS (Include Zip Code)
Metallurgy & Materials Research Branch
Division of Reactor Safety Research
Nuclear Regulatory Commission
Mail Stop 1130 SS
Washington, DC 20555

10. PROJECT/TASK/WORK UNIT NO.

11. CONTRACT NO.: NRC-04-78-227

13. TYPE OF REPORT: Dissertation

PERIOD COVERED (Inclusive dates)

15. SUPPLEMENTARY NOTES

14. (Leave blank)

16. ABSTRACT (200 words or less)

Exact methods are used to obtain J from a single load displacement record for different configurations based on dimensional analysis and deformation theory of plasticity to imply the dependence of the load on crack length and displacement. The methods also permit the evaluation of the crack length increment a and hence complete J-R curves can be constructed. Formulae for T_{mat} and T_{app} are presented as well. Conditions for the existence of the so-called n-factor are stated, and subsequent simplifications of the general method by its use are shown. Results of analysis of experimental work for different configuration material combinations are presented showing the adequacy of the general methodology.

17. KEY WORDS AND DOCUMENT ANALYSIS

17a. DESCRIPTORS

17b. IDENTIFIERS/OPEN-ENDED TERMS

18. AVAILABILITY STATEMENT: Unlimited

19. SECURITY CLASS (This report): Unclassified

21. NO. OF PAGES

20. SECURITY CLASS (This page): Unclassified

22. PRICE: $

UNITED STATES
NUCLEAR REGULATORY COMMISSION
WASHINGTON, D. C. 20555

OFFICIAL BUSINESS
PENALTY FOR PRIVATE USE, $300

POSTAGE AND FEES PAID
U.S. NUCLEAR REGULATORY
COMMISSION